Università degli Studi di Palermo

SCUOLA POLITECNICA

Dipartimento di Ingegneria Civile, Ambientale, Aerospaziale, dei Materiali

Dottorato di Ricerca in Ingegneria Civile e Ambientale

Ingegneria delle Strutture

XXV Ciclo

Coor.: Prof. Orazio Giuffrè

Ph.D. Thesis

Analysis and design of elastic plastic structures subjected to dynamic loads

Candidato:
Arch. Pietro Tabbuso

Relatore:
Ch.mo Prof. Luigi Palizzolo

S.S.D. ICAR/08

Pietro Tabbuso
Printed in Palermo, January 2015
e-mail:pietro.tabbuso@unipa.it
e-mail:p.tabbuso@alice.it

Thesis of the Ph.D. course in *Structural Engineering*
Department of Civil, Environmental, Aerospace, Materials Engineering
University of Palermo
Viale delle Scienze - 90128 Palermo, ITALY
Tutor: Prof. Luigi Palizzolo

"Repetition is the only form of permanence
that nature can achieve."[1]

[1] G. Santayana, Soliloquies in England, 1922.

Contents

List of Figures

List of Tables

Preface

In the last decades, the concept of "optimization" has reached considerable value in many different fields of scientific research and, in particular, it has assumed great importance in the field of structural mechanics, as one can see through the large scientific literature produced on the topic of "structural optimization"(see e.g. [24, 52, 81]).

The present study describes and shows the scientific path followed in the three years of doctoral studies.

The state of the art concerning the optimization of elastic plastic structures subjected to quasi-static loads was already well established at the beginning of the Ph.D. course. Actually, it was already faced the study of structures subjected to quasi-static cyclic loads able to ensure different structural behaviors in relation to different intensity levels of the applied loads (see e.g. [1, 2, 6, 47, 57]).

In such a scientific context and with the aim to refer to cases of great practical interest, e.g. civil and industrial buildings affected by catastrophic events such as earthquakes and strong wind loads, the research effort has been addressed to reach an optimal design problem formulation for elastic perfectly-plastic structures subjected to static and dynamic loads, rigorously taking into account the dynamic and random nature of the loads and the non-linear behavior of the material.

Solving a structural optimization design problem means the reaching, among all the feasible designs, of the one which minimizes or maximizes a suitable chosen quantity according to given constraints usually representing some required behaviors for the structure. The formulation of the relevant search problem requires the choice of the structural model together with the definition of some parameter used as design variables, the choice of an objective function, and the imposition of suitable admissibility conditions.

In particular, the minimum volume of resistant structure has been chosen as objective function for a structure constituted by beam elements, in the hypothesis of small strains and displacements. The cross sections of the beams have been completely defined by means of a geometric parameter (thickness) used in the optimization problem as design variable. Furthermore the admissibility conditions of the problem have been used to impose different structural behaviors.

As known, a structure made of elastic plastic material subject to loads, which are variable in a quasi-static and/or in a dynamic manner, can exhibit five different structural behaviors depending on the relevant load intensity: the purely elastic behavior in which the structure does not suffer any plastic strain and the stress does not reach the yielding condition at no point; the elastic shakedown behavior in which the structure responds in an elastic manner after a first initial phase where there is the production of some limited plastic deformations; the plastic shakedown or low cycle fatigue behavior in which one can assist in the cycle to the production of plastic deformation of opposite sign that can lead to fatigue failure; the ratchetting or incremental collapse behavior for which there is the production of increasing plastic deformations along the load path; finally, the instantaneous collapse behavior for which the structure is immediately transformed into a mechanism.

Some practical considerations permit to say that a civil or industrial building made of elastic perfectly plastic material must behave in an elastic manner for permanent loads, must shake down for a combination of permanent and exceptional loads with low intensity, in such a way to exploit all the ductility resource that the structure possesses beyond the elastic limit, and should not instantaneously collapse for a combination of permanent and exceptional loads with high intensity. In particular, the adaptation behavior and the instantaneous collapse are studied by means of the shakedown theory and limit analysis respectively. This choice is particularly fruitful since both are first-order theories which do not require the solution of incremental elastic plastic analysis problems. It is useful to remember that the shakedown theory is based on a dual couple of theorems. These theorem, commonly known as Melan [65] and Koiter [60] theorems, permit to establish if the shakedown occurs in the structure subjected to quasi-static loads just looking at the elastic response.

Even the limit analysis is founded on a dual couple of well-known theorems which allow to identify the origin of a local or global mechanism of plastic zones (instantaneous collapse) for a structure subject to a monotonically increasing quasi-static load.

Referring to the classical shakedown theory and to international standards, the optimal design problem has been first formulated by modeling the seismic load through the response spectrum and calculating the purely elastic response through the modal combination. This response from a theoretical point of view has been idealized as the response to a quasi-static and perfectly cyclic load. Obviously, in order to simultaneously impose the shakedown and the collapse behavior, two different seismic responses, related to different probabilities of exceedance during the life of the structure, have been considered.

This approach has been used for the optimal design formulation of structures subjected to wind and seismic loads. In order to take into account some dangerous phenomena for the optimal structures such as the bucking and the $P - \Delta$ effects, various specializations have been proposed. Furthermore, the optimization of existing buildings equipped with seismic isolation system has been studied.

In order to more rigorously formulate the optimal design problem of structures subjected to seismic loads, a further scientific development has been reached making reference to the so-called "dynamic shakedown theory" which allows a better formulation of the optimal design problem of structures subject to dynamic actions.

This theory was born with the pioneering work of Ceradini [19]. Then it has experienced an enormous theoretical development in the eighties and nineties, and in the present thesis, it is used in the optimal design problem in order to take into account the real dynamic nature of seismic and wind loads.

The Ceradini's theorem is an extension in the dynamic range of the Melan's one. However, there are some theoretical differences. The former investigates the conditions under which a structure made of elastic plastic material subjected to a single dynamic and infinite load history, eventually shakes down ("restricted shakedown"), while the latter considers the same structure but subjected to an unknown quasi-static load within a given load domain. These difference can be overcome by the "unrestricted shakedown theory" in which the dynamic loads are conceived to appertain to a particular excitation domain so that the structure is exposed to an infinite and unknown sequence of potentially active excitations like in the classical theory. Following the unrestricted dynamic shakedown approach a complete optimal design formulation has been given.

The bibliographic study conducted on "dynamic shakedown" during the last part of the Ph.D. course have led to a new and original interpretation of the dynamic shakedown analysis problem in a probabilistic key. This modeling has paved the way to an additional and unexpected scientific improvement of the optimal design with the dynamic shakedown criterion in which the loads are modeled in all their stochastic nature. It should be noted, that optimal design problem with probabilistic constraints are placed in that recent line of research called Reliability-based design optimization (RBDO). An RBDO problem is formulated as a minimum volume problem with deterministic and probabilistic constraints. The research in this topics are still in progress and perhaps they will constitute the subjects of future developments.

Finally, consolidated linearization techniques have been used for the solution of formulated problems with continuous variables while a new heuristic algorithms, suitably modified and adapted for multi-constrained problems, have been used for the solution of the formulated design problems with both continuous and discrete variables.

It is worth remarking that this thesis contains the main part of the research done by Pietro Tabbuso at the Department of Civil, Environmental, Aerospace and Materials Engineering, University of Palermo. Furthermore, it contains original results, and some outcomes from the work done in collaboration [7–13, 49, 71–73].

Outline of the thesis

This thesis is composed of six chapters. After the present preface, in Chapter 1 the classical quasi-static shakedown theory, on which the first optimal design formulations have been developed, is recalled. In particular, the classical shakedown theorems together with the methods for the determination of the shakedown safety factor are reported.

In Chapter 2, the dynamic shakedown analysis is discussed following its historical evolution. Furthermore, an original probabilistic assessment of dynamic shakedown is given. This chapter constitutes the basis for a second group of optimal design formulations and paves the way for future developments.

Chapter 3 constitutes the core of the thesis because it collects all the proposed optimal design formulations. First, some optimal design formulations of structures subjected to idealized quasi-static loads are proposed and then, an unrestricted shakedown design is formulated for seismically excited buildings.

Obviously an optimization problem, whether it is formulated with continuous or discrete variables, has to be solved with appropriate computational procedures. In addition to the consolidated linearization techniques, in this thesis, reference has been made to a new heuristic algorithms, called harmony search method, and some improvements have been proposed. All these issues are briefly discussed in Chapter 4.

Chapter 5 collects all the most significant numerical applications which concern frame structures. After a probabilistic dynamic shakedown analysis of a structure subject to wind load, the minimum volume design is searched with all the proposed formulations. In some cases the Bree diagram of the obtained structure is plotted and the special structural features are discussed.

Finally, some conclusive comments are reported in Chapter 6.

Chapter 1

The classical shakedown theory

In this first chapter, the fundamental relations that govern the analysis problem of elastic perfectly plastic continua subjected to quasi-statically variable loads are reported and, thereafter, the basic concepts of the classical shakedown theory are shown together with the methods to obtain the shakedown safety factor.

1.1 The elastic perfectly plastic problem

Let consider an elastic perfectly plastic solid body of volume V and surface S (Figure 1.1) in the hypothesis of small strains and displacements, referred to a rectangular Cartesian coordinate system x_i, $(i = 1, 2, 3)$.

It is subjected to body forces F_i, to surface tractions T_i applied on the part S_1 of S, to imposed displacements $u_i = U_i$ on $S_2 = S - S_1$, and also to imposed strains ϑ_{ij} in V (for instance of thermal origin), varying all these actions in a quasi-static manner so that time is not the physical time, but just some parameter specifying the loading sequence.

Denoting with σ_{ij} the Cauchy stress tensor, the equilibrium equation are:

$$\sigma_{ij,j} + F_i = 0 \quad \text{in } V, \tag{1.1}$$

$$\sigma_{ij} n_j = T_i \quad \text{on } S_1 \tag{1.2}$$

where n_j is the unit external normal of S. Further, denoting with ϵ_{ij} the strain tensor, the compatibility equations are:

$$\epsilon_{ij} = e_{ij} + p_{ij} + \vartheta_{ij} \quad \text{in } V, \tag{1.3}$$

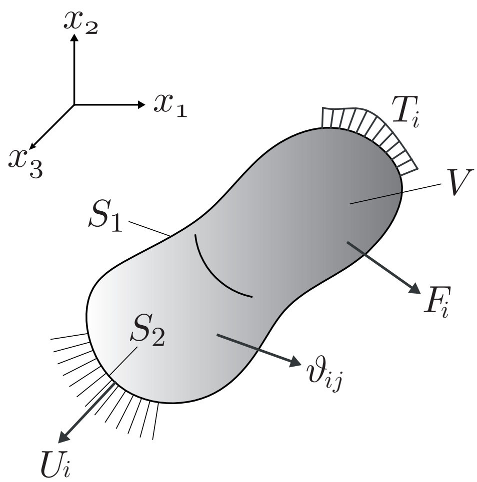

Figure 1.1: Sketch of an elastic perfectly plastic solid body.

$$\epsilon_{ij} = \frac{1}{2}(u_{i,j} + u_{j,i}) \quad \text{in } V, \tag{1.4}$$

$$u_i = U_i \quad \text{on } S_2 \tag{1.5}$$

where e_{ij} and p_{ij} are the elastic and the plastic strains. The elastic behavior of the material is described by Hooke's law:

$$e_{ij} = C_{ijhk}\sigma_{hk} \quad \text{in } V \quad \text{or, equally} \tag{1.6}$$

$$\sigma_{ij} = E_{ijhk}e_{hk} \quad \text{in } V \tag{1.7}$$

where C_{ijhk} is the usual (constant, symmetric and positive definite) compliance tensor while $E_{ijhk} = C_{ijhk}^{-1}$ is the elasticity tensor.

The elastic range in the stress space is defined by the following inequality:

$$\varphi(\sigma_{ij}) \leq 0 \quad \text{in } V \tag{1.8}$$

where $\varphi = \varphi(\sigma_{ij})$ is a convex yield function independent of plastic strain. The plastic strain rates are given by the usual normality rule:

$$\dot{p}_{ij} = \frac{\partial \varphi}{\partial \sigma_{ij}}\dot{\lambda} \quad \text{in } V \tag{1.9}$$

together with the side equations

$$\varphi \leq 0 \quad \dot{\lambda} \geq 0 \quad \text{in } V, \tag{1.10}$$

$$\varphi \dot{\lambda} = 0 \quad \dot{\varphi} \dot{\lambda} = 0 \quad \text{in } V, \tag{1.11}$$

where the over dot means time derivative.

Equations (1.1) to (1.11) govern the so-called elastic perfectly plastic problem. Solving this problem, at least in principle, it's possible to known, through the use of some step by step procedures, the response of the elastic perfectly plastic continuum in terms of stresses, strains and displacements, when the loading history is fully specified.

1.2 The classical shakedown theorems

An elastic plastic structure, subjected to variable or cyclic loads, can exhibit different behaviors. When the intensity of applied loads is sufficiently low, so that all the inequalities (1.8) are strictly satisfied in each point of V, the structural response is purely elastic and hence the deformation is completely recovered during the unloading. When at least in one point of the body, the relation (1.8) holds as equality, there is the production of plastic deformations, according to the flow rules expressed by the relations (1.9) to (1.11), and the structural behavior could be one of four types: elastic shakedown, alternating plasticity or plastic shakedown, ratchet or incremental collapse and instantaneous collapse (Figure 1.2).

Elastic shakedown means that the structure, after a first transient phase in which some plastic deformation appear over the body, is able to react in an elastic manner and the possible production of plastic deformation is a stable phenomenon (Figure 1.2a). Indeed, if the plastic deformations do not stop but, maintaining the same absolute value, they change theirs sign at every cycle, the structure could fail for low-cycle fatigue and the name given to this behavior is alternating plasticity or plastic shakedown (Figure 1.2b). It may also happen that the plastic strains continue to develop in every cycle so that the structure becomes unserviceable due to large displacements and excessive strains, so it is said that the structure is exposed to ratchet or incremental collapse (Figure 1.2c). Finally, the structure could instantaneously collapses if the loads intensities are higher than the loads-carrying plastic capacity so that plastic strains are unconstrained at first cycle (Figure 1.2d).

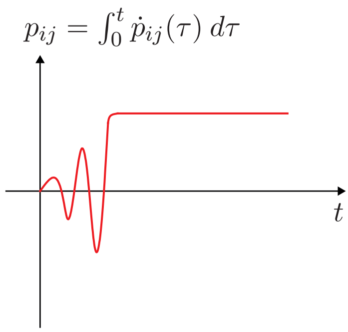

(a) Elastic shakedown;

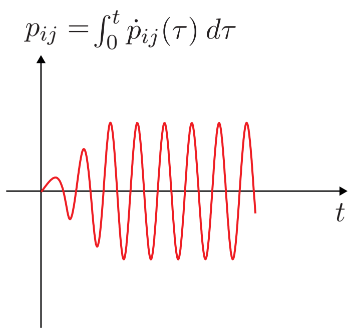

(b) Alternating plasticity;

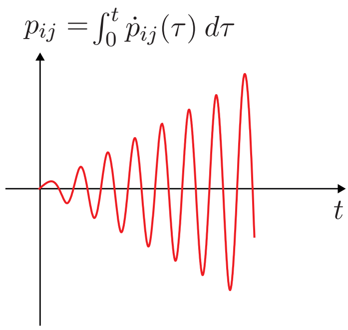

(c) Incremental collapse;

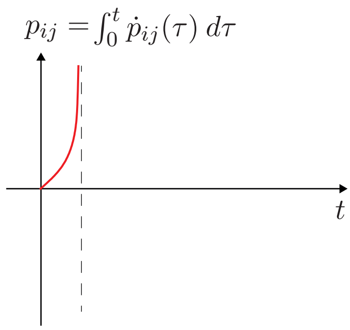

(d) Instantaneous collapse;

Figure 1.2: Structural behaviors beyond the elastic limit.

It is easy to understand that the elastic shakedown is a safe criterion to treat elastic-plastic structures because it permits the developing of some plastic strain in a first transient phase allowing the structure to respond in an elastic manner during the stationary response.

Before to continue, let make some remarks on the applied loads. Generally speaking, loads are random in nature as well as random is their evolution in time. Furthermore the structures could be subject to different independent load histories. If one wants to treat quasi-static loads in a deterministic manner, a simple way could be to estimates the maximum and minimum value that they assume for each independent load history and than to refer to the so-called "load domain". Every load path inside the loads domain will be called in the following "admissible load history" (ALH). At least in principle, solving the problem shown in section (1.1) for every admissible load history, it is possible to say if the structures is able to shake down or not. Indeed, being the real load history not known, there are infinite ALHs, and therefore, it is not possible to solve infinite analysis problems.

A dual couple of well-known theorems permit to say if a structure shakes down or not, overcoming the difficult related to an incremental elastic plastic analysis. One of them is the static theorem given first, in a general form by Melan [65] whose extended the work of Bleich [14] who proved the static shakedown theorem for a system of beams of ideal I-cross sections.

The static shakedown theorem or Melan's theorem, in its form suitable to the present context, can be stated as follows:

Theorem 1.2.1. *a necessary and sufficient condition for an elastic perfectly plastic structures to shake down is that there exist a time independent self-stress field ρ_{ij} that superimposed to the purely elastic (fictitious) stress history σ_{ij}^E nowhere violates the yielding law:*

$$\varphi\left(\sigma_{ij}^E(t) + \rho_{ij}\right) < 0 \quad \text{in } V \tag{1.12}$$

for any admissible load history inside the domain.

When the load domain is convex and could be represented, without loss of generality, trough a simplex Π of m vertices each of which will be called "basic load condition", using the "convex hull theorem" (see e.g. [61, 74]), there is a notable simplification on the shakedown condition. In fact, for an elastic plastic structure subjected to loads within a convex loads domain whose basic loads are denoted with F_i^b, T_i^b, ϑ_{ij}^b, U_i^b, $b = 1, 2, \ldots, m$,

Theorem 1.2.2. *a necessary and sufficient condition for shakedown is that there exist a time independent self-stress field ρ_{ij} that superimposed to the purely elastic stress response to any basic load conditions $\sigma_{ij}^{E(b)}$ nowhere violates* *the yielding law:*

$$\varphi\left(\sigma_{ij}^{E(b)} + \rho_{ij}\right) < 0 \quad \forall b \in I(m), \quad \text{in } V. \tag{1.13}$$

In this way the shakedown is ensured for any quasi-static load history $F_i(t)$, $T_i(t)$, $\vartheta_{ij}(t)$, $U_i(t)$ inside the convex loads domain that is possible to construct as a linear convex combination of the basic load conditions:

$$F_i(t) = \sum_{b=1}^{m} \mu^b(t) F_i^b, \tag{1.14}$$

$$T_i(t) = \sum_{b=1}^{m} \mu^b(t) T_i^b \tag{1.15}$$

$$\vartheta_{ij}(t) = \sum_{b=1}^{m} \mu^b(t) \vartheta_{ij}^b \tag{1.16}$$

$$U_i(t) = \sum_{b=1}^{m} \mu^b(t) U_i^b \tag{1.17}$$

where the coefficients $\mu^b(t)$ are required to satisfy the admissibility conditions that are:

$$\mu^b(t) \geq 0 \quad \forall b \in I(m), \tag{1.18}$$

$$\sum_{b=1}^{m} \mu^b(t) = 1. \tag{1.19}$$

being t a parameter specifying the loading sequence.

In 1950 Neal [69] presented a shakedown analysis method for frames by analyzing possible mechanisms of plastic flow extended in a special form for beams and frames by Neal and Symonds [70]. It was Koiter [60], who formulated a general kinematic approach to shakedown for continuous solid body.

Before to show the Koiter's theorem in its suitable form to the case of body subjected to a convex load domain, let define the plastic accumulation mechanism (PAM). This is a set of m plastic strain fields $\bar{p}_{ij}^b$, related to the m basic load conditions, such that the work done by them is positive and that their result is compatible:

$$\bar{p}_{ij} = \sum_{b=1}^{m} \bar{p}_{ij}^b = \frac{1}{2}(\bar{u}_{i,j}^r + \bar{u}_{j,i}^r) \quad \text{in } V, \quad \bar{u}_i^r = 0 \text{ on } S_2. \tag{1.20}$$

being $\bar{u}_i^r$ the residual displacement field related to $\bar{p}_{ij}$.

The kinematic shakedown theorem or Koiter's theorem can be stated as follows:

Theorem 1.2.3. *a necessary and sufficient condition for an elastic perfectly plastic structures to not shake down is that the total external work done by the basic loads is greater than the total plastic dissipation work:*

$$\sum_{b=1}^{m} \int_V \sigma_{ij}^{E(b)} \bar{p}_{ij}^b \, dV > \sum_{b=1}^{m} \int_V D\left(\bar{p}_{ij}^b\right) \, dV \tag{1.21}$$

where

$$D\left(\bar{p}_{ij}^b\right) = \sigma_{ij}^b \bar{p}_{ij}^b \tag{1.22}$$

is the unit volume plastic dissipation related to the b^{th} plastic strain field.

In equation (1.22) σ_{ij}^b is the stress field corresponding to $\bar{p}_{ij}^b$ trough the plastic flow rules.

It is worth noticing that the shakedown theory is a generalization of the limit analysis whose objective, as known is to evaluate, through a dual couple of well-known theorems, the origin of a local or global mechanism for a structure subject to a monotonically increasing quasi-static load. In fact, when one refers to a single basic load condition of the load domain and hence, the convex domain degenerates in a single vertex, the Melan and Koiter theorems are identical to the theorems of limit analysis.

1.3 The shakedown safety factor

With the aim to define a suitable safety index with respect to the shakedown of a structure subjected to an ALH, let consider that the convex domain Π, already defined in section (1.2), can expand or shrink homotetically depending on a single parameter ξ, so that:

$$\bar{F}_i^b = \xi F_i^b \quad \forall b \in I(m), \tag{1.23}$$

$$\bar{T}_i^b = \xi T_i^b \quad \forall b \in I(m), \tag{1.24}$$

$$\bar{\vartheta}_{ij}^b = \xi \vartheta_{ij}^b \quad \forall b \in I(m), \tag{1.25}$$

$$\bar{U}_i^b = \xi U_i^b \quad \forall b \in I(m), \tag{1.26}$$

being $\bar{F}_i^b$, $\bar{T}_i^b$, $\bar{\vartheta}_{ij}^b$, $\bar{U}_i^b$ the amplified basic load conditions.

When this parameter will take that particular limit value ξ^*, called shakedown limit multiplier, such that for all values $\xi \leq \xi^*$ the body elastically shakes down under the load domain amplified by ξ, it will assume the meaning of shakedown safety factor against the global crisis of the structure and its value is a significant measure of the structural safety. The determination of ξ^* is achieved through the application of the Melan's theorem or Koiter's theorem. These theorems are here recalled in the form of the lower bound and upper bound theorem for shakedown, because it is more appropriate to the purposes of the present thesis.

The lower bound theorem may be stated as follows: a number $\xi^s > 0$ is a statical load multiplier if, correspondingly, a self-equilibrated generalized stress field, ρ_{ij}, can be found such that the stress field $\hat{\sigma}_{ij}^b = \xi^s \sigma_{ij}^{E(b)} + \rho_{ij}$, being $\sigma_{ij}^{E(b)}$ the purely elastic stress response to b^{th} basic load condition, are each plastically admissible, i.e.

$$\varphi\left(\hat{\sigma}_{ij}^b\right) \equiv \varphi\left(\xi^s \sigma_{ij}^{E(b)} + \rho_{ij}\right) < 0 \quad \forall b \in I(m), \quad \text{in } V. \tag{1.27}$$

From the above theorem it is possible to say that no statical load multiplier can be greater than the limit load multiplier, so $\xi^s \leq \xi^*$.

The upper bound theorem may be stated as follows: a number $\xi^c > 0$ is a kinematical load multiplier if it identifies with the ratio between the total plastic dissipation promoted in the structure by a plastic accumulation mechanism and the total external work done by the basic loads and that mechanism, i.e.

$$\xi^c = \sum_{b=1}^{m} \int_V D\left(\bar{p}_{ij}^b\right) dV \Bigg/ \sum_{b=1}^{m} \int_V \sigma_{ij}^{E(b)} \bar{p}_{ij}^b \, dV \tag{1.28}$$

From the above theorem it is possible to say that no kinematical load multiplier can be lower than the limit load multiplier, so $\xi^c \geq \xi^*$.
The lower bound and upper bound theorem permit to write:

$$\xi^* = \max \xi^s = \min \xi^c \tag{1.29}$$

and so, the limit load multiplier or shakedown safety factor can be determined as the greatest statical multiplier or the lowest kinematical multiplier.

On the basis of the lower bound theorem, and hence on the Melan's theorem, the shakedown safety factor can be determined trough the solution of the following mathematical programming problem:

$$\xi^* = \max_{\xi^s,\, \rho_{ij}} \xi^s \tag{1.30a}$$

subjected to:

$$\varphi\left(\hat{\sigma}^b_{ij}\right) \equiv \varphi\left(\xi^s \sigma^{E(b)}_{ij} + \rho_{ij}\right) \leq 0 \quad \forall b \in I(m), \quad \text{in } V \tag{1.30b}$$

$$\rho_{ij,j} = 0 \quad \text{in } V, \quad \rho_{ij} n_j = 0 \quad \text{on } S_1. \tag{1.30c}$$

On the other hand, making reference to the upper bound theorem and hence to the Koiter's theorem, it' s possible to determinate the shakedown safety factor with the following mathematical programming problem:

$$\xi^* = \min_{\bar{p}^b_{ij}, \bar{u}^r_i} \xi^c = \min_{\bar{p}^b_{ij}, \bar{u}^r_i} \sum_{b=1}^{m} \int_V \sigma^b_{ij} \bar{p}^b_{ij} \, dV \tag{1.31a}$$

subjected to:

$$\bar{p}_{ij} = \sum_{b=1}^{m} \bar{p}^b_{ij} = \frac{1}{2}(\bar{u}^r_{i,j} + \bar{u}^r_{j,i}) \quad \text{in } V, \quad \bar{u}^r_i = 0 \text{ on } S_2, \tag{1.31b}$$

$$\sum_{b=1}^{m} \int_V \sigma^b_{ij} \bar{p}^b_{ij} \, dV = 1. \tag{1.31c}$$

Chapter 2

The dynamic shakedown theory

The concept of shakedown for quasi-static variable loads (Chapter 1) was first introduced in the thirties by the Austrian engineers Bleich [14] and Melan [65] which proposed the first "static" shakedown theorem. The second "kinematic" shakedown theorem is due to Koiter [60] who generalized the work of Neal and Symonds [70].

The introduction of dynamic shakedown concept was proposed by Ceradini [19] in 1969, who enunciated and proved the first dynamic shakedown theorem for elastic perfectly plastic solid bodies. This theorem is equivalent, as far as dynamic range is concerned, to the Bleich-Melan's theorem and reduces to it if inertia and damping forces may be neglected. Very similar arguments was the subject of a study published by Ho [55] in 1972. The second dynamic shakedown theorem for elastic perfectly plastic bodies is due to Corradi and Maier [30]. A theoretical reorganization of dynamic shakedown is due to Polizzotto [75], who first proposed a distinction between restricted and unrestricted dynamic shakedown. Restricted shakedown deals with a specified load history , while "unrestricted" is shakedown dealing with a load scheme allowing for load repetition. A complete and general treatment of dynamic shakedown for structures with an elastic-plastic rate-independent material model is object of a recent survey by Polizzotto et al. [79].

In the following sections, the Ceradini's theorem will be first recalled in its original form. Later, the theoretical aspect related to the "restricted" and to the "unrestricted" dynamic shakedown will be introduced, and consequently the related methods for the determination of the dynamic shakedown safety factor. It is worth noticing that the "kinematical type" dynamic shakedown theorem (see e.g. [30]) will be here disregarded because it does not represent a dual theorem of the Ceradini's one. Actually, for completeness, a dual kinematical dynamic shakedown theorem will be presented in the unrestricted dynamic shakedown context. Finally, a new probabilistic assessment of dynamic shakedown will be given.

2.1 The Ceradini's theorem

In this section the Ceradini's theorem will be given in its original form [19]. At this purpose, first, the governing equations of the dynamic elastic perfectly plastic analysis problem will be introduced. Then, a fictitious linear elastic analysis will be defined. The latter permit the right enunciation of the Ceradini's theorem whose proof is here disregarded for brevity.

Let consider an elastic perfectly plastic solid body of volume V and surface S, referred to a rectangular Cartesian coordinate system x_i, $(i = 1, 2, 3)$ in the hypothesis of small strains and displacements (Figure 2.1). It is subjected to the following external actions variable in the infinite time interval $t\,[0, +\infty]$: body forces $F_i(t)$, surface tractions $T_i(t)$ applied on free surface S_1 of S, imposed displacements $u_i(t) = U_i(t)$ on the constrained part S_2 of S, and imposed strains (e.g. thermal strains) $\vartheta_{ij}(t)$.

It is assumed that: the loading process varies so rapidly in time that inertia and damping forces cannot be neglected, the material satisfy the Drucker's stability conditions, the plastic deformations are instantaneous and the yield surface is fixed and bounded in all directions.

Let $\sigma_{ij}(t)$, $\epsilon_{ij}(t)$, $u_i(t)$, be the stress tensor, the strains tensor and the displacement components of the real dynamic elastic plastic body's response to the external actions with the given initial conditions $u_i(0) = u_i^0$, $\dot{u}_i(0) = \dot{u}_i^0$.

The equilibrium is expressed by the following equations:

$$\sigma_{ij,j}(t) + F_i(t) = \mu\ddot{u}_i(t) + \chi\dot{u}_i(t) \quad \text{in } V, \tag{2.1}$$

$$\sigma_{ij}(t)n_j = T_i(t) \quad \text{on } S_1, \tag{2.2}$$

where $\mu = \mu(x)$ is the mass density, $\chi = \chi(x)$ is the viscous damping coefficient and n_j is the unit external normal to S_1. The compatibility equations are:

$$\epsilon_{ij}(t) = e_{ij}(t) + p_{ij}(t) + \vartheta_{ij}(t) \quad \text{in } V, \tag{2.3}$$

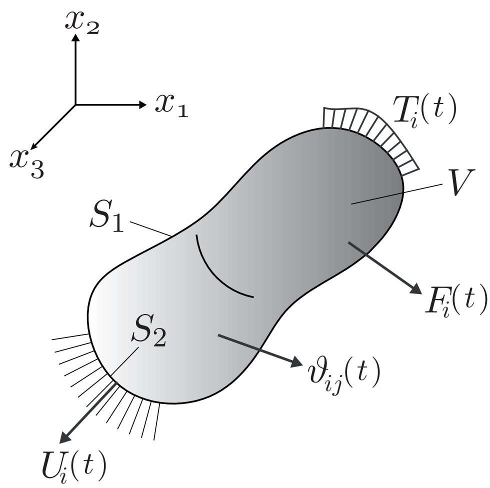

Figure 2.1: Sketch of an elastic perfectly plastic solid body under dynamic actions.

$$\epsilon_{ij}(t) = \frac{1}{2}\left[u_{i,j}(t) + u_{j,i}(t)\right] \quad \text{in } V, \tag{2.4}$$

$$u_i(t) = U_i(t) \quad \text{on } S_2, \tag{2.5}$$

being $e_{ij}(t)$ and $p_{ij}(t)$ the elastic and the plastic strains. Furthermore, the elastic behavior of the material is described by Hooke's law:

$$e_{ij}(t) = C_{ijhk}\sigma_{hk}(t) \quad \text{in } V \quad \text{or, equally} \tag{2.6}$$

$$\sigma_{ij} = E_{ijhk}e_{hk} \quad \text{in } V, \tag{2.7}$$

where C_{ijhk} is the compliance tensor and E_{ijhk} its inverse.

The elastic range is defined by the following inequality:

$$\varphi(\sigma_{ij}) \leq 0 \quad \text{in } V, \tag{2.8}$$

being φ the yield functions. Moreover, the elastic perfectly plastic behavior is governed by the following flow rules:

$$\dot{p}_{ij} = \frac{\partial\varphi}{\partial\sigma_{ij}}\dot{\lambda}, \quad \dot{\lambda} \geq 0, \quad \varphi\dot{\lambda} = \dot{\varphi}\dot{\lambda} = 0, \quad \text{in } V. \tag{2.9}$$

At least in principle, using the eqs. (2.1) to (2.9), it is possible to solve the analysis problem of the referenced elastic-perfectly plastic continuous, and then, to check if the body shakes down or not. Instead, Ceradini proved that it is possible to establish the conditions under which the body shakes down starting from a fictitious purely elastic response of the same body.

At this purpose, let consider a fictitious purely elastic response to the given external actions with arbitrary initial conditions $\bar{u}_i(0) = \bar{u}_i^0$, $\dot{\bar{u}}_i(0) = \dot{\bar{u}}_i^0$. Quantities referring to fictitious response will be represented with a bar superscript. It is quite obvious that the fictitious response differs from the real one because the plastic strains are neglected and because the arbitrary initial conditions. As a consequence, inertia and damping forces are different in the real process and in the fictitious one.

So, assuming that the material behavior is indefinitely elastic, the fictitious response is governed by the following set of equations. The equilibrium is held by:

$$\bar{\sigma}_{ij,j}(t) + F_i(t) = \mu\ddot{\bar{u}}_i(t) + \chi\dot{\bar{u}}_i(t) \quad \text{in } V, \tag{2.10}$$

$$\bar{\sigma}_{ij}(t)n_j = T_i(t) \quad \text{on } S_1, \tag{2.11}$$

the compatibility is expressed by:

$$\bar{\epsilon}_{ij}(t) = \bar{e}_{ij}(t) + \vartheta_{ij}(t) \quad \text{in } V, \tag{2.12}$$

$$\bar{\epsilon}_{ij}(t) = \frac{1}{2}\left[\bar{u}_{i,j}(t) + \bar{u}_{j,i}(t)\right] \quad \text{in } V, \tag{2.13}$$

$$\bar{u}_i(t) = U_i(t) \quad \text{on } S_2 \tag{2.14}$$

and the elasticity is described by:

$$\bar{e}_{ij}(t) = C_{ijhk}\bar{\sigma}_{hk}(t) \quad \text{in } V \quad \text{or, equally} \tag{2.15}$$

$$\bar{\sigma}_{ij} = E_{ijhk}\bar{e}_{hk} \quad \text{in } V. \tag{2.16}$$

The first dynamic shakedown theorem or Ceradini's theorem [19, 20] was establishes both as a sufficient condition that as a necessary and sufficient condition.

Let show first that a sufficient dynamic shakedown condition:

Theorem 2.1.1. *if a fictitious response $\bar{\sigma}_{ij}(t)$, $\bar{\epsilon}_{ij}(t)$, $\bar{u}_i(t)$ and a time independent residual stress distribution ρ_{ij} may be found so that:*

$$\varphi\left(\bar{\sigma}_{ij}(t) + \rho_{ij}\right) < 0 \quad in\ V, \quad t \in [0, +\infty], \tag{2.17}$$

than the dynamic shakedown will occur in the real response.

The latter theorem has been enunciated as a sufficient condition because the condition (2.17) may be violated during the first transient phase.

In fact, let consider that the magnitude of external actions decreases monotonically in time after a first phase of high intensity. If the structure shakes down, plastic deformations will cease at a certain instant t^* even if the condition of equation (2.17) is violated during the interval $[0, t^*]$.

In this case the dynamic shakedown theorem can be enunciated as a necessary and sufficient condition:

Theorem 2.1.2. *a necessary and sufficient condition for dynamic shakedown is that there exist a fictitious response $\bar{\sigma}_{ij}(t)$, $\bar{\epsilon}_{ij}(t)$, $\bar{u}_i(t)$, a time independent residual stress distribution ρ_{ij} and a finite time $t^* \geq 0$ such that the resulting stress field nowhere violates the yielding condition in the structure at any time $t \geq t^*$ so that:*

$$\varphi\left(\bar{\sigma}_{ij}(t) + \rho_{ij}\right) < 0 \quad in\, V, \quad \forall t \geq t^*. \tag{2.18}$$

Ceradini proved that the sufficient condition, above exposed theorem (2.1.1), became also necessary when the external actions are periodic, in other word: if the external actions are periodic and if the body in the real dynamic process shakes down, then at least a fictitious response must exist which superimposed to a suitable residual stress distribution satisfy the inequalities (2.17). It is noteworthy that the proofs of the above theorems (2.1.1,2.1.2) were given first for undamped structures and then for structures in which the viscous damping is considered (see e.g. [19, 20]).

A particular mention should be made of the work of Gavarini [41], who proved the following theorem in the case of periodic external actions:

Theorem 2.1.3. *a necessary and sufficient condition for dynamic shakedown for a structure subjected to periodic external actions is that there exist a fictitious stress response $\bar{\sigma}^s_{ij}(t)$, a time independent residual stress distribution ρ_{ij} such that the resulting stress field nowhere violates the yielding condition*

$$\varphi\left(\bar{\sigma}^s_{ij}(t) + \rho_{ij}\right) < 0 \quad in\, V, \quad t \in [0, +\infty], \tag{2.19}$$

being $\bar{\sigma}^s_{ij}(t)$ the steady-state stress history.

The Gavarini's theorem results very useful in practical applications, in fact, in the case of discrete structures with linearized yield surface, the determination of the shakedown safety factor can be bring back to a simple linear programming problem (see e.g. [21]).

Finally, it is important to recall that the dynamic shakedown theorems remain valid even for that particular load history made by load cycles spaced out by intervals such that the body is brought at rest thanks to internal damping, as proved by Ceradini [19] in his first work. This fact will be used later in order to define a probabilistic assessment of dynamic shakedown and in the unrestricted dynamic shakedown context.

2.2 A unified treatment of dynamic shakedown

The classical shakedown theory (Chapter 1), is deeply rooted on the concept that all the load combinations, potentially active at the present time, remain potentially active in the future and no load condition, different from those expressed by the load domain, are allowed in the future. This means that all future potential events are simple repetitions of the present ones. The actual possibility of loads to be repeated any number of times in the future creates a kind of permanent load history typical of quasi-static shakedown theory in such a way that the structure eventually adapts. In contrast with quasi-static shakedown, dynamic shakedown, as proposed by Ceradini [19, 20], has been associated with loading histories fully specified at all times from $t = 0$ to $t = +\infty$.
On comparing them, one notices that they have two different approach to consider the loading history.

In Ceradini's approach, the loads repetition is not allowed and the shakedown depends only in the future loading events, not on the present nor on the past ones. Therefore, the Ceradini's theorem has a more restricted meaning than the classical shakedown one.

For the above reasons and with the aim to establish a link between the classical and the dynamic shakedown theory, Polizzotto [75] proposed a theoretical reorganization of shakedown dealing with dynamic agencies. He made a distinction between "restricted" and "unrestricted" dynamic shakedown. Restricted shakedown deals with a specified load history , while "unrestricted" is shakedown dealing with a load scheme allowing for load repetition.

In other words, with restricted dynamic shakedown only the load conditions acting after a long term are responsible of the shakedown occurrence, whereas the loads acting in a first phase are irrelevant with respect to shakedown since they constituted isolated unrepeatable load conditions that in any case may produce only finite plastic deformations. With unrestricted dynamic shakedown, all load conditions are equally responsible of the shakedown occurrence because every individual load is always potentially active during the structure's life.

2.2.1 The restricted dynamic shakedown

The Ceradini's theorem belongs to the restricted dynamic shakedown theory, in fact, it refers to a single infinite load history. Making reference to the work of Polizzotto [76] and considering the elastic perfectly plastic problem posed in the section (2.1), for the purpose of the present subsection let recall the Ceradini's theorem in a more general form:

Theorem 2.2.1. *a necessary and sufficient condition for dynamic shakedown is that there exist a finite time, $t^* \geq 0$, and some initial condition, $(\bar{u}_i^0, \dot{\bar{u}}_i^0, \bar{p}_{ij}^0)$, such that the purely elastic stress response to the given load history, $\bar{\sigma}_{ij}(t)$, proves to be inside the yield surface at any subsequent time, $t \geq t^*$, so that:*

$$\varphi\left(\bar{\sigma}_{ij}(t)\right) < 0 \quad in\; V, \quad \forall t \geq t^*. \tag{2.20}$$

Considering that the initial plastic strains give rise to a residual stress distribution and that the initial displacement and velocity govern the free-vibration motion, let the stress response $\bar{\sigma}_{ij}(t)$ in equation (2.20) be given in the form:

$$\bar{\sigma}_{ij}(t) = \bar{\sigma}_{ij}^E(t) + \bar{\sigma}_{ij}^F(t) + \rho_{ij} \tag{2.21}$$

where $\bar{\sigma}_{ij}^E(t)$ is the purely elastic response to the loads $F_i(t)$, $T_i(t)$, $\vartheta_{ij}(t)$, with arbitrary but fixed initial conditions, $\bar{\sigma}_{ij}^F(t)$ is the stress history associated with a free motion or natural vibration of the structure considered as purely elastic and ρ_{ij} is a time-independent self-stress field. With a change of the time variable:

$$t = t^* + \tau \tag{2.22}$$

the inequality (2.21) can be rewritten as:

$$\varphi\left(\bar{\sigma}_{ij}^E(t^* + \tau) + \bar{\sigma}_{ij}^F(\tau) + \rho_{ij}\right) < 0 \quad \text{in } V, \quad \forall \tau \geq 0, \tag{2.23}$$

in which $\bar{\sigma}_{ij}^E(t^* + \tau)$, $\tau \geq 0$, is the elastic stress response truncated backward at time t^*, that is the elastic stress response to the loads $F_i(t^* + \tau)$, $T_i(t^* + \tau)$, $\vartheta_{ij}(t^* + \tau)$, $\tau \geq 0$, with arbitrary but fixed initial conditions specified at $\tau = 0$, while $\bar{\sigma}_{ij}^F(\tau)$ is a free-motion stress field with initial conditions specified at $\tau = 0$. In the following, a finite time $t^* \geq 0$ for which the inequality (2.23) holds as equality will be called "separation time" because ideally it separates the elastic plastic phase to the purely elastic one.

With the above considerations an alternative form of the shakedown theorem can be formulated:

Theorem 2.2.2. *a necessary and sufficient condition for dynamic shakedown is that there exist a finite time, $t^* \geq 0$, a free motion stress field $\bar{\sigma}_{ij}^F(\tau)$, and a time-independent self-stress field, ρ_{ij}, such that the sum of these stresses with the elastic stress response truncated backward at t^*, $\bar{\sigma}_{ij}^E(t^* + \tau)$, proves to be inside the yield surface at any time $\tau \geq 0$.*

This alternative form of the shakedown theorem is completely equivalent to the previous one.

As proved by Polizzotto [76] if there exist a separation time, t^*, and hence the structure shakes down, every time of the interval, $J(t^*) = \{t : t \geq t^*\}$, is a separation time. Furthermore, for a structure which shakes down, the shortest separation time is a lower bound with respect to the adaptation time t^a.

From a physical point o view, the free-motion stress $\bar{\sigma}_{ij}^F$, are representative of the dynamic effect produced by the plastic strains over the body's motion during the transient phase up to the adaptation time t^a. The analogous static effect are represented by ρ_{ij}. As shown before, in Ceradini's approach [19, 20], these effects are simulated by means of fictitious initial conditions fixed at remote time $t = 0$.

With the new definition of the restricted dynamic shakedown theorem (2.2.2), it is easy to understand that the actual initial conditions associated with the loading history have no influence on the capacity of the structure to adapt to the given load history. In fact, assuming that in (2.23) $\bar{\sigma}_{ij}^E$ is associated with zero initial conditions, the analogous response in case of nonzero initial conditions, say $\bar{\sigma}_{ij}^{E1}$, can be expressed as $\bar{\sigma}_{ij}^{E1} = \bar{\sigma}_{ij}^E + \bar{\sigma}_{ij}^{EF}$, with $\bar{\sigma}_{ij}^{EF}$ being the free-motion stress generated by the mentioned initial conditions. Thus, inequality (2.23) becomes:

$$\varphi\left(\bar{\sigma}_{ij}^{E}(t^{*}+\tau)+\bar{\sigma}_{ij}^{EF}(\tau)+\bar{\sigma}_{ij}^{F}(\tau)+\rho_{ij}\right)<0, \quad \text{in } V, \quad \forall\tau\geq 0, \tag{2.24}$$

which coincides with (2.23) because the addend $\bar{\sigma}_{ij}^{EF}(\tau)+\bar{\sigma}_{ij}^{F}(\tau)$ does represent a free-motion stress field like $\bar{\sigma}_{ij}^{F}(\tau)$. This fact is beneficial because the actual initial conditions, like the initial residual stresses, are hardly known in practice.

Another issue is that the Ceradini's theorem looks for the conditions under which the overall plastic dissipation work does not diverge with time, treating the load in an infinite interval. So, if the load act in a finite interval, the plastic dissipation work cannot diverge and hence the theorem is defective.

In fact, let consider that the load history has a finite duration, say $0 \leq t \leq T$, always it is possible to choose a time $t^{*} > T$, such that $\bar{\sigma}_{ij}^{E}$ is a free-motion stress and thus the inequality (2.23) can be always satisfied by taking $\bar{\sigma}_{ij}^{F} = -\bar{\sigma}_{ij}^{E}$. In other word, for T finite, shakedown always occurs because after $t^{*} > T$ no further plastic strains can be produced and the theorem gives no indication about whether shakedown occurs before the given loading history extinguishes.

With the aim to define a suitable shakedown safety factor, let the given loads, $F_i(t)$, $T_i(t)$, $\vartheta_{ij}(t)$, be multiplied by a positive scalar, ξ, and let the following problem:

$$\xi^{*} = \max_{\left(\xi,\,\bar{\sigma}_{ij}^{F},\,\rho_{ij}\right)} \xi^{s} \tag{2.25a}$$

subjected to:

$$\varphi_r\left(\xi\bar{\sigma}_{ij}^{E}(t^{*}+\tau)+\bar{\sigma}_{ij}^{F}(\tau)+\rho_{ij}\right)\leq 0 \quad (r=1,2,\ldots,m), \quad \text{in } V, \quad \forall\tau\geq 0, \tag{2.25b}$$

be solved for a fixed separation time t^{*}. The maximum value of ξ, $\xi^{*}\left(t^{*}\right)$, determined by solving the problem (2.25), specifies the interval of the load amplifier, $0 \leq \xi \leq \xi^{*}$, for which the fixed t^{*} is a separation time, and hence the structure shakes down. In particular the meaning of ξ^{*} can be stated as follow:

- for any $\xi < \xi^{*}\left(t^{*}\right)$, the structure shakes down and its minimum adaptation time is not greater than t^{*};

- for any $\xi > \xi^{*}\left(t^{*}\right)$, the structure does not shake down and its minimum adaptation time is greater than t^{*};

- for any $\xi = \xi^* (t^*)$, the structure shakes down and its minimum adaptation time is equal to t^*.

The optimal value of $\xi^* (t^*)$, which will be called "safety factor for fixed minimum adaptation time" in the following, turns out to be a non-decreasing function of t^*, in fact increasing t^* is equivalent to reducing the number of constraints in the problem (2.25).

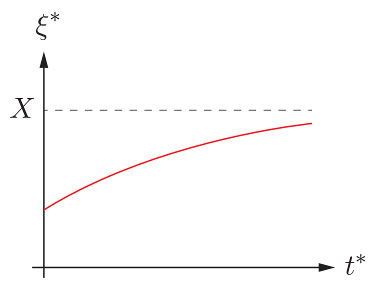

(a) Asymptotic case, non-periodic loading;

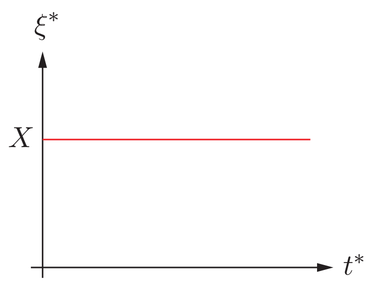

(b) Costant case, periodic loading;

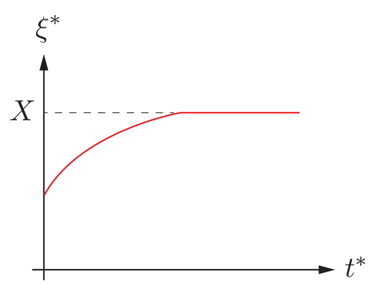

(c) Intermediate case, non-periodic loading followed by a periodic one;

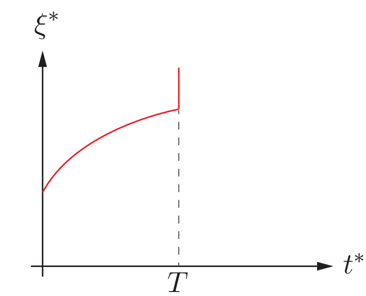

(d) Unbounded case, loading of limited duration;

Figure 2.2: Typical shapes of the curve $\xi = \xi^* (t^*)$ representing the shakedown safety factor for fixed separation time.

Typical shapes of the function $\xi = \xi^* (t^*)$ are shown in Figure 2.2. When the forcing function is a non-periodic one, which becomes less heavy as the time elapses, the function $\xi^*(t^*)$ increases monotonically and it reaches a maximum, X, for $t^* \to \infty$, as shown in Figure 2.2a. In Figure 2.2b, $\xi^*(t^*)$ is a constant. This important case corresponds to a periodic loading, assuming that the backward truncated elastic stress response $\bar{\sigma}_{ij}^E(t^* + \tau)$ is the steady-state response. When the loading history becomes periodic after some time has elapsed, the function $\xi^*(t^*)$ increases first and then remains constant. This case, as shown in Figure 2.2c, is an intermediate case of the two ones above. Finally, in Figure 2.2d, $\xi^*(t^*)$ exists only for $0 \leq t \leq T$, while $\xi^* \to \infty$ when $t^* \to T$. This case is relevant to a forcing function that act for a finite interval and it is called unbounded case.

It is now possible to define the "shakedown safety factor" of the structure subjected to the given loading history as the maximum value, X, of the multiplier ξ such that for any $\xi < X$ there exists some finite t^* for which the problem (2.25) has solutions. Since $\xi^*(t^*)$ is, for every finite t^*, the maximum value of ξ for which the problem (2.25) has solutions and since $\xi^*(t^*)$ is a non-decreasing function, the shakedown safety factor for restricted dynamic shakedown can be found as follow:

$$X = \lim_{t^* \to \infty} \xi^*(t^*) = \max_{(t^*)} \xi^*(t^*). \tag{2.26}$$

It is noteworthy, that a dual problem can be set in which one looks for the minimum adaptation time for a fixed load multiplier. In the author's opinion such a problem has no practical interest because it can be simply substituted by a real dynamic elastic plastic analysis.

2.2.2 The unrestricted dynamic shakedown

In real applications, all the load histories are known only for finite time intervals, and infinite duration load histories (e.g. periodic loading) are just extrapolations of finite duration. To respond to this necessity, a theoretical development of dynamic shakedown theory was given by Polizzotto [75] who treated the unrestricted shakedown theory, following an interesting idea proposed by Ceradini [19] in his first paper devoted the dynamic shakedown.

Polizzotto [75] noted that the loading history of limited duration (called excitations) had to be introduced in the loading scheme, and that they should to be repeated any number of times. In this way, he could built a dynamic shakedown theory consistent with the classical one.

In fact, as pointed out by Ceradini [19], when the infinite load history is allowed to be any sequence of excitations, belonging to a set of excitations, Ω, with indefinite intervals of zero-load between two subsequent excitations in which the structure can be consider motionless thanks to damping, the dynamic shakedown condition is simplified in the sense that $t^* = 0$. Furthermore the fictitious free vibration stress history $\bar{\sigma}^F$ can be neglected and the fictitious stress history $\bar{\sigma}^E$ is now associated with the same initial condition of the given loadings. In the following this sequence of excitations will be called "indefinite load history".

With this premises Polizzotto [75] established the "unrestricted" dynamic shakedown theory consistent with the classical one. He build a loading scheme that is a straight-forward generalization of that used in the quasi-static shakedown replacing the static load by the excitation and the static load domain by the excitation domain. Any sequence of excitations within this domain is permitted and every two subsequent excitations being separated by a zero-load period of arbitrary lengths. In this way, the link between the classical and the dynamic shakedown theory is established. It is worth noting that the unrestricted dynamic shakedown theory has been applied to many themes of structural engineering (see e.g. [10, 15, 16]).

In fact, if the duration of all excitations tends to become infinitely small, the excitations, considered as a periodic actions each with an infinitely large frequency and a null period, tend to become static load and, therefore the above load scheme is transformed into a static one.

Let now refer to the elastic perfectly plastic solid body, already defined at the beginning of the section (2.1), and, for more clarity, let consider the forces acting upon the structure and the generic stress response with a compact notation, so that:

$$\boldsymbol{P} = \{F_i, T_i, \vartheta_{ij}, U_i\}, \tag{2.27}$$

$$\boldsymbol{\sigma} = \{\sigma_{ij}\}. \tag{2.28}$$

Let define Π a set of finite dynamic excitations each of which is represented by a vectorial function $\boldsymbol{P} = \boldsymbol{P}(\tau)$, where τ is the time variable, $0 \leq \tau \leq t_f$, and t_f the final instant of the excitation. By hypothesis, all the excitations have the same length. This condition, for instance, can be easily met by the addition of a zero-load queues to the shorter excitation.

Without loss of generality, one can assume that Π is a bounded region of the multidimensional space that can be represented as a simplex of n vertices. These vertices represent the "basic excitations", that is a discrete set of assigned excitations (Figure 2.3), denoted as:

$$\boldsymbol{P}_k = \boldsymbol{P}_k(\tau), \quad k = 1, 2, \ldots, n, \quad 0 \leq \tau \leq t_f. \tag{2.29}$$

Thus the typical excitation $\boldsymbol{P}(\tau)$ as belonging to the convex domain Π can be represented as a linear convex combination of the basic excitations $\boldsymbol{P}_k(\tau)$, that is

$$\boldsymbol{P}(\tau) = \sum_{k=1}^{n} \mu_k \boldsymbol{P}_k(\tau) \tag{2.30}$$

where the coefficients μ_k are required to satisfy the admissibility conditions, that are:

$$\mu_k \geq 0 \quad \text{for } k = 1, 2, \ldots, n, \tag{2.31a}$$

$$\sum_{k=1}^{n} \mu_k = 1. \tag{2.31b}$$

An admissible loading history (ALH), $\hat{P}(t)$, being $t \geq 0$ the general time variable, can be constructed to have the shape of a sequence of admissible excitations. The analytic representation of an ALH can be given in the following form:

$$\hat{\boldsymbol{P}}(t) = \sum_{k=1}^{n} \mu_k^{(p)} \boldsymbol{P}_k(q) + \boldsymbol{P}^0 \tag{2.32}$$

where $\boldsymbol{P}^0$ is a fixed (permanent) load and where both p and q are function of t:

$$p = p(t) = 1 + \mathrm{Int}\,(t/t_f) \tag{2.33a}$$

$$q = q(t) = t - t_f\,\mathrm{Int}\,(t/t_f) \tag{2.33b}$$

In particular, p is the excitation ordering index while q is the partial time variable. Here, the function $\mathrm{Int}\,(x)$ gives the maximum integer not greater than x. With this representation the time axis is subdivided into intervals of equal length t_f ordered sequentially according to the integer values given by the function $p(t)$. It is worth noting that the coefficients $\mu_k^{(p)}$ of equation (2.32) must satisfy the admissibility conditions (2.31) for every p value.

Varying the coefficients $\mu_k^{(p)}$ in all admissible ways, all the potentially active load histories are then obtained. A sketch of such dynamic load model with zero permanent load is shown in Figure 2.4. It is worth noting that in this figure the zero-load periods have been disregarded.

Such a load scheme has the possibility for every admissible excitations to be unlimitedly repeated. As a consequence the condition for (unrestricted) dynamic shakedown identify with the classical quasi-static ones, that are the Bleich-Melan theorem (1.2.1) and the Koiter-Neal-Symond theorem (1.2.2), but with the difference that in the present context a fictitious dynamic elastic stress response is involved.

In order to enunciate the unrestricted dynamic shakedown theorems, let consider just the basic load conditions instead of all the admissible ones.

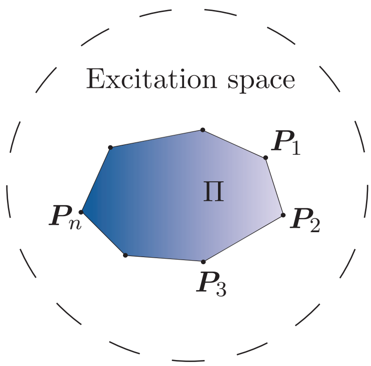

Figure 2.3: Sketch of the excitation domain Π whose vertices are the basic excitations $\boldsymbol{P}_k(\tau)$.

The unrestricted dynamic shakedown theorem of static type, in its form suitable to the present context, consider the fictitious dynamic elastic stress response to the basic excitations, $\bar{\boldsymbol{\sigma}}_k^E$, the elastic response to the permanent load, $\boldsymbol{\sigma}^0$, together with a time-independent self stress field $\boldsymbol{\rho}$ (expressed here in a compact notation). It can be phrased as follow:

Theorem 2.2.3. *for an elastic perfectly plastic structure subjected to an admissible load history belonging to a given excitation domain* Π_k*, and to fixed load, the unrestricted dynamic shakedown occurs if, and only if, there exist a time independent self-stress field,* $\boldsymbol{\rho}$*, such that, on superposing it to the basic*

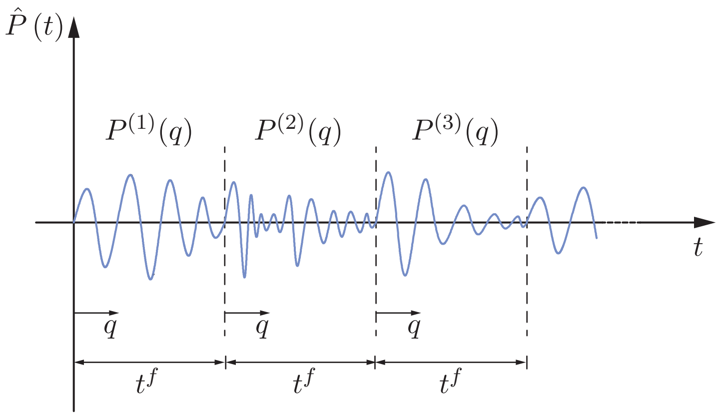

Figure 2.4: Sketch of an admissible load history.

elastic stress responses, $\bar{\boldsymbol{\sigma}}_k^E + \boldsymbol{\sigma}^0$*, the resulting stresses nowhere violate the plastic yielding condition:*

$$\varphi\left(\bar{\boldsymbol{\sigma}}_k^E(\tau) + \boldsymbol{\sigma}^0 + \boldsymbol{\rho}\right) < 0 \quad in\ V, \quad 0 \leq \tau \leq t_f. \tag{2.34}$$

being, $k = 1, 2, \ldots, n$.

The unrestricted dynamic shakedown theorem of kinematic type, in its form suitable to the present context, beside the fictitious dynamic elastic stress response to the basic excitations, $\bar{\boldsymbol{\sigma}}_k^E + \boldsymbol{\sigma}^0$, considers plastic accumulation mechanism (PAM), that is a set of plastic strain rate fields, $\dot{\boldsymbol{p}}_k(\tau)$, $0 \leq \tau \leq t_f$, $k = 1, 2, \ldots, n$, such that the corresponding ratchet strain fields $\Delta\boldsymbol{p}$, given by:

$$\Delta\boldsymbol{p} = \sum_{k=1}^{n} \int_0^{t_f} \dot{\boldsymbol{p}}_k(\tau)\, d\tau \quad \text{in } V \tag{2.35}$$

be a compatible field with zero displacement on S_2. It can be phrased as follow:

Theorem 2.2.4. *for an elastic perfectly plastic structure subjected to an admissible load history belonging to a given excitation domain* Π_k *and to fixed load, the unrestricted dynamic shakedown occurs if, and only if, the energy inequality*

$$\sum_{k=1}^{n} \int_0^{t_f} \int_V \left[D\left(\dot{\boldsymbol{p}}_k\right) - \left(\bar{\boldsymbol{\sigma}}_k^E + \boldsymbol{\sigma}^0\right) : \dot{\boldsymbol{p}}_k\right] dV\, d\tau > 0 \tag{2.36}$$

is satisfied for all PAMs, being D the plastic dissipation function.

Let all the admissible excitations be defined within a scalar multiplier $\xi > 0$, that is

$$\boldsymbol{P}(\tau) = \xi \tilde{\boldsymbol{P}}(\tau), \tag{2.37}$$

where $\tilde{\boldsymbol{P}}(\tau)$ denotes the excitations belonging to a reference domain $\tilde{\Pi}$. In this way, even the basic excitations, $\tilde{\boldsymbol{P}}_k(\tau)$, of $\tilde{\Pi}$ can be expressed in the following form:

$$\boldsymbol{P}_k(\tau) = \xi \tilde{\boldsymbol{P}}_k(\tau). \tag{2.38}$$

The unrestricted dynamic shakedown safety factor ξ^* (or limit load multiplier) is that particular value of ξ, such that the dynamic shakedown occurs for all $\xi \leq \xi^*$, while does not for all $\xi > \xi^*$.

Two alternative approach for the determination of ξ^* depending on the referenced theorem are available. The first approach, called static approach because it is based on the unrestricted dynamic shakedown theorem of static type (2.2.3), permit to evaluate ξ^* as the maximum value of ξ for which the condition (2.34) written with $\bar{\boldsymbol{\sigma}}_k^E(\tau) = \xi \tilde{\boldsymbol{\sigma}}_k^E(\tau)$ can be satisfied, namely

$$\xi^* = \max_{\xi,\,\boldsymbol{\rho}} \xi \tag{2.39a}$$

subjected to:

$$\varphi_r\left(\xi \tilde{\boldsymbol{\sigma}}_k^E(\tau) + \boldsymbol{\sigma}^0 + \boldsymbol{\rho}\right) \leq 0 \quad \text{in } V, \quad 0 \leq \tau \leq t_f, \tag{2.39b}$$

and to the conditions of self-equilibrium on $\boldsymbol{\rho}$.

The kinematic approach to unrestricted dynamic shakedown, according to the theorem (2.2.4), is obtainable writing $\bar{\boldsymbol{\sigma}}_k^E(\tau) = \xi \tilde{\boldsymbol{\sigma}}_k^E(\tau)$, and looking for that PAM such as minimize the ratio between the total plastic dissipation reduced by the total work of fixed load, and the total external work done by the excitations $\tilde{\boldsymbol{P}}_k$, namely

$$\xi^* = \min_{\dot{\boldsymbol{p}}_k} \sum_{k=1}^{n} \int_0^{t_f} \int_V D\left(\dot{\boldsymbol{p}}_k\right)\, dV\, d\tau - \int_V \boldsymbol{\sigma}^0 : \Delta \boldsymbol{p}\, dV \tag{2.40a}$$

subjected to:

$$\sum_{k=1}^{n} \int_0^{t_f} \int_V \tilde{\boldsymbol{\sigma}}_k^E : \dot{\boldsymbol{p}}_k\, dV\, d\tau, \tag{2.40b}$$

and to the compatibility conditions on

$$\Delta \boldsymbol{p} = \sum_{k=1}^{n} \int_{0}^{t_f} \dot{\boldsymbol{p}}_k \, d\tau \tag{2.41}$$

2.3 A probabilistic assessment of dynamic shakedown

As already mentioned at the beginning of the section (2.2.2), an interesting idea about the practical application of dynamic shakedown theory is present in the first paper of Ceradini [19] dedicated to dynamic shakedown. In that paper, the case of loading scheme made of excitations paused by arbitrary interval in which the structure can be considered motionless due to to internal damping is reported.

For such load, called in this thesis arbitrary load history, when it is allowed to be any sequence of excitations belonging to a set of excitations, Ω, with arbitrary time intervals of zero-load between two subsequent excitations, the dynamic shakedown condition of the Ceradini's theorem (2.1.2) is simplified in the sense that $t^* = 0$. Furthermore, for an arbitrary load history, the intervals of no-motion make neglegible the free vibration stress history $\bar{\sigma}^F$, so the fictitious stress history $\bar{\sigma}^E$ can be associated with the same initial condition of the given loading.

The following theorem, in its form suitable to the present context can be stated:

Theorem 2.3.1. *a necessary and sufficient condition for an elastic perfectly plastic structure to dynamically shakes down when subjected to an arbitrary load history, and to fixed load, is that there exist a time independent self-stress field and a fictitious elastic stress response, such that on superposing these stresses, the resulting stress nowhere violate the yielding condition during every excitation of the arbitrary load history.*

The latter theorem is a straightforward extension of the Melan's theorem (1.2.1) to dynamics, the only difference is that inertia and damping forces are involved in the determination of the stress response.

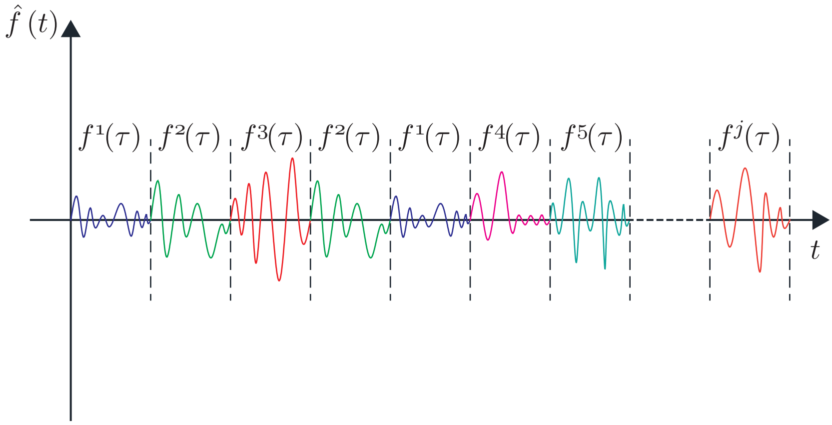

Figure 2.5: Sketch of an arbitrary excitation history $\hat{f}(t)$.

Let consider an arbitrary excitation history, $\hat{f}(t)$, made by a sequence of j excitations, $f^i(\tau)$, $i = 1, 2, \ldots, j$, paused by an arbitrary interval of no motion. Every single excitation, $f^i(\tau)$, is allowed to be repeated any number of time and by hypothesis all the excitations have the same length, t^f. An example of $\hat{f}(t)$ is sketched in Figure 2.5.

Let $\bar{\sigma}^i(\tau)$, $i = 1, 2, \ldots, j$, the fictitious elastic response to the i^{th} excitation $f^i(\tau)$. On the basis of the theorem (2.3.1), and considering an elastic perfectly plastic structure subjected to the arbitrary load history, $\hat{f}(t)$, it is possible to find the related shakedown safety factor, solving the following problem:

$$\xi^* = \max_{\xi,\,\boldsymbol{\rho}} \xi \tag{2.42a}$$

subjected to:

$$\varphi\left(\xi\boldsymbol{\sigma}^i(\tau) + \boldsymbol{\sigma}^0 + \boldsymbol{\rho}\right) \leq 0 \quad \text{in } V, \quad 0 \leq \tau \leq t_f, \quad i = 1, 2, \ldots, j, \tag{2.42b}$$

and to the conditions of self-equilibrium on $\boldsymbol{\rho}$, being φ the yield functions, and $\boldsymbol{\sigma}^0$ the fictitious elastic response to fixed loads.

With the aim to define a probabilistic shakedown safety factor for an elastic perfectly plastic structure dynamically excited by a stochastic load, let consider for simplicity the following normal stochastic process with assigned power

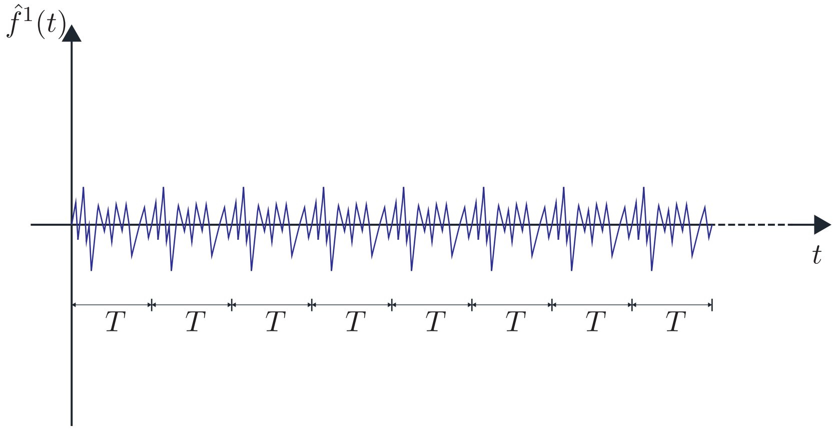

Figure 2.6: Sketch of a normal stochastic process for a single realization of the random variable.

spectral density $S(\omega)$:

$$f(t) = \sum_{i=1}^{l} C_i \cos(\omega_i t + \Phi_i) \tag{2.43}$$

where $C_i = \sqrt{2S(\omega_i)\Delta\omega}$ is the maximum power for any circular frequency ω_i, $\Delta\omega = \omega_c/l$ is the sample frequency (being ω_c the cut-off frequency and l a suitable number of cosine waves) and Φ_i is a random phase angle uniformly distributed in $0 \div 2\pi$.

For a single realization of the random variable Φ_i, one obtains a forcing function $\hat{f}^1(t)$, as sketched in Figure 2.6, whose period is $T = 2\pi/\Delta\omega$. The part of the function inside the period T will be called in the following "stationary segment".

In real applications, one can consider the stationary segments as well as isolated excitations paused by intervals of no motion. For this reason, the forcing function, $\hat{f}^1(t)$, constituted by an infinite repetition of the stationary segment, $f^1(\tau)$, $0 \leq \tau \leq T$, can be viewed as an arbitrary excitation history, as sketched in Figure 2.7. In the last figure, for more clarity, the derived arbitrary excitation history has the same name of the original one. It is quite obvious that the set Ω related to $\hat{f}^1(t)$ is constituted by a single excitation that is $f^1(\tau)$,

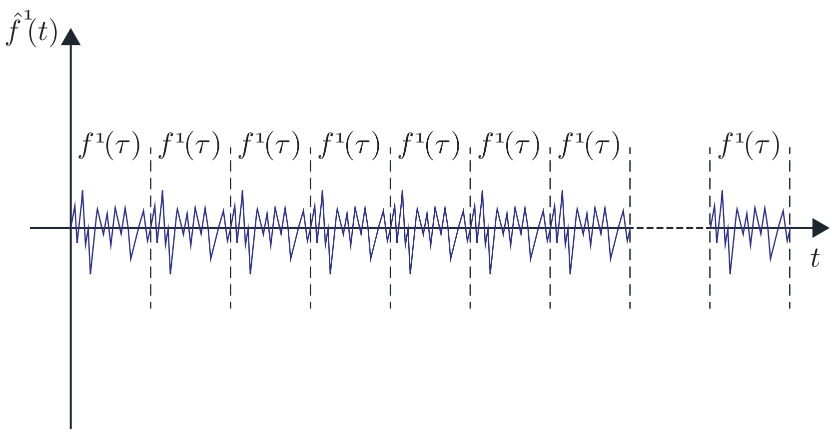

Figure 2.7: Sketch of an arbitrary excitation history derived from a single realization of the random variable of the normal stochastic process.

$0 \leq \tau \leq T$.

For an elastic perfectly plastic structure dynamically excited by $\hat{f}^1(t)$, once determined the stress response $\boldsymbol{\sigma}^1(\tau)$ of the structure to a stationary segment of the non-amplified load $f_1(t)$ it's possible to find throughout the solution of the problem (2.42) the shakedown safety factor, or shakedown multiplier, ξ^1. In particular, if $\xi^1 \geq 1$ the structure will shake down, if $\xi^1 < 1$ it will not shake down.

Let consider another realization of the random variable for which one obtains a sample $\hat{f}^2(t)$ or its equivalent representation, as sketched in Figure 2.8. Also in this case, it's possible to know the shakedown safety factor ξ^2.

Let now shuffle the stationary segments of the first $\hat{f}^1(t)$ and the second $\hat{f}^2(t)$ arbitrary short excitation history in a new one $\hat{f}^{1,2}(t)$ (Figure 2.9) for which is possible to find a shakedown multiplier $\xi^{1,2}$. Evidently, the shakedown multiplier $\xi^{1,2}$ will coincide with the lower multiplier between ξ^1 and ξ^2. For instance, if $\xi^1 < \xi^2$ than $\xi^{1,2} \equiv \xi^1$ because the plastic demand induced on the structure by a stationary segment of $\hat{f}^1(t)$ is greater than that induced by any stationary segments of $\hat{f}^2(t)$. Obviously this operation may be repeated countless time due to the possible infinite realizations.

This means that every time one simulates a sample of the type $f^1(t)$ and

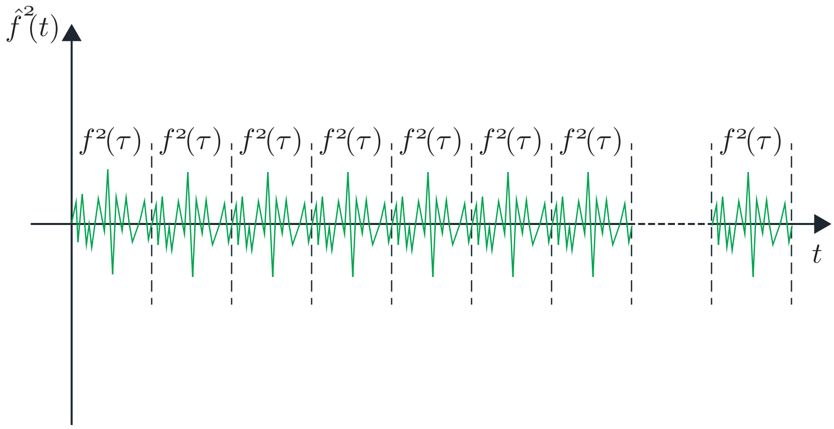

Figure 2.8: Sketch of an arbitrary excitation history derived from a second realization of the random variable of the normal stochastic process.

finds the corresponding multiplier ξ^1, actually (in the context of dynamic shakedown), is watching in a time window of an arbitrary short excitation history for which the observed event is that with the greater plastic demand and also the one with the lower shakedown multiplier.

The concept of "arbitrary excitation history" guarantees the validity of founded the shakedown multiplier that, as known, has no sense for a single load history with finite time duration (see e.g. [78, 79]). Moreover, this representation is a realistic one to model wind loads on buildings, in fact, the wind blows for finite intervals paused by period for which the structure can be considered motionless. It should be noted that the concept of dynamic excitation domain [79] has been here neglected because a probabilistic assessment of dynamic shakedown multiplier can't be established when loads belong to a convex domain of excitations as explained by De Martino and Di Paola [32].

The concept of structural reliability is based on the definition of a limit state function that separates the safe region from the unsafe one for a structure standing in an uncertain environment.

In this section, the dynamic shakedown has been chosen as limit state, in other words, it's considered as safe that structural behavior in which the

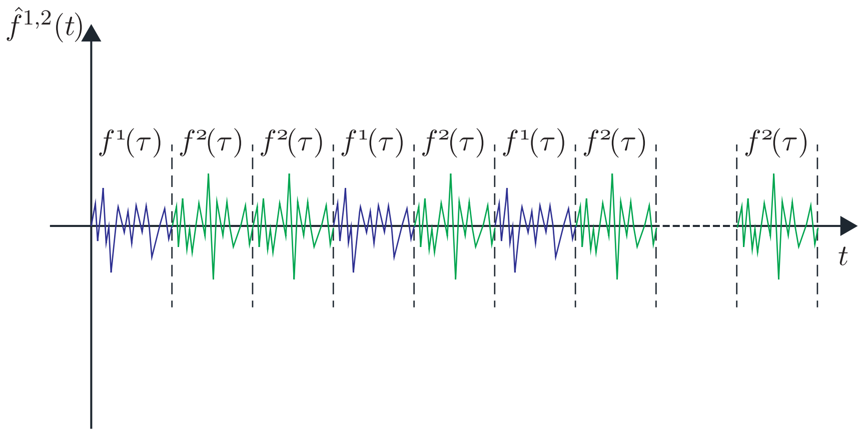

Figure 2.9: Shuffled arbitrary excitation history.

structure is able to react in a purely elastic manner after that some plastic deformations have been produced. If the structure exceeds this limit, it could suffer very dangerous phenomena as the incremental collapse (excessive accumulation of plastic strain) or the alternating plasticity collapse (production of plastic strain in the cycle with the possibility of failure for fatigue) or it may even instantaneously collapse.

To better understand the failure region, it can be useful to show the different structural behaviors that a structure made of elastic perfectly plastic material can have in the steady-state response through the Bree-like diagram. As one can see in Figure 2.10, indicating with ξ and ξ^0 the dynamic load multiplier and the fixed load multiplier respectively, it is possible to distinguish five different structural behaviors: purely elastic (E), elastic shakedown (S), low cycle fatigue or plastic shakedown(F), incremental collapse or ratcheting (R) and instantaneous collapse (I). The presence of fixed load or quasi-static one does not affect the discussion so far produced.

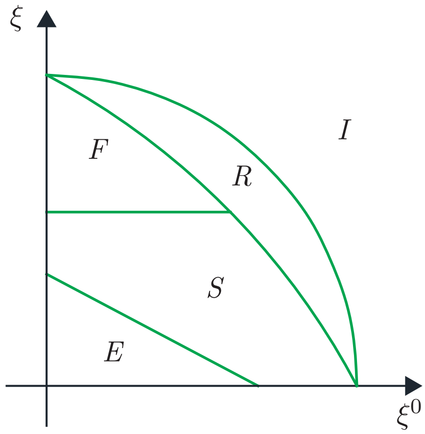

Figure 2.10: Typical Bree-like diagram.

Once defined the failure region, let $\boldsymbol{\theta} \in \mathbb{R}^n$ a vector that contains all the uncertain parameters regarding both the structural behavior and the load conditions. Let $q : \mathbb{R}^n \mapsto [0, \infty)$ be a prescribed probability density function (PDF) representing the values that the set of uncertain parameters $\boldsymbol{\theta} = [\theta_1, \theta_2, \cdots, \theta_n]$ can assume. Without loss of generality this parameters can be assumed as independent so that $q(\boldsymbol{\theta}) = \prod_{j=1}^{n} q_j(\theta_j)$, where $q_j : \mathbb{R}^n \mapsto [0, \infty)$ is the one-dimensional PDF for each θ_j. The failure probability can be formulated in a generic form as

$$P(F) = \int \mathbb{I}_F(\boldsymbol{\theta})\, q(\boldsymbol{\theta})\, d\boldsymbol{\theta} \tag{2.44}$$

where $F \subset \mathbb{R}^n$ is the failure region specified as the exceedance of an uncertain load multiplier ξ over its shakedown value ξ^* so that $F = \{\boldsymbol{\theta} : \xi(\boldsymbol{\theta}) > \xi^*(\boldsymbol{\theta})\}$, $\mathbb{I}_F : \mathbb{R}^n \mapsto \{0, 1\}$ is an indicator function that is $\mathbb{I}_F(\boldsymbol{\theta}) = 1$ when $\boldsymbol{\theta} \in F$ and $\mathbb{I}_F(\boldsymbol{\theta}) = 0$ otherwise. Due to the large number of uncertainties involved, this problem is very complex to solve and usually the solution is reached with methods based on simulation. These tools are robust and they are able to provide the probability of failure of an uncertain structure with stochastic load conditions.

Chapter 3

Optimal design of structures

This chapter is devoted to the formulations of the optimal design of elastic perfectly plastic structures subjected to dynamic loads.

As known, the two fundamental problems of structural mechanics are the analysis and the design problem. In the first problem, the structure and the applied loads are fully described as well as the safety criterion that has to be satisfied. In the second, the geometry of the structure or other parameters are free variables, and consequently, only the loads scheme is fully known. Generally speaking, also in this case, the material characteristics can be considered known as well as the safety criterion to respect. To solve an analysis problem, one has to determinate the complete response of the structure to the applied loads, and then, to verify that this response satisfy (locally and/or globally) some chosen safety criteria. Solving a structural design problem means the reaching, among all the feasible designs, of the one which minimizes or maximizes a chosen quantity (e.g. the cost, the volume, the stiffness etc.) according to some required conditions for the structure.

To formulate an optimal design problem, one has to make three different decisions each of which assumes a crucial role in the overall process:

1. Selection and definition of the structural model;

2. Choice and definition of the eligibility criterion for the optimization problem to solve;

3. Choice of the solution procedure.

The first decision concerns the choice and the related formalization of the structural model, namely, the choice of the structural type, of the loads model, and, of the constitutive material behavior.

The second operation is related to the definition of the optimization problem to solve together with the constrains that the optimal design has to respect. This decision making is the most important among the above described phases: obviously, a wrong formulation can led to bad results and, in addition it can require prohibitive computational costs. For the mathematical formalization of an optimal design problem, three basic elements have to be introduced:

a) the design variables;

b) the objective function;

c) the constraint equations.

In an optimization problem, it is usually required to modify the structural geometry through the variation, within a prescribed range, of suitable design parameters which completely describe the structure. These parameters are referred to as design variables and they can define the geometry, the topology or the shape of a structural system. Furthermore, the design variables can be distinguished in continuous or discrete variables. The former can assume any value within a continuous range of variation while the latter employ values belonging to a list of allowable parameters. The computational effort related to the solution of an optimization problem formulated with discrete variables is more difficult from a computational point of view than a problem with continuous variable. Nevertheless, recent heuristic methods permit to solve discrete variable problems saving computational time reposing on the powerful of modern computers.

The objective function is a function (or functional) of the design variables. The different values that the objective function can assume, permit to compare different designs and to choose the best one in accordance with the particular adopted criterion. In structural optimization, the minimum volume, being proportional to the cost of the structure, is the most frequently adopted objective function.

Often it is also necessary to define more than a single objective function. For this type of problems the optimum is no longer represented by a single value, but by the so-called “Pareto’s optimum”. There are some techniques that allow to bring back a multi-objective problem into a single-objective one. One of these consists in the definition of a composite objective function, i.e. a function that is a linear combination of the other according to suitable weight coefficients. Another technique is to choose a single objective function among the others and turning the other functions into constraints of the problem.

Another key element in the mathematical formulation of the optimal design problem is represented by so-called constraint equations. A design is defined feasible if it satisfies certain conditions regarding local and/or global behavior of the structure and, if necessary, specific limits on the design variables. The latter are, in general, represented by technological constraints which ensure no execution difficulty and, above all, that no theoretical hypotheses are violated. However, the former are more important because they represent the safety criterion that the design has to respect.

The typical optimal design formulation can be expressed as follow:

$$f^* = \min_{\boldsymbol{x}} f(\boldsymbol{x}) \tag{3.1a}$$

subjected to:

$$g_j(\boldsymbol{x}) \leq 0 \qquad j = 1, 2, \ldots, n_g \tag{3.1b}$$

$$h_k(\boldsymbol{x}) = 0 \qquad k = 1, 2, \ldots, n_h \tag{3.1c}$$

where $f(x)$ is the objective function to minimize, $\boldsymbol{x}$ is the vector of design variables, while g_j and h_k represent respectively the inequality and the equality constraints.

As already said, the last and decisive decision is the choice of procedures for the numerical solution of the problem. The optimal design problem is indeed a constrained minimization problem. The search for the optimal solution has to be done among all feasible designs, i.e. among those that satisfy all the constraints of the problem. Over the past decades, many algorithms to solve optimization problems have been proposed, and many of these are included as subroutine of the most common numerical software.

In the present thesis reference has been made to the so-called “sizing optimization problem with stress constraints” in which the minim volume of a frame structure has been searched treating as variables the thicknesses of the cross sections of all the beam elements. The structure has been considered subjected to multiple loads combination and thus different stress constrains have been imposed to the optimal design formulations.

3.1 Optimal design of frames under quasi-static cyclic loads

In this section, a first group of formulations are proposed idealizing the seismic loads on the structure as a perfect cyclic quasi-static load and taking into account inertia and damping effects in an approximate way trough the use of the response spectrum method. Furthermore, other formulations taking into account dangerous phenomena such as buckling, P-Δ effects are exposed.

3.1.1 General formulation

Let consider a (discrete) elastic perfectly plastic plane frame, constituted by n_b Euler-Bernoulli beam elements and n_n free nodes in the range of "small" displacements and deformations, subjected to an assigned loading history variable in time quasi-statically.

The v^{th} element geometry is fully described by the s components of the vector $\boldsymbol{t}_v$ so that $\boldsymbol{t} = \left[\boldsymbol{t}_1^T, \boldsymbol{t}_2^T, \ldots, \boldsymbol{t}_{n_b}^T\right]^T$ represents the $n_b \times s$ super-vector collecting all the design variables. It is worth noting that here and in what follows, the apex $(\cdot)^T$ means transpose of the relevant quantity.

Let introduce the n_f-vectors $\boldsymbol{u}$ and $\bar{\boldsymbol{F}}$ collecting the nodes' displacements and the loads acting upon them, the n_d-vectors $\boldsymbol{q}$ and $\boldsymbol{Q}$ grouping the generalized strains and stresses respectively, being $n_f = 3 \cdot n_n$ the total number of degrees of freedom of the free nodes and $n_d = 6 \cdot n_b$ the number of total stresses and strains at the end of the beams.

Geometric compatibility between strains and nodes' displacements can be imposed:

$$\boldsymbol{q} = \boldsymbol{C}\boldsymbol{u} \tag{3.2}$$

being $\boldsymbol{C}$ a compatibility matrix depending on the geometry only.

Let assume that for each element plastic deformations can occur just at plastic nodes, which are conceived as sources from which plastic strains spread within the element volume according to fixed shape function (see e.g. [28, 29]).

Generally plastic nodes and element nodes are not coincident so the vector $\boldsymbol{q}$ can be expressed as:

$$\boldsymbol{q} = \boldsymbol{e} + \boldsymbol{G}_p \boldsymbol{p} \tag{3.3}$$

being $\boldsymbol{e}$ the elastic strain vector at element nodes, $\boldsymbol{p}$ the plastic strain vector at plastic nodes and $\boldsymbol{G}_p$ a matrix which applied to the plastic strains provides element nodal strains.

The elasticity equations read:

$$\boldsymbol{Q} = \boldsymbol{D}_e \boldsymbol{e} + \boldsymbol{Q}^* \tag{3.4}$$

where $\boldsymbol{D}_e$ is the block diagonal matrix containing all the elastic stiffness matrices of the n_b beam elements constituting the structure and $\boldsymbol{Q}^*$ is the vector collecting the perfectly clamped element generalized stresses.

Equilibrium at element nodes is expressed by n_f equations:

$$\boldsymbol{C}^T \boldsymbol{Q} = \bar{\boldsymbol{F}} \tag{3.5}$$

where $\boldsymbol{C}^T$ is the equilibrium matrix.

Using eqs. (3.2) to (3.5) and after some simple manipulations, one can obtains the following equilibrium equation in terms of displacements and plastic strains:

$$\boldsymbol{K}\boldsymbol{u} - \boldsymbol{B}\boldsymbol{p} = \boldsymbol{F} \tag{3.6}$$

in which $\boldsymbol{K} = \boldsymbol{C}^T \boldsymbol{D}_e \boldsymbol{C}$ is the structure stiffness matrix, $\boldsymbol{B} = \boldsymbol{C}^T \boldsymbol{D}_e \boldsymbol{G}_p$ is the so-called pseudo-force matrix and $\boldsymbol{F} = \bar{\boldsymbol{F}} + \boldsymbol{F}^*$ is the equivalent nodal load vector being $\boldsymbol{F}^* = -\boldsymbol{C}^T \boldsymbol{Q}^*$ the vector collecting the loads directly acting upon the elements. Furthermore the generalized stress response evaluated at the plastic nodes $\boldsymbol{P} = \boldsymbol{G}_p^T \boldsymbol{Q}$ is given by:

$$\boldsymbol{P} = \boldsymbol{B}^T \boldsymbol{u} - \boldsymbol{D}\boldsymbol{p} + \boldsymbol{P}^* \tag{3.7}$$

being $\boldsymbol{D} = \boldsymbol{G}_p^T \boldsymbol{D}_e \boldsymbol{G}_p$ the block diagonal stiffness matrix related to the plastic nodes and $\boldsymbol{P}^* = \boldsymbol{G}_p^T \boldsymbol{Q}^*$ the analogous of $\boldsymbol{P}$ but just due to $\boldsymbol{F}^*$.

Internal stresses at each cross section of the structure cannot lie outside of the yield surface, hence the vector $\boldsymbol{P}$ has to respect the following inequality:

$$\boldsymbol{\varphi} = \boldsymbol{N}^T \boldsymbol{P} - \boldsymbol{R} \leq \boldsymbol{0} \tag{3.8}$$

where $\boldsymbol{\varphi}$ is the piece-wise linearized yield vector, $\boldsymbol{N}$ is block diagonal matrix of unit external normal to the piece-wise linear convex yield surface and $\boldsymbol{R}$ is the plastic resistance vector. When at least one of inequalities (3.8) holds as equality, plastic strain can occur according to the following plastic flow rules:

$$\dot{\boldsymbol{p}} = \boldsymbol{N}\dot{\boldsymbol{\lambda}},\ \dot{\boldsymbol{\lambda}} \geq \boldsymbol{0},\ \boldsymbol{\varphi}^T\dot{\boldsymbol{\lambda}} = \boldsymbol{0},\ \dot{\boldsymbol{\varphi}}^T\dot{\boldsymbol{\lambda}} = \boldsymbol{0} \tag{3.9}$$

in which $\boldsymbol{\lambda}$ represent the vector of plastic multipliers and the over dot means time derivative of the relevant quantity. It is worth noting that time is not the physical time, but just some parameter specifying the loading sequence.

For an assigned loading history, eqs. (3.6) to (3.9) govern the analysis problem of elastic perfectly plastic plane frames. This problem is usually solved by means of a step-by-step procedure (see e.g. [45]).

Very often structures are subjected to the contemporaneous action of fixed and cyclic loads. Therefore, let denote with $\boldsymbol{F}_0$ the reference fixed mechanical load and with $\boldsymbol{F}_c$ the reference mechanical and/or kinematical cyclic load varying in a quasi-static manner. Let assume that the cyclic load identifies with a convex polygonal load path with vertices corresponding to a set of m mutually independent load vectors, say $\boldsymbol{F}_{ci}$, $\forall i \in I(m) \equiv \{1, 2, \ldots, m\}$.

For assigned element geometry vector $\boldsymbol{t}$ and loads, it is possible to know the purely elastic (fictitious) stress response in the following manner:

$$\boldsymbol{u}_0 = \boldsymbol{K}^{-1}\boldsymbol{F}_0, \tag{3.10}$$

$$\boldsymbol{P}_0 = \boldsymbol{B}^T\boldsymbol{u}_0 + \boldsymbol{P}_0^*, \tag{3.11}$$

and

$$\boldsymbol{u}_{ci} = \boldsymbol{K}^{-1}\boldsymbol{F}_{ci} \quad \forall i \in I(m), \tag{3.12}$$

$$\boldsymbol{P}_{ci} = \boldsymbol{B}^T\boldsymbol{u}_{ci} + \boldsymbol{P}_{ci}^* \quad \forall i \in I(m). \tag{3.13}$$

On the basis of the classical shakedown theory (1.2) and of the limit analysis, it is possible to formulate a minimum volume design problem which contemporary satisfy different limit conditions (see e.g. [44, 46, 48]). In particular, referring to different intensity levels of loads, trough the use of some positive scalar parameters $\xi \geq 0$, it is possible to impose to the optimal structure different behaviors, so that the optimal design problem with stress constraints can be formulated as follow:

$$V^* = \min_{\boldsymbol{t},\boldsymbol{\rho},\boldsymbol{\rho}_i} V(\boldsymbol{t}) \tag{3.14a}$$

subjected to:

$$\boldsymbol{\varphi}_e = \boldsymbol{N}^T (\xi_{e1} \boldsymbol{P}_0 + \xi_{e2} \boldsymbol{P}_{ci}) - \boldsymbol{R} \leq \boldsymbol{0}, \tag{3.14b}$$

$$\boldsymbol{\varphi}_{si} = \boldsymbol{N}^T (\xi_{s1} \boldsymbol{P}_0 + \xi_{s2} \boldsymbol{P}_{ci} + \boldsymbol{\rho}) - \boldsymbol{R} \leq \boldsymbol{0} \quad \forall i \in I(m), \tag{3.14c}$$

$$\boldsymbol{A}^T \boldsymbol{\rho} = \boldsymbol{0}, \tag{3.14d}$$

$$\boldsymbol{\varphi}_{li} = \boldsymbol{N}^T (\xi_{l1} \boldsymbol{P}_0 + \xi_{l2} \boldsymbol{P}_{ci} + \boldsymbol{\rho}_i) - \boldsymbol{R} \leq \boldsymbol{0} \quad \forall i \in I(m), \tag{3.14e}$$

$$\boldsymbol{A}^T \boldsymbol{\rho}_i = \boldsymbol{0} \quad \forall i \in I(m). \tag{3.14f}$$

In this problem, equation (3.14a) represents the so-called "objective function" posed in terms of volume V (function of the design variable vector $\boldsymbol{t}$) whose optimal value is V^*.

Further, eqs. (3.14b) to (3.14f) represent the so-called "stress constraints" of the design problem. In particular, equation (3.14b), as one can see, is utilized to impose an elastic behavior to the structure when it is subjected to the amplified loads $\xi_{e1}\boldsymbol{F}_0$ and $\xi_{e2}\boldsymbol{F}_{ci}$, $\forall i \in I(m)$, being ξ_{e1} and ξ_{e2} two suitable chosen positive scalars.

Equation (3.14c) is utilized to imposed the shakedown behavior to the structure when it subjected to the loads $\xi_{s1}\boldsymbol{F}_0$ and $\xi_{s2}\boldsymbol{F}_{ci}$,$\forall i \in I(m)$, being ξ_{s1} and ξ_{s2} two chosen multipliers. In fact, being $\boldsymbol{\rho}$ an arbitrary self-stress vector, equation (3.14c) represents the admissibility condition required by the Melan's theorem. In addition, the mentioned self-stress condition is imposed by equation (3.14d) in which $\boldsymbol{A}^T$ is the equilibrium matrix related to the plastic nodes (see e.g. [46, 48]). In particular, $\boldsymbol{A} = \boldsymbol{C}_p\boldsymbol{C}$ is a compatibility matrix with $\boldsymbol{C}_p$ matrix that when applied to element node displacements provides plastic strains evaluated at strain points ($\boldsymbol{C}_p\boldsymbol{G}_p = \boldsymbol{I} = \boldsymbol{G}_p^T\boldsymbol{C}_p^T$).

As mentioned in Chapter 1, the shakedown analysis is a generalization of the limit one. In fact, when it is possible to find an independent self-stress vector for each admissibility condition related to each basic load condition, the Melan's theorem become the lower bound theorem of limit analysis in which multiple load conditions are considered. This fact is exploited in equation (3.14e) to prevent the instantaneous collapse of the structure when it is subjected to the loads $\xi_{l1}\boldsymbol{F}_0$ and $\xi_{l2}\boldsymbol{F}_{ci}$,$\forall i \in I(m)$, where ξ_{l1} and ξ_{l2} are two chosen parameters. Moreover, in this equation, $\boldsymbol{\rho}_i$, $\forall i \in I(m)$, are a set of independent self-stress vectors constrained to respect the self-stress conditions trough the equation (3.14f).

In problem (3.14) $\boldsymbol{\varphi}_e$, $\boldsymbol{\varphi}_{si}$, $\boldsymbol{\varphi}_{li}$ represent the plastic potential vectors related to the elastic, to the shakedown and to the instantaneous collapse limit respectively. It is worth noting that further constraints can be imposed on the design variables as shown later on this chapter.

3.1.2 Formulation for frame under seismic loads

In this context, the aim of the present subsection is to provide an appropriate formulation of the optimal design problem for structures subjected to earthquakes or strong winds. As reported in many international structural standards, a useful technique to evaluate the seismic response of structures is the so-called "response spectrum" method.

As known, since only a few degrees of freedom are dynamically significant, to know the seismic response of the structure some condensation procedures can be adopted transforming a consistent system into a lumped one (e.g. shear type frame). In order to evaluate the seismic response of the structure let refer to the lumped system just subjected to an horizontal ground acceleration a_g. The frame is modeled as a Multi-Degree-Of-Freedom (MDOF) structure, such that the total number of degrees of freedom is equal to n_f with $n_f < n_n \times 3$ The dynamic equilibrium equations can be written in the following form:

$$\boldsymbol{M}\ddot{\boldsymbol{u}}_f(t) + \boldsymbol{V}\dot{\boldsymbol{u}}_f(t) + \boldsymbol{K}_f\boldsymbol{u}_f(t) = -\boldsymbol{M}\boldsymbol{\tau}a_g(t), \tag{3.15}$$

being τ the $(n_f \times 1)$ influence vector; $\boldsymbol{u}_f$ represents the displacement vector related to the structure dynamic degree of freedom and the following initial conditions $\boldsymbol{u}_f(0) = \mathbf{0}$, $\dot{\boldsymbol{u}}_f(0) = \mathbf{0}$ hold.

In equation (3.15) $\boldsymbol{M}$ and $\boldsymbol{V}$ are the mass and damping matrices (with dimensions $n_f \times n_f$), respectively. In addition $\boldsymbol{K}_f$ is a condensed stiffness matrix of order n_f obtained as:

$$\boldsymbol{K}_f = \boldsymbol{E}^T\boldsymbol{K}\boldsymbol{E}, \tag{3.16}$$

where $\boldsymbol{E}$ is an appropriate condensation and/or reordering matrix. Furthermore, $\boldsymbol{M}$, $\boldsymbol{A}$ and $\boldsymbol{K}_f$ are assumed to be positive definite matrices, $\ddot{\boldsymbol{u}}_f(t)$ and $\dot{\boldsymbol{u}}_f(t)$ are the acceleration and velocity$(n_f \times 1)$ vectors of the system, respectively, and the over dot means time derivative of the relevant quantity.

As it is usual, the dynamic characteristics of the structural behavior are identified in terms of natural frequencies as well as damping coefficients. In this framework, as usual, the following coordinate transformation is adopted:

$$\boldsymbol{u}_f(t) = \boldsymbol{\Phi}\boldsymbol{y}(t), \tag{3.17}$$

being $\boldsymbol{y}(t)$ the modal displacement vector and $\boldsymbol{\Phi}$ the so-called modal matrix of order $(n_f \times n_f)$, normalized with respect to the mass matrix and whose columns are the eigenvectors of the undamped structure, given by the solution to the following eigenproblem:

$$\boldsymbol{K}_f^{-1}\boldsymbol{M}\boldsymbol{\Phi} = \boldsymbol{\Phi}\boldsymbol{\Omega}^{-2}, \tag{3.18a}$$

$$\boldsymbol{\Phi}^T\boldsymbol{M}\boldsymbol{\Phi} = \boldsymbol{I}, \tag{3.18b}$$

$$\boldsymbol{\Phi}^T\boldsymbol{K}_f\boldsymbol{\Phi} = \boldsymbol{\Omega}^2, \tag{3.18c}$$

In equations (3.18), besides the already known symbols, $\boldsymbol{I}$ represents the identity matrix while $\boldsymbol{\Omega}^2$ is a diagonal matrix listing the square of the natural frequencies of the structure.

Once the modal matrix $\boldsymbol{\Phi}$ has been determined, the structure can be defined as a classically-damped one if

$$\boldsymbol{\Phi}^T\boldsymbol{V}\boldsymbol{\Phi} = \boldsymbol{\Xi} \tag{3.19}$$

is a diagonal matrix whose j^{th} component is equal to $2\zeta_j\omega_j$, being ω_j and ζ_j the j^{th} natural frequency and the j^{th} damping coefficient, respectively. It is worth noting that in the present subsection all the structural modes are taken into account and no truncation technique is used.

Making reference to the so-called seismic response spectra $S(T)$ (with T period of the structure), commonly used in earthquake engineering (see e.g. [23, 25, 68]), once the natural frequencies and the modal matrix are known, the displacement vector due to the j^{th} mode can be determined as follow:

$$\boldsymbol{u}_{fj} = \boldsymbol{\Phi}_j \frac{\boldsymbol{\Phi}_j^T\boldsymbol{M}\boldsymbol{\tau}S\left(T_j\right)}{\omega_j^2}, \tag{3.20}$$

and the complete response of the MDOF system is obtainable combining in a full quadratic way all the mode's responses trough the following relation:

$$E_\ell = \sqrt{\sum_k \sum_j \rho_{jk} E_{j\ell} E_{k\ell}} \tag{3.21}$$

where E_ℓ is the typical ℓ^{th} component of the combined effect of the evaluated quantity $\boldsymbol{u}_f$ or $\boldsymbol{P} = \boldsymbol{B}^T \boldsymbol{E} \boldsymbol{u}_f$. In equation (3.21) $E_{j\ell}$ and $E_{k\ell}$ represent the ℓ^{th} components of the effect related to the j^{th} and k^{th} mode respectively, while ρ_{jk} is the correlation coefficient between j^{th} and k^{th} modes:

$$\rho_{jk} = \frac{8\zeta^2 \beta_{jk}^{3/2}}{(1+\beta_{jk})\left[(1+\beta_{jk})^2 + 4\zeta^2\beta_{jk}\right]} \tag{3.22}$$

in which $\beta_{jk} = T_k/T_j$, being T_j and T_k the periods of the j^{th} and k^{th} mode.

The solution of the seismic analysis problem obtained by referring to appropriate response spectra allows to model the seismic load as a perfect cyclic (quasi-static) one, accounting just for the relevant response peak values obtainable by equations (3.20) and (3.21). This idealization of the structural response is necessary to specialize the problem (3.14) to the case of structures subjected to earthquake loading. It is worth noting that, although quasi-static field, the response spectrum takes into account inertial and damping effects.

Now, once assumed that the structure can suffer the action of fixed and seismic loads (as above modeled), it is necessary to individuate appropriate admissible load combinations which characterize some prefixed limit state of the structure during its lifetime. Therefore, as usual, three admissible load combinations of fixed and seismic loads are chosen, and in particular:

1. the first combination is given by the action of the solely fixed loads $\boldsymbol{F}_0$. When the structure is subjected to this load combination the elastic stress response $\boldsymbol{P}_0$ can be evaluated trough the equations (3.10) and (3.11);

2. the second combination characterizes the so-called serviceability conditions; it is given as superimposition of reduced fixed loads $\boldsymbol{F}_{s0} = \xi_{s0}\boldsymbol{F}_0$, $0 < \xi_{s0} < 1$, and seismic actions of relatively low intensity. In particular, the seismic effects are related with the response spectra S_s defined as a function of a high up-crossing probability in the structure's lifetime. When the structure is subjected to this load combination the elastic stress response to the fixed load $\boldsymbol{P}_{s0}$ can be evaluated trough the equations (3.10) and (3.11), while the elastic stress response to the seismic loads $\boldsymbol{P}_s$ can be evaluated trough the equations (3.20) and (3.21);

3. finally, the third combination characterizes the so-called ultimate load conditions; it is given as superimposition of reduced fixed loads $\boldsymbol{F}_{l0} = \xi_{l0}\boldsymbol{F}_0$, $0 < \xi_{l0} < 1$, and seismic actions of high intensity. In particular, the seismic effects are related with the response spectrum S_l defined as function of a low up-crossing probability in the structure's lifetime. When the structure is subjected to this load combination the elastic stress response to the fixed load $\boldsymbol{P}_{l0}$ can be evaluated trough the equations (3.10) and (3.11), while the elastic stress response to the seismic loads $\boldsymbol{P}_l$ can be evaluated trough the equations (3.20) and (3.21);

In correspondence of each load combination a related limit state must be imposed on the structure behavior, and in particular:

1. the structure must behave in a purely elastic manner when subjected to the first load combination;
2. the structure must respond eventually in an elastic manner when subjected to the second load combination (i.e. the structure must shakes down);
3. the structure must prevent the instantaneous collapse when subjected to the last load combination.

Taking into account all the remarks previously reported it is possible to formulate an optimal design problem for elastic perfectly plastic frames subjected to the above described combinations of fixed and seismic loads.

In order to generalize. let assume that the design variables can alternatively belong to a continuous and/or to a discrete domain, so that the minimum volume design problem can be formulated as follows:

$$V^* = \min_{\boldsymbol{t},\boldsymbol{\rho},\boldsymbol{\rho}_i} V(\boldsymbol{t}), \tag{3.23a}$$

subjected to:

$$t_d \in T_d, \quad (d = 1, 2, \ldots, n_d), \tag{3.23b}$$

$$t_c^{\min} \leq t_c \leq t_c^{\max} \quad (c = n_d + 1, n_d + 2, \ldots, n_b \times s), \tag{3.23c}$$

$$\boldsymbol{H}\boldsymbol{t} \geq \bar{\boldsymbol{h}}, \tag{3.23d}$$

$$\boldsymbol{\varphi}_e = \boldsymbol{N}^T \boldsymbol{P}_0 - \boldsymbol{R} \leq \mathbf{0}, \tag{3.23e}$$

$$\boldsymbol{\varphi}_{si} = \boldsymbol{N}^T \left[\boldsymbol{P}_{s0} + (-1)^i \boldsymbol{P}_s + \boldsymbol{\rho}\right] - \boldsymbol{R} \leq \mathbf{0} \quad (i = 1, 2), \tag{3.23f}$$

$$\boldsymbol{A}^T \boldsymbol{\rho} = \mathbf{0}, \tag{3.23g}$$

$$\boldsymbol{\varphi}_{li} = \boldsymbol{N}^T \left[\boldsymbol{P}_{l0} + (-1)^i \boldsymbol{P}_l + \boldsymbol{\rho}_i\right] - \boldsymbol{R} \leq \mathbf{0} \quad (i = 1, 2), \tag{3.23h}$$

$$\boldsymbol{A}^T \boldsymbol{\rho}_i = \mathbf{0} \quad (i = 1, 2). \tag{3.23i}$$

In problem (3.23), eqs. (3.23b) to (3.23d) represent suitably imposed technological constraints to the design variables. In particular, in equations (3.23b) and (3.23c) t_d $(d = 1, 2, \ldots, n_d)$ are the design variables related to the discrete domains T_d, while t_c $(c = n_d + 1, n_d + 2, \ldots, n_b \times s)$ are the ones related to continuous domains with defined lower $t_c^{\min}$ and upper $t_c^{\max}$ bounds. Finally, in equations (3.23d) $\boldsymbol{H}$ is the so-called technological constraint matrix and $\bar{\boldsymbol{h}}$ a technological vector.

3.1.3 Formulation considering element slenderness

In section (3.1) the considered load combinations and the particular structure typology are related with a response that can be strongly influenced by other dangerous effects, as well as some other limits can be imposed to ensure the full usability of the relevant structure subjected to seismic actions. The cited dangerous effects (P-Δ effects and buckling) will be taken into account in the relevant optimization problem as specified in the present subsection.

Dealing with structures constituted by slender elements, it is advisable to suitably take into account the risk of buckling as well as the P-Delta effects. For the relevant described frame it suffices that these dangerous effects be accounted for the pillars.

In order to take into account the so-called P-Δ effects, a suitable distribution of bending moments acting on the structural nodes has been considered. Such nodal load distribution is determined by multiplying the global vertical nodal forces times the drifts at each story deduced by the elastic response to the relevant standard loads of the structure in its initial configuration (Figure 3.1). The elastic response to the defined bending nodal loads represents a suitable approximate evaluation of the searched P-Δ effects.

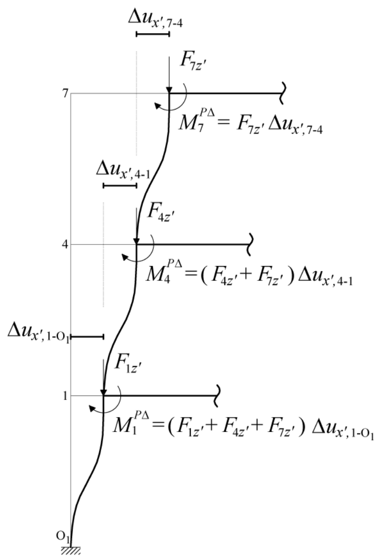

Figure 3.1: Structural scheme utilized for the computation of the P-Δ effects

Furthermore, the following approach can be utilized in order to take into account the buckling effect on the pillars, determining the approximate value of the relevant critical load.

Let us assume a shear type behavior for the frame. The critical load of the typical pillar can be obtained by referring to the scheme plotted in Figure 3.2, in which $d_{2z} = d_z(H)$ is the transversal elastic displacement of the 2^{th} extreme of the typical pillar, k_t is the spring stiffness computed as the total floor shear stiffness, E is the material Young's modulus and $I_{\min}$ is the minimum moment of inertia of the relevant pillar cross section.

The total potential energy functional related to the typical pillar sketched in Figure 3.2 can be written as follows:

$$\mathcal{V} = \frac{1}{2}\int_0^H \left(EI_{\min}d_z''^{\,2} - Pd_z'^{\,2}\right)\,dx. \tag{3.24}$$

By imposing the stationariness of the above defined functional, the following differential equation is obtained:

$$EI_{\min}d_z'''' - Pd_z'' = 0. \tag{3.25}$$

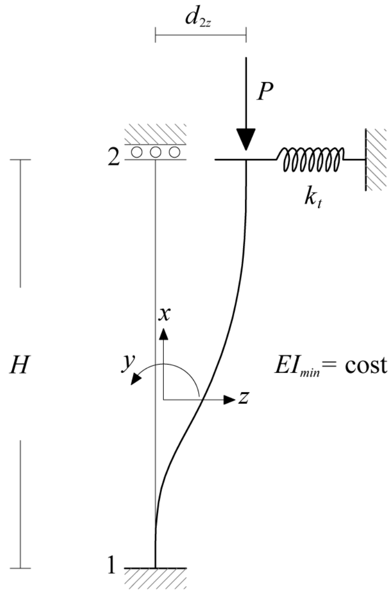

Figure 3.2: Beam mechanical scheme utilized for the computation of limit buckling load.

The general integrals of equation (3.25), here skipped for the sake of brevity, can be particularized by imposing the following boundary conditions:

$$d_{1z} = d_z(0) = 0, \tag{3.26a}$$

$$d_{1y} = -d'_{1z} = -d'_z(0) = 0, \tag{3.26b}$$

$$d_{2y} = -d'_{2z} = -d'_z(H) = 0, \tag{3.26c}$$

$$d'''_z(H) + \alpha^2 d'_z(H) - \frac{k_t}{EI_{\min}} d_z(H) = 0, \tag{3.26d}$$

in which $\alpha^2 = P/EI_{\min}$, as usual, and k_t is the total floor shear stiffness.

The resulting equation system can provide a non trivial solution (in terms of integration constants) only if the related coefficient matrix is a singular one. Therefore, imposing the singularity of the cited matrix, and neglecting the trivial solution $\alpha = 0$, the following relation holds:

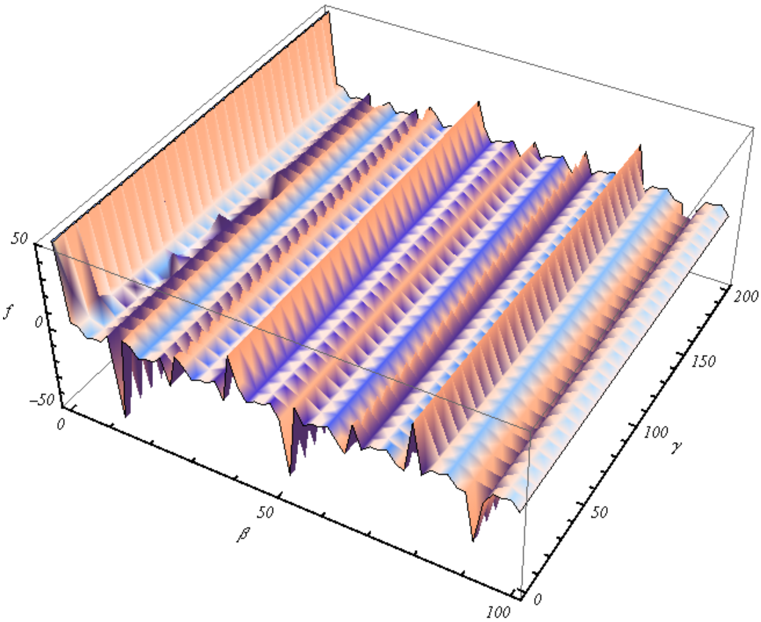

Figure 3.3: Sketch of equation (3.29).

$$\cot\beta - \sec\beta = \frac{2k_t}{\dfrac{EI_{\min}}{H^3} - k_t\beta}, \tag{3.27}$$

where $\beta = \alpha H$ has been defined.

Equation (3.27) cannot be solved in a closed form. So, putting:

$$\gamma = \frac{k_t H^3}{EI_{\min}}, \tag{3.28}$$

it is possible to define a function:

$$f(\beta, \gamma) = \frac{2\gamma}{\beta^3 - \gamma\beta} - \cot\beta + \sec\beta, \tag{3.29}$$

the zeros of which represent the solution of equation (3.27).

In order to obtain the solution, function $f(\beta, \gamma)$ in equation (3.29) has been sketched in Figure 3.3 for suitably chosen ranges of the relevant variables. To the aim of the chapter, it is of interest to obtain the first value of β for which

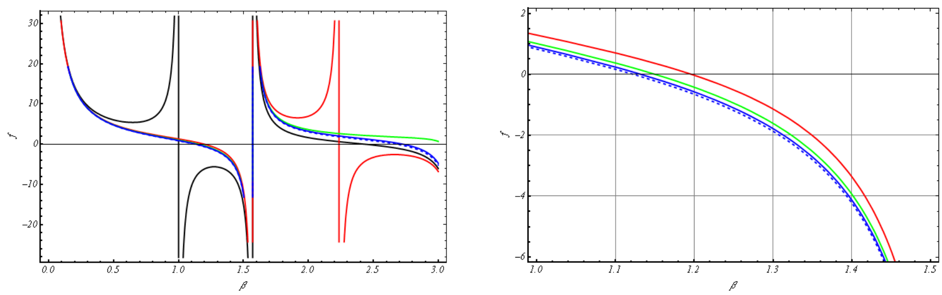

(a) Sketch of equation (3.29) for different values of γ: (black) $\gamma = 1$; (red) $\gamma = 5$; (green) $\gamma = 10$; (blue) $\gamma = 40$; (dashed blue) $\gamma = 50$; in the range $0 \leq \beta \leq 3$.

(b) Sketch of equation (3.29) for different values of γ: (black) $\gamma = 1$; (red) $\gamma = 5$; (green) $\gamma = 10$; (blue) $\gamma = 40$; (dashed blue) $\gamma = 50$; in the range $1 \leq \beta \leq 1.5$.

Figure 3.4: Sketches of equation (3.29) for different values of γ

$f(\beta, \gamma)$ is equal to zero. In order to do that, an examination Figure 3.3 suggests to focus the attention in the range $0 < \beta \leq 5$.

Therefore, $f(\beta, \gamma)$ has been sketched in Figure 3.4a for different values of γ by varying β. An examination of this figure shows that for $\gamma > 10$ all the sketched functions seem to possess the same zeroing β. This remark is confirmed by an examination of Figure 3.4b in which the same functions as in Figure 3.4a have been reported zooming in the range $1 \leq \beta \leq 1.5$.

An examination of this graphs suggests that the zero of equation (3.29) can be assumed given for $\beta \cong 1.125$, so that the critical load for the pillar plotted in Figure 3.2 can be given by:

$$P_{cr} = 1.266 \frac{EI_{\min}}{H^2}, \tag{3.30}$$

It is worth noticing that if the frame contains some cross bracing element, even for it the buckling effect must be taken into account. Obviously, in this case the limit load is provided by the well-known Eulero's formula $P_{cr} = \pi^2 EI_{\min}/\ell^2$, being ℓ the length of the relevant cross bracing element and $I_{\min}$ the minimum moment of inertia of its cross section.

Taking into account all the remarks previously reported and considering the optimal design formulation (3.23) of section (3.1), the following improved design problem accounting for element slenderness can be formulated:

$$V^* = \min_{\boldsymbol{t},\boldsymbol{\rho},\boldsymbol{\rho}_{l1},\boldsymbol{\rho}_{l2}} V(\boldsymbol{t}), \tag{3.31a}$$

subjected to:

$$t_d \in T_d, \quad (d = 1, 2, \ldots, n_d), \tag{3.31b}$$

$$t_c^{\min} \leq t_c \leq t_c^{\max} \quad (c = n_d + 1, n_d + 2, \ldots, n_b \times s), \tag{3.31c}$$

$$\boldsymbol{Ht} \geq \bar{\boldsymbol{h}}, \tag{3.31d}$$

$$\boldsymbol{\varphi}_e = \bar{\boldsymbol{N}}^T \left(\boldsymbol{P}_0 + \tilde{\boldsymbol{P}}_0 \right) - \bar{\boldsymbol{R}} \leq \boldsymbol{0}, \tag{3.31e}$$

$$\boldsymbol{\varphi}_{s1} = \bar{\boldsymbol{N}}^T \left(\boldsymbol{P}_{s0} + \boldsymbol{P}_s + \tilde{\boldsymbol{P}}_{s1} + \boldsymbol{\rho} \right) - \bar{\boldsymbol{R}} \leq \boldsymbol{0}, \tag{3.31f}$$

$$\boldsymbol{\varphi}_{s2} = \bar{\boldsymbol{N}}^T \left(\boldsymbol{P}_{s0} - \boldsymbol{P}_s + \tilde{\boldsymbol{P}}_{s2} + \boldsymbol{\rho} \right) - \bar{\boldsymbol{R}} \leq \boldsymbol{0}, \tag{3.31g}$$

$$\boldsymbol{A}^T \boldsymbol{\rho} = \boldsymbol{0}, \tag{3.31h}$$

$$\boldsymbol{\varphi}_{l1} = \bar{\boldsymbol{N}}^T \left(\boldsymbol{P}_{l0} + \boldsymbol{P}_l + \tilde{\boldsymbol{P}}_{l1} + \boldsymbol{\rho}_{l1} \right) - \bar{\boldsymbol{R}} \leq \boldsymbol{0}, \tag{3.31i}$$

$$\boldsymbol{\varphi}_{l2} = \bar{\boldsymbol{N}}^T \left(\boldsymbol{P}_{l0} - \boldsymbol{P}_l + \tilde{\boldsymbol{P}}_{l2} + \boldsymbol{\rho}_{l2} \right) - \bar{\boldsymbol{R}} \leq \boldsymbol{0}, \tag{3.31j}$$

$$\boldsymbol{A}^T \boldsymbol{\rho}_{l1} = \boldsymbol{0}, \quad \boldsymbol{A}^T \boldsymbol{\rho}_{l2} = \boldsymbol{0}. \tag{3.31k}$$

In problem (3.31), besides the already known symbols, $\bar{\boldsymbol{N}}$ is the matrix of the unit external normals to the elastic domain and $\bar{\boldsymbol{R}}$ is the plastic resistance vector both defined taking into account the pillar slenderness. Actually, depending on the slenderness of the relevant element, the shape of the limit domain can change and, as a consequence, matrix $\bar{\boldsymbol{N}}$ and vector $\bar{\boldsymbol{R}}$ change; in particular, vector $\bar{\boldsymbol{R}}$ will assume as suitable limit for the axial force, alternatively, the minimum between the values $N_0 = \sigma_y A$, being σ_y the material yield stress and A the measure of the relevant cross section area, and P_{cr}/η with P_{cr} given in equation (3.30) and η appropriate safety factor.

Furthermore, vector $\tilde{\boldsymbol{P}}_0$ collects the element node stress response related to the P-Δ effects when just the first load combination act. Vectors $\tilde{\boldsymbol{P}}_{s1}$ and $\tilde{\boldsymbol{P}}_{s2}$ collect the element node stress response related to the P-Δ effects when the second load combination acts in the two opposite loading directions. Finally, $\tilde{\boldsymbol{P}}_{l1}$ and $\tilde{\boldsymbol{P}}_{l2}$ collect the element node stress response related to the P-Δ effects when the third load combination acts in the two opposite loading directions.

3.1.4 Formulation for structures with limited ductility

Due to the complexity of the relevant structural problem to be formulated, where some constraints will be introduced related with quantities characterizing the structure behavior above the elastic limit, even if an elastic plastic analysis is not effected, it needs to recall some fundamentals related to the inelastic response of the structure as synthetically reported here after.

Let refer to the structure model as above described and let it be subjected to a known quasi-statically load $\boldsymbol{F} = \boldsymbol{F}(t)$, variable in time in the interval $0 \leq t \leq t_f$. Furthermore, as usual, a finite number of cross sections are chosen as points (strain points) in which the plastic admissibility conditions have to be satisfied.

The elastic plastic structural response at time t is governed by the following relations:

$$\boldsymbol{K}\boldsymbol{u} - \boldsymbol{B}\boldsymbol{p} = \boldsymbol{F}, \tag{3.32a}$$

$$\boldsymbol{P} = \boldsymbol{B}^T\boldsymbol{u} - \boldsymbol{D}_p\boldsymbol{p} + \boldsymbol{P}^*, \tag{3.32b}$$

$$\boldsymbol{\varphi} = \boldsymbol{N}^T\boldsymbol{P} - \boldsymbol{R} \leq \boldsymbol{0}, \tag{3.32c}$$

$$\dot{\boldsymbol{p}} = \boldsymbol{N}\dot{\boldsymbol{\lambda}}, \tag{3.32d}$$

$$\dot{\boldsymbol{\lambda}} \geq 0, \quad \boldsymbol{\varphi}^T\dot{\boldsymbol{\lambda}} = 0, \quad \dot{\boldsymbol{\varphi}}^T\dot{\boldsymbol{\lambda}} = 0, \tag{3.32e}$$

$$\boldsymbol{p} = \int_0^t \boldsymbol{N}\dot{\boldsymbol{\lambda}}(\tau)\, d\tau. \tag{3.32f}$$

The solving set can be deduced from equations (3.32) with appropriate replacements:

$$-\boldsymbol{\varphi} = \boldsymbol{R} - \boldsymbol{N}^T\left(\boldsymbol{B}^T\boldsymbol{K}^{-1}\boldsymbol{F} + \boldsymbol{P}^*\right) - \boldsymbol{N}^T\left(\boldsymbol{B}^T\boldsymbol{K}^{-1}\boldsymbol{B} - \boldsymbol{D}_p\right)\boldsymbol{N}\int_0^t \dot{\boldsymbol{\lambda}}(\tau)\, d\tau \tag{3.33a}$$

$$-\boldsymbol{\varphi} \geq \boldsymbol{0}, \quad \dot{\boldsymbol{\lambda}} \geq \boldsymbol{0}, \quad \boldsymbol{\varphi}^T\dot{\boldsymbol{\lambda}} = 0, \quad \dot{\boldsymbol{\varphi}}^T\dot{\boldsymbol{\lambda}} = 0, \tag{3.33b}$$

and must be satisfied for all t $0 \leq t \leq t_f$.

At least in principle equations (3.33), plus the appropriate initial conditions at $t = 0$, can be integrated with respect to time t in order to obtain the vectors $\boldsymbol{\varphi}$ and $\dot{\boldsymbol{\lambda}}$, and, trough equations (3.32), the elastic plastic structural response.

Anyway, in practice, in order to obtain a numerical solution it is necessary that the problem becomes discrete also with respect to time, subdividing the time axis into f sub-intervals with the same width $\delta t = t_f/f$. During the typical sub-interval k, $((k-1)\delta t \leq t \leq k\delta t)$, the unknown time function $\dot{\boldsymbol{\lambda}}(\tau)$, $\forall \tau = (t - (k-1)\delta t) \in (0, \delta t)$, is modeled so as to be expressed in terms of time independent unknown non-negative vector $\boldsymbol{Y}^k$, i.e.:

$$\dot{\boldsymbol{\lambda}}(\tau) = \boldsymbol{h}(\tau)\boldsymbol{Y}^k, \quad \boldsymbol{Y}^k \geq \boldsymbol{0} \tag{3.34}$$

where $\boldsymbol{h}(\tau)$ is a square dimensional matrix with non-negative entries and such that:

$$\int_0^{\delta t} \boldsymbol{h}(\tau)\, d\tau = \boldsymbol{I} \tag{3.35}$$

being $\boldsymbol{I}$ the identity matrix.

Due to the modeling problem (3.34) and (3.35), elastic unloading can occur just at the discretization instants, every element remains either in the elastic regime or in the elastic plastic one during each step, and the equation $\dot{\boldsymbol{\varphi}}^T\dot{\boldsymbol{\lambda}} = 0$ in (3.33b) become meaningless.

Equations (3.33) can not be satisfied at some instant $\tau \in (0, \delta t)$, however, they must be satisfied in an integrated, holonomic form (see e.g. [45]), i.e.:

$$\boldsymbol{Z}^k \equiv -\boldsymbol{\varphi}^k = -\int_0^{\delta t} \boldsymbol{h}^T(\tau)\boldsymbol{\varphi}^T(\tau)\, d\tau = \boldsymbol{S}\boldsymbol{Y}^k + \boldsymbol{b}^k \tag{3.36a}$$

$$\boldsymbol{Z}^k \geq \boldsymbol{0}, \quad \boldsymbol{Y}^k \geq \boldsymbol{0}, \quad \left(\boldsymbol{Y}^k\right)^T \boldsymbol{Z}^k = 0 \tag{3.36b}$$

A step-wise constant shape for $\dot{\boldsymbol{\lambda}}$ is very often chosen $\boldsymbol{h}(\tau) = \boldsymbol{h} = \boldsymbol{I}\,(1/\delta t)$. In such a case, it results:

$$\boldsymbol{S} = -\boldsymbol{N}^T\left(\boldsymbol{B}^T\boldsymbol{K}^{-1}\boldsymbol{B} - \boldsymbol{D}_p\right)\boldsymbol{N} = -\boldsymbol{N}^T\boldsymbol{G}_p^T\left(\boldsymbol{D}\boldsymbol{C}\boldsymbol{K}^{-1}\boldsymbol{C}^T\boldsymbol{D} - \boldsymbol{D}\right)\boldsymbol{N}\boldsymbol{G}_p \tag{3.37a}$$

$$\boldsymbol{b}^k = \boldsymbol{R} + \boldsymbol{S}\sum_{j=1}^{k-1}\boldsymbol{Y}^j - \boldsymbol{N}^T\boldsymbol{B}^T\boldsymbol{K}^{-1}\boldsymbol{F}^k - \boldsymbol{N}^T\boldsymbol{P}^{*k} \tag{3.37b}$$

where $\boldsymbol{S}$ is a time-independent symmetric structural matrix which transforms plastic activation $\boldsymbol{Y}^k$ into the opposite of the plastic potential $\boldsymbol{\varphi}^k$, and $\boldsymbol{b}^k$ is a known vector depending on the pertinent loading at step k and on the sum of the increments of the plastic activation intensity vectors accumulated at step $k-1$.

In virtue of the effected time discretization, problem (3.33) transforms into the following sequence of linear complementarity problems:

$$\boldsymbol{Z}^k \geq \mathbf{0}, \quad \boldsymbol{Y}^k \geq \mathbf{0}, \quad \left(\boldsymbol{Y}^k\right)^T \boldsymbol{Z}^k = 0, \quad (k = 1, 2, \ldots, f). \tag{3.38}$$

It is worth noting that in the case of perfect plasticity $\boldsymbol{S}$ is a semi-defined positive matrix (see e.g. [63]) and as a consequence, neither the existence of a bounded solution $\boldsymbol{Y}^k$, nor its uniqueness is guaranteed. If equations (3.37a) admit an unbounded solution $\boldsymbol{Y}^k$ (at least somewhere in the structure) , instantaneous collapse occurs; if they admit a vanishing solution solution $\boldsymbol{Y}^k$, the full structure is elastic; if they admit a finite no vanishing solution $\boldsymbol{Y}^k$, the structure exhibits an elastic plastic behavior. In this last case, every two solutions to the same problem must differ by a stress-less (i.e. compatible, corresponding to a mechanism) set of plastic deformations (see e.g. [63]).

On the basis of the above considerations, problem (3.23) may be rewritten in the following form:

$$V^* = \min_{\boldsymbol{t},\boldsymbol{Y},\boldsymbol{Y}_i} V(\boldsymbol{t}), \tag{3.39a}$$

subjected to:

$$t_d \in T_d, \quad (d = 1, 2, \ldots, n_d), \tag{3.39b}$$

$$t_c^{\min} \leq t_c \leq t_c^{\max} \quad (c = n_d + 1, n_d + 2, \ldots, n_b \times s), \tag{3.39c}$$

$$\boldsymbol{H}\boldsymbol{t} \geq \bar{\boldsymbol{h}}, \tag{3.39d}$$

$$\boldsymbol{\varphi}_e = \boldsymbol{N}^T \boldsymbol{P}_0 - \boldsymbol{R} \leq \mathbf{0}, \tag{3.39e}$$

$$\boldsymbol{\varphi}_{si} = \boldsymbol{N}^T \left[\boldsymbol{P}_{s0} + (-1)^i \boldsymbol{P}_s\right] - \boldsymbol{S}\boldsymbol{Y} - \boldsymbol{R} \leq \mathbf{0} \quad (i = 1, 2), \tag{3.39f}$$

$$\boldsymbol{Y} \geq \mathbf{0}, \tag{3.39g}$$

$$\boldsymbol{\varphi}_{li} = \boldsymbol{N}^T \left[\boldsymbol{P}_{l0} + (-1)^i \boldsymbol{P}_l\right] - \boldsymbol{S}\boldsymbol{Y}_i - \boldsymbol{R} \leq \mathbf{0} \quad (i = 1, 2), \tag{3.39h}$$

$$\boldsymbol{Y}_i \geq \mathbf{0}, \quad (i = 1, 2). \tag{3.39i}$$

It should be noted that this problem formulation (3.39) is completely equivalent to the previous one (3.23) substituting just the self-stress vectors $\boldsymbol{\rho}$ with the fictitious plastic activation intensity vectors $\boldsymbol{Y}$.

The results obtainable by means of the described analyses are very consistent but, unfortunately, they cannot give complete information with respect to relevant ductility and/or functionality limits. Actually, as known, due to the special loading model assumed in the present case, the amount of plastic deformation occurring during the transient phase can be provided just by making recourse to suitable bounding techniques based on the perturbation method [74]. With particular reference to the elastic shakedown behavior, a chosen measure of the plastic deformation can be bounded by means of the following relation:

$$|\bar{U}| \leq \frac{1}{2\omega} \hat{\boldsymbol{Y}}^T \boldsymbol{S} \hat{\boldsymbol{Y}} \tag{3.40a}$$

$$\omega > 0 \tag{3.40b}$$

where $|\bar{U}|$ is the kinematic quantity to be bounded, $\omega > 0$ is the perturbation multiplier and $\hat{\boldsymbol{Y}}$ is the plastic multiplier vector related to the perturbed yield domain.

In this way, problem (3.39) can be improved in order to take into account limited ductility by means of equations (3.40):

$$V^* = \min_{\boldsymbol{t}, \hat{\boldsymbol{Y}}, \boldsymbol{Y}_i, \omega} V(\boldsymbol{t}), \tag{3.41a}$$

subjected to:

$$t_d \in T_d, \quad (d = 1, 2, \ldots, n_d), \tag{3.41b}$$

$$t_c^{\min} \leq t_c \leq t_c^{\max} \quad (c = n_d + 1, n_d + 2, \ldots, n_b \times s), \tag{3.41c}$$

$$\boldsymbol{H}\boldsymbol{t} \geq \bar{\boldsymbol{h}}, \tag{3.41d}$$

$$\boldsymbol{\varphi}_e = \boldsymbol{N}^T \boldsymbol{P}_0 - \boldsymbol{R} \leq \boldsymbol{0}, \tag{3.41e}$$

$$\boldsymbol{\varphi}_{si} = \boldsymbol{N}^T \left[\boldsymbol{P}_{s0} + (-1)^i \boldsymbol{P}_s\right] - \boldsymbol{S}\hat{\boldsymbol{Y}} + \omega \hat{\boldsymbol{R}} - \boldsymbol{R} \leq \boldsymbol{0} \quad (i = 1, 2), \tag{3.41f}$$

$$\hat{\boldsymbol{Y}} \geq \boldsymbol{0}, \tag{3.41g}$$

$$\boldsymbol{\varphi}_{li} = \boldsymbol{N}^T \left[\boldsymbol{P}_{l0} + (-1)^i \boldsymbol{P}_l\right] - \boldsymbol{S}\boldsymbol{Y}_i - \boldsymbol{R} \leq \boldsymbol{0} \quad (i = 1, 2), \tag{3.41h}$$

$$\boldsymbol{Y}_i \geq \boldsymbol{0}, \quad (i = 1, 2). \tag{3.41i}$$

$$\frac{1}{2} \hat{\boldsymbol{Y}}^T \boldsymbol{S} \hat{\boldsymbol{Y}} + \omega \left(|U_{te}|_{\max} - \bar{U}_t\right) \leq 0 \tag{3.41j}$$

$$\omega > 0 \tag{3.41k}$$

where, besides the already known symbols, $\hat{\boldsymbol{R}}$ is the linear perturbation mode vector , $\bar{U}_t$ is the imposed bounding value on the total chosen displacement and $|U_{te}|_{\max}$ the elastic part of the relevant displacement, computed as maximum absolute value of the response related to the combination of load characterizing the serviceability conditions.

3.2 Optimal design of frames under dynamic loads

In this section, a second group of optimal design problem formulations are presented making reference to the so-called "repeated seismic excitation model" in which seismic waves are represented trough a spectral decomposition as a convex domain of excitations. With this special load model it is possible to formulate an optimization problem in which the seismic actions are treated in all their dynamic nature. Furthermore, some special formulations for base-isolated structure are exposed.

3.2.1 General formulation

Let consider an elastic perfectly plastic frame structure constituted by n_b Euler-Bernoulli beams. The v^{th} element geometry is fully described by the s components of the vector $\boldsymbol{t}_v$ so that $\boldsymbol{t} = \left[\boldsymbol{t}_1^T, \boldsymbol{t}_2^T, \ldots, \boldsymbol{t}_{n_b}^T\right]^T$ represents the $n_b \times s$ super-vector collecting all the design variables. The structure is subjected to mechanical nodal forces as well as to mechanical and/or kinematical element loads, all actions varying in time interval $[0, t_f]$ dynamically.

For an assigned structure design ($\boldsymbol{t} = \bar{\boldsymbol{t}}$) and for an assigned load history, in the hypothesis of small displacements and deformations the elastic perfectly plastic structure behavior is described by the following relations:

$$\boldsymbol{M}\ddot{\boldsymbol{u}} + \boldsymbol{V}\dot{\boldsymbol{u}} + \boldsymbol{K}\boldsymbol{u} - \boldsymbol{B}\boldsymbol{p} = \boldsymbol{F} \quad \forall t \in [0, t_f], \tag{3.42a}$$

$$\boldsymbol{P} = \boldsymbol{B}^T\boldsymbol{u} - \boldsymbol{D}_p\boldsymbol{p} + \boldsymbol{P}^* \quad \forall t \in [0, t_f], \tag{3.42b}$$

$$\boldsymbol{\varphi} = \boldsymbol{N}^T\boldsymbol{P} - \boldsymbol{R} \leq \boldsymbol{0} \quad \forall t \in [0, t_f], \tag{3.42c}$$

$$\dot{\boldsymbol{p}} = \boldsymbol{N}\dot{\boldsymbol{\lambda}} \quad \forall t \in [0, t_f], \tag{3.42d}$$

$$\dot{\boldsymbol{\lambda}} \geq 0, \quad \boldsymbol{\varphi}^T\dot{\boldsymbol{\lambda}} = 0, \quad \dot{\boldsymbol{\varphi}}^T\dot{\boldsymbol{\lambda}} = 0, \quad \forall t \in [0, t_f], \tag{3.42e}$$

$$\boldsymbol{u} = \boldsymbol{u}^0, \ \dot{\boldsymbol{u}} = \dot{\boldsymbol{u}}^0, \ \boldsymbol{p} = \boldsymbol{p}^0, \quad \text{for } t = 0, \tag{3.42f}$$

where, besides the already known symbols, $\boldsymbol{u}^0$, $\dot{\boldsymbol{u}}^0$, $\boldsymbol{p}^0$, represent the initial conditions in terms of displacement, velocity, and plastic strains respectively.

When the load history and the initial conditions are known, it is always possible (at least in principle) to obtain the exact elastic plastic response of the structure by integrating the equations (3.42). Effectively, to obtain the solution is necessary to discretize the problem with respect to time, subdividing the time axis into small intervals. The solution can be reached making reference to direct methods based on the concept of tangent stiffness, or by indirect methods, such as the mode superposition methods, that may refer to the Colonnetti's decomposition principle (see e.g. [17, 43, 50, 77]).

Let assume now that $\boldsymbol{F}$, as function of time t, is identified with any load path that does not exceed a given excitation domain Π of convex polygonal shape with vertices corresponding to a set of n mutually independent nodal excitations of finite duration, say $\xi \boldsymbol{F}_k(\tau)$, $k \in I(n) \equiv \{1, 2, \ldots, n\}$, $0 \leq \tau \leq t_f$, where $\xi > 0$ is the load multiplier and t_f is the final instant of each basic excitation.

On changing ξ, Π expands or shrinks homothetically with respect to the reference excitation domain, obtained for $\xi = 1$. A load path inside Π, obtained as linear convex combination of the basic excitations $\boldsymbol{F}_k$, constitutes an admissible loading history (ALH), that is a potentially active load history for the structure.

On choosing a special ALH, the consequent response of the structure can be obtained, for instance, by a step-by-step procedure based on the equation set (3.42), plus the appropriate initial conditions at $t = 0$, but this is not the job here. This operation, in fact, should be carried out on all the infinite ALHs belonging to Π, in order to establish some safety margins for the structure. On the contrary, making reference to the "unrestricted dynamic shakedown theorems" (subsection 2.2.2), it is possible to assess the condition under which the structure has the ability to eventually shake down in the elastic regime (or adapt to the loads) when subjected to loads arbitrarily varying within Π.

In particular, the static type theorem (2.2.3) and the kinematic type theorem (2.2.4) permit to known that particular value of ξ, called shakedown safety factor ξ^*, such that dynamic shakedown occurs for all $\xi \leq \xi^*$, while does not for all $\xi > \xi^*$. For the computation of ξ^*, in subsection (2.2.2), two alternative approaches, based on these theorems, have been given.

For the purpose of the present section, making reference to frame structures and using the notation of this chapter, let recall the first (static) approach. Let indicate with $\boldsymbol{P}_k(\tau)$, $k \in I(n) \equiv \{1, 2, \ldots, n\}$, $0 \leq \tau \leq t_f$, the purely elastic (fictitious and dynamic) response to the basic excitations $\boldsymbol{F}_k(\tau)$, and with $\boldsymbol{P}_0$ the purely elastic (fictitious) response to a fixed (permanent) load $\boldsymbol{F}_0$.

With the above positions the shakedown safety factor can be evaluated with the following linear programming problem:

$$\xi^* = \max_{\xi,\,\boldsymbol{\rho}} \xi \tag{3.43a}$$

subjected to:

$$\boldsymbol{\varphi} = \boldsymbol{N}^T \left(\boldsymbol{P}_0 + \boldsymbol{\rho}\right) + \xi \check{\boldsymbol{P}} - \boldsymbol{R} \leq \mathbf{0}, \tag{3.43b}$$

$$\boldsymbol{A}^T \boldsymbol{\rho} = \mathbf{0}, \tag{3.43c}$$

where:

$$\check{\boldsymbol{P}} = \max_{k \in I(n)} \max_{0 \leq \tau \leq t_f} \boldsymbol{N}^T \boldsymbol{P}_k(\tau) \tag{3.44}$$

is the elastic envelope stress vector which select for each yielding mode the maximum of the plastic demand in time [26, 27, 64].

On the basis of the unrestricted dynamic shakedown theory, it is possible to formulate a minimum volume design problem which satisfy the shakedown limit conditions. In particular, referring to different intensity levels of loads, trough the use of some positive scalar parameters $\xi \geq 0$, it is possible to impose to the optimal structure different behaviors, so that the optimal design problem with stress constraints can be formulated as follow:

$$V^* = \min_{\boldsymbol{t},\boldsymbol{\rho}} V(\boldsymbol{t}) \tag{3.45a}$$

subjected to:

$$\boldsymbol{\varphi}_e = \xi_{e1} \boldsymbol{N}^T \boldsymbol{P}_0 + \xi_{e2} \check{\boldsymbol{P}} - \boldsymbol{R} \leq \mathbf{0}, \tag{3.45b}$$

$$\boldsymbol{\varphi}_s = \xi_{s1} \boldsymbol{N}^T \boldsymbol{P}_0 + \xi_{s2} \check{\boldsymbol{P}} + \boldsymbol{N}^T \boldsymbol{\rho} - \boldsymbol{R} \leq \mathbf{0}, \tag{3.45c}$$

$$\boldsymbol{A}^T \boldsymbol{\rho} = \mathbf{0}, \tag{3.45d}$$

where equation (3.45b) represents the stress constraint on the elastic behavior, equation (3.45c) the stress constraint on the shakedown behavior and equation (3.45d) the so-called equilibrium condition.

In contrast to what has been done for the optimal design of frames subjected to cyclic loads (section 3.1), the formulation (3.45) does not include any constraints on the instantaneous collapse condition. Indeed, if the instantaneous collapse must be prevented for each ALH, no load $\boldsymbol{F}_k(\tau)$, $k \in I(n)$, within the interval $[0, t_f]$ should be a plastic collapse load. This operation, although theoretically possible, is unfeasible from a practical standpoint, as one can see from the following formulation in which just the instantaneous collapse is prevented:

$$V^* = \min_{\boldsymbol{t}, \boldsymbol{\rho}_{lk\tau}} V(\boldsymbol{t}) \tag{3.46a}$$

subjected to:

$$\boldsymbol{\varphi}_{lk\tau} = \boldsymbol{N}^T \left(\xi_{l1}\boldsymbol{P}_0 + \xi_{l2}\boldsymbol{P}_k(\tau) + \boldsymbol{\rho}_{lk\tau}\right) - \boldsymbol{R} \leq \boldsymbol{0}, \quad \forall k \in I(n),\ \forall \tau \in [0, t_f]\,, \tag{3.46b}$$

$$\boldsymbol{A}^T \boldsymbol{\rho}_{lk\tau} = \boldsymbol{0}, \quad \forall k \in I(n),\ \forall \tau \in [0, t_f]\,. \tag{3.46c}$$

Adopting a time discretization, the problem (3.46) could be solved with classical techniques, but the number of variables to manage would be huge.

An approximate technique to prevent the instantaneous collapse for the optimal structure is to select from the stress response $\boldsymbol{P}_k(\tau)$, $k \in I(n)$, $0 \leq \tau \leq t_f$, a finite number of peak stress response $\boldsymbol{P}_z$, $z \in I(w) \equiv \{1, 2, \ldots, w\}$, according to a suitable criterion, as described in the next section.

In this way, a unitary formulation of the design problem for structure subjected to dynamic loads can be done by enriching the problem (3.45) with a further constraint which allows to prevent the instantaneous collapse in an approximate manner:

$$V^* = \min_{\boldsymbol{t}, \boldsymbol{\rho}} V(\boldsymbol{t}) \tag{3.47a}$$

subjected to:

$$\boldsymbol{\varphi}_e = \xi_{e1}\boldsymbol{N}^T\boldsymbol{P}_0 + \xi_{e2}\check{\boldsymbol{P}} - \boldsymbol{R} \leq \boldsymbol{0}, \tag{3.47b}$$

$$\boldsymbol{\varphi}_s = \xi_{s1}\boldsymbol{N}^T\boldsymbol{P}_0 + \xi_{s2}\check{\boldsymbol{P}} + \boldsymbol{N}^T\boldsymbol{\rho} - \boldsymbol{R} \leq \boldsymbol{0}, \tag{3.47c}$$

$$\boldsymbol{A}^T\boldsymbol{\rho} = \boldsymbol{0}, \tag{3.47d}$$

$$\boldsymbol{\varphi}_{lz} = \boldsymbol{N}^T \left(\xi_{l1}\boldsymbol{P}_0 + \xi_{l2}\boldsymbol{P}_z + \boldsymbol{\rho}_{lz}\right) - \boldsymbol{R} \leq \boldsymbol{0} \quad \forall z \in I(w), \tag{3.47e}$$

$$\boldsymbol{A}^T\boldsymbol{\rho}_{lz} = \boldsymbol{0} \quad \forall z \in I(w), \tag{3.47f}$$

3.2.2 Formulation considering repeated seismic loads

With the aim to specialize the optimal design formulation (3.47) to the case of frame structures subjected to seismic action let recall the so-called "seismic excitation model" proposed by Borino and Polizzotto [15].

A seismic wave can be represented as a time history of the ground acceleration $\ddot{u}_g(\tau)$, $0 \leq \tau \leq t_f$ and, usually it is expressed as a superposition of r single frequency wave components of the discrete spectrum ω_i:

$$\ddot{u}_g(\tau) = \sum_{i=1}^{n} E(\tau)\left(\alpha_i \cos \omega_i \tau + \beta_i \sin \omega_i \tau\right) \quad \forall i \in I(r) \tag{3.48}$$

in which α_i and β_i are two constants representing both power an phase of each wave component and t_f is the final instant of acceleration history. Furthermore, $E(\tau)$ is an envelope shape function aimed at modeling the evolutive character of the seismic wave, that typically is given by:

$$E(\tau) = \frac{\tau}{t_{\max}} \exp\left(1 - \frac{\tau}{t_{\max}}\right) \tag{3.49}$$

where $t_{\max}$ is the instant of expected maximum acceleration intensity.

Equation (3.48) represents a two-parameter family of waves. A convex domain of excitations Π of this wave family is obtained by allowing α_i, β_i to range each within the closed interval $[-c_i, +c_i]$, where the r scalars c_i are given. This means that the point (α_i, β_i) of the (α_i, β_i)-plane ranges within a square Ω_i of side $2c_i$ and center at origin (Figure 3.5). A subset of Π is then composed of r-frequency waves as (3.48), each of which is represented by r points (α_i, β_i), one for every square Ω_i, and possesses a maximum power not exceeding $2\left({c_1}^2 + {c_2}^2 + \ldots + {c_r}^2\right)$.

With the aim to describe an admissible excitation history belonging to the convex domain of excitations Π, let adopt the following positions:

$$c_0 = \sum_{i=1}^{r} c_i \tag{3.50}$$

and

$$\nu_i = \frac{c_i}{c_0}, \quad \forall i \in I(r), \tag{3.51}$$

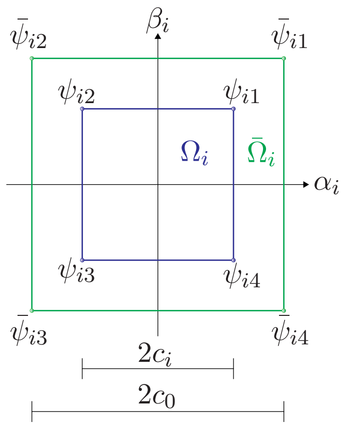

Figure 3.5: Square Ω_i of edge $2c_i$ whose point $(\alpha_i,\ \beta_i)$ represent the i^{th} spectral component of seismic wave and square $\bar{\Omega}_i$ of edge $2c_0$.

so that the four vertices of each square Ω_i, that are the basic wave components, can be obtained as:

$$\psi_{ij}(\tau) = \nu_i \bar{\psi}_{ij}(\tau), \quad j = 1, 2, 3, 4, \quad \forall i \in I(r), \tag{3.52}$$

where:

$$\bar{\psi}_{i1}(\tau) = c_0 E(\tau)\,(+\cos\omega_i\tau + \sin\omega_i\tau) \quad \forall i \in I(r) \tag{3.53a}$$

$$\bar{\psi}_{i2}(\tau) = c_0 E(\tau)\,(+\cos\omega_i\tau - \sin\omega_i\tau) \quad \forall i \in I(r) \tag{3.53b}$$

$$\bar{\psi}_{i3}(\tau) = c_0 E(\tau)\,(-\cos\omega_i\tau + \sin\omega_i\tau) \quad \forall i \in I(r) \tag{3.53c}$$

$$\bar{\psi}_{i4}(\tau) = c_0 E(\tau)\,(-\cos\omega_i\tau - \sin\omega_i\tau) \quad \forall i \in I(r) \tag{3.53d}$$

are the vertices of an external square $\bar{\Omega}_i$ of edge length $2c_0$, as one can see in Figure 3.5.

In this way, in perfect analogy with the repeated excitation model described in Chapter 2, an admissible excitation history can be obtained as a linear convex combination of the basic excitations ψ_{ij}, $j = 1, 2, 3, 4$, $\forall i \in I(r)$. So we can write:

$$\ddot{u}_g(\tau) = \sum_{i=1}^{r} \sum_{j=1}^{4} \gamma_{ij} \nu_i \bar{\psi}_{ij}(\tau) \quad \forall i \in I(r), \tag{3.54}$$

where the coefficients γ_{ij} are required to satisfy the admissibility conditions:

$$\gamma_{ij} \geq 0 \quad \text{for } j = 1, 2, 3, 4 \quad \forall i \in I(r), \tag{3.55}$$

$$\sum_{i=1}^{4} \gamma_{ij} = 1 \quad \forall i \in I(r). \tag{3.56}$$

Equation (3.54) may be rewritten in the following form by setting $\chi_{ij} = \gamma_{ij}\nu_i$:

$$\ddot{u}_g(\tau) = \sum_{i=1}^{r} \sum_{j=1}^{4} \chi_{ij} \bar{\psi}_{ij}(\tau) \tag{3.57}$$

where the new coefficients χ_{ij} have to respect the following admissibility conditions:

$$\chi_{ij} \geq 0 \quad \text{for } j = 1, 2, 3, 4 \quad \forall i \in I(r) \tag{3.58a}$$

$$\sum_{i=1}^{n} \sum_{j=1}^{4} \chi_{ij} = 1 \tag{3.58b}$$

$$\sum_{j=1}^{4} \chi_{ij} = \nu_i \quad \forall i \in I(r) \tag{3.58c}$$

Equation (3.57) under the constraints (3.58) is a representation of an admissible loading history belonging to Π. Every ALH has a complete spectrum $\omega_1, \omega_2, \ldots, \omega_r$ and it is obtained as a linear convex combination of 4^r basic waves (Figure 3.6).

However, it is in general computationally convenient to disregard constraint (3.58c), with the consequence that (3.57) becomes a linear convex combination of only the $4r$ basic single frequency wave (3.53) but with the disadvantages that there is a magnification of the maximum power related to each wave component.

The frequencies ω_i are chosen coincident with the r natural frequencies of the structure whereas the parameters c_i are taken as:

$$c_i = \sqrt{8\zeta_i \omega_i S_g(\omega_i)} \quad \forall i \in I(r) \tag{3.59}$$

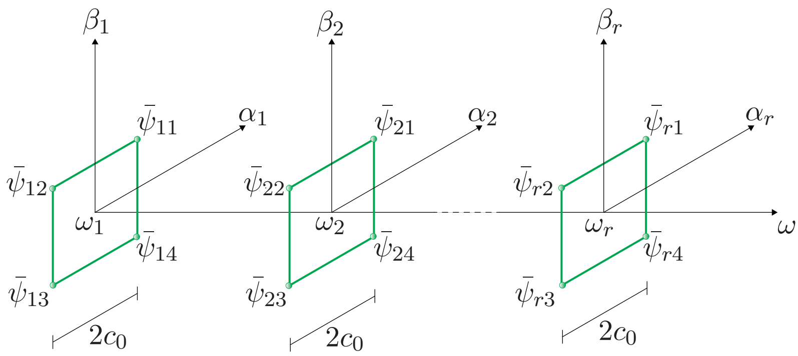

Figure 3.6: Three-dimensional space (ω, α, β) of single frequency seismic wave.

where the ζ_i coefficients denote the damping ratios of the structure and $S_g(\omega_i)$ is given by:

$$S_g(\omega_i) = \frac{\left[1 + 4\zeta_g^2 (\omega_i/\omega_g)^2\right] S_0}{\left[1 - (\omega_i/\omega_g)^2\right]^2 + 4\zeta_g^2 (\omega_i/\omega_g)^2} \quad \forall i \in I(r). \tag{3.60}$$

Here $S_g(\omega)$ denotes the power spectral density function of a simple oscillator, with natural frequency ω_g and damping ratio ζ_g, which according to the Kanai and Tajimi ground filter model (see e.g. [87]) simulates the ground response to seismic wave from the deep rock bed with uniform power density S_w.

For the further developments, it is convenient to rewrite the repeated seismic excitation model as described by equations (3.57), (3.58a) and (3.58b) with the substitution of the couple indices i and j there appearing with a single one, say $k = 1, 2, \ldots, n$. Thus, on relabelling the basic excitations (3.53) as $\bar{\psi}_k(\tau)$ the preceding excitation model is now given in the form:

$$\ddot{u}_g(\tau) = \sum_{k=1}^{n} \chi_k \bar{\psi}_k(\tau) \quad \forall k \in I(n), \tag{3.61}$$

where the coefficients χ_k must satisfy the admissibility conditions

$$\chi_k \geq 0 \quad \forall k \in I(n), \tag{3.62a}$$

$$\sum_{k=1}^{n} \chi_k = 1. \tag{3.62b}$$

As shown in section (3.2) for the optimal design formulation, what matters to impose shakedown and limit constraints are the basic excitations histories $\bar{\psi}_k(\tau)$, and consequently the related purely elastic response.

At this purpose, let consider an elastic perfectly plastic frame whose behavior is described by the equations (3.42) subgected to the k^{th} horizontal ground acceleration $\bar{\psi}_k(\tau)$, $0 \leq \tau \leq t_f$. In order to evaluate the purely elastic seismic response of the structure (thus assuming $\boldsymbol{p} = \boldsymbol{0}$), let refer a lumped lumped system obtained trough standard condensation procedures. The equilibrium equation is:

$$\boldsymbol{M}\ddot{\boldsymbol{u}}_f(\tau) + \boldsymbol{V}\dot{\boldsymbol{u}}_f(\tau) + \boldsymbol{K}_f\boldsymbol{u}_f(\tau) = -\boldsymbol{M}\boldsymbol{\tau}\bar{\psi}_k(\tau), \tag{3.63}$$

where $\boldsymbol{u}_f$ represents the displacement vector related to the structure dynamic degree of freedom, $\boldsymbol{K}_f = \boldsymbol{E}^T\boldsymbol{K}\boldsymbol{E}$ is the condensed stiffness matrix, being $\boldsymbol{E}$ a suitable condensation matrix, $\boldsymbol{\tau}$ is the influence vector.

Equation (3.63) together with the appended initial conditions, here assumed as $\boldsymbol{u}_f(0) = \boldsymbol{0}$ and $\dot{\boldsymbol{u}}_f(0) = \boldsymbol{0}$, may be solved by the classical modal analysis techniques.

Let be $\boldsymbol{\Phi}$ the modal matrix whose columns are the eigenvectors of the dynamic matrix ${\boldsymbol{K}_f}^{-1}\boldsymbol{M}$ normalized with respect to $\boldsymbol{M}$. Due to the symmetry of the matrices $\boldsymbol{M}$ and $\boldsymbol{K}_f$ the eigenvectors are orthogonal with respect to $\boldsymbol{M}$ and $\boldsymbol{K}_f$, that is:

$$\boldsymbol{\Phi}^T\boldsymbol{M}\boldsymbol{\Phi} = \boldsymbol{I}, \tag{3.64}$$

$$\boldsymbol{\Phi}^T\boldsymbol{K}_f\boldsymbol{\Phi} = \boldsymbol{\Omega}_D^2, \tag{3.65}$$

where $\boldsymbol{I}$ is the identity matrix and $\boldsymbol{\Omega}_D^2$ is a diagonal matrix whose diagonal elements are the square of the natural radian frequencies ω_r. Let assume that the system is classically damped, then:

$$\boldsymbol{\Phi}^T\boldsymbol{V}\boldsymbol{\Phi} = \boldsymbol{\Lambda}_D, \tag{3.66}$$

where $\boldsymbol{\Lambda}_D$ is a diagonal matrix whose diagonal elements are $2\zeta_r\omega_r$, being ζ_r the damping ratio in the modal space. By means of the modal transformation:

$$\boldsymbol{u}_f(\tau) = \boldsymbol{\Phi}\boldsymbol{y}(\tau), \tag{3.67}$$

equation (3.63) is rewritten in the decoupled form:

$$\ddot{y_r}(\tau) + 2\zeta_r\omega_r\,\dot{y_r}(\tau) + \omega_r^2 y_r = g_r(\tau), \tag{3.68}$$

where

$$g_r(\tau) = \mathbf{\Phi}_r^T \boldsymbol{M}\boldsymbol{\tau}\bar{\psi}_k(\tau), \tag{3.69}$$

is the forcing function of the r^{th} oscillator in the modal space. In equation (3.69) $\mathbf{\Phi}_r$ is the r^{th} eigenvector. Integrating the equations of motion (3.68) for all the decoupled oscillators, it is possible to obtain $\boldsymbol{u}_f(\tau)$ trough the coordinate transformation (3.67), and hence the response of the system to the k^{th} seismic input $\bar{\psi}_k(\tau)$ in terms of structure node displacements $\boldsymbol{u}_k(\tau) = \boldsymbol{E}\boldsymbol{u}_f(\tau)$ and generalized stresses $\boldsymbol{P}_k(\tau) = \boldsymbol{B}^T\boldsymbol{u}_k(\tau)$.

Now, once assumed that the structure can suffer the action of fixed and seismic loads (as above modeled), it is necessary to individuate appropriate admissible load combinations which characterize some prefixed limit state of the structure during its lifetime. Therefore, as usual, three admissible load combinations of fixed and seismic loads are chosen, and in particular:

1. the first combination is given by the action of the solely fixed loads $\boldsymbol{F}_0$ for which it is possible to known the elastic stress response $\boldsymbol{P}_0$, imposing $\boldsymbol{p} = \boldsymbol{0}$ and neglecting damping and inertia forces;

2. the second combination characterizes the so-called serviceability conditions; it is given as superimposition of reduced fixed loads $\boldsymbol{F}_{s0} = \xi_{s0}\boldsymbol{F}_0$, $0 < \xi_{s0} < 1$, and a repeated seismic excitation model $\bar{\psi}_{sk}(\tau)$, $k \in I(n)$, $0 \le \tau \le t_f$ whose power spectral density function S_{sg} is regulated by a low uniform power density S_{sw}. When the structure is subjected to this load combination the purely elastic stress response to the fixed load $\boldsymbol{P}_{s0}$ and the purely elastic stress response $\boldsymbol{P}_{sk}(\tau)$ to the k^{th} basic seismic input $\bar{\psi}_k(\tau)$, can be evaluated trough the above exposed techniques;

3. finally, the third combination characterizes the so-called ultimate load conditions; it is given as superimposition of reduced fixed loads $\boldsymbol{F}_{l0} = \xi_{l0}\boldsymbol{F}_0$, $0 < \xi_{l0} < 1$, and a repeated seismic excitation model $\bar{\psi}_{lk}(\tau)$, $k \in I(n)$, $0 \le \tau \le t_f$ whose power spectral density function S_{lg} is regulated by a high uniform power density S_{lw}. When the structure is subjected to this load combination the purely elastic stress response to

the fixed load $\boldsymbol{P}_{l0}$ and the purely elastic stress response $\boldsymbol{P}_{lk}(\tau)$ to the k^{th} basic seismic input $\bar{\psi}_k(\tau)$, can be evaluated trough the above exposed techniques.

In correspondence of each load combination a related limit state must be imposed on the structure behavior, and in particular:

1. the structure must behave in a purely elastic manner when subjected to the first load combination;

2. the structure must respond eventually in an elastic manner when subjected to the second load combination (i.e. the structure dynamically shakes down);

3. the structure must prevent the instantaneous collapse when subjected to the last load combination.

As reported in the previous subsection (3.2.1) in order to prevent the instantaneous collapse in an approximate way, some peak stress responses have to be selected from the stress response $\boldsymbol{P}_{lk}(\tau)$, $k \in I(n)$, $0 \leq \tau \leq t_f$. Therefore let define:

$$\boldsymbol{P}_{l1} = \max_{k \in I(n)} \max_{0 \leq \tau \leq t_f} \boldsymbol{P}_{lk}(\tau), \tag{3.70}$$

$$\boldsymbol{P}_{l2} = \min_{k \in I(n)} \min_{0 \leq \tau \leq t_f} \boldsymbol{P}_{lk}(\tau), \tag{3.71}$$

$$\boldsymbol{P}_{l3} = \boldsymbol{G}_N \boldsymbol{P}_{l1} + \boldsymbol{G}_M \boldsymbol{P}_{l2}, \tag{3.72}$$

$$\boldsymbol{P}_{l4} = \boldsymbol{G}_N \boldsymbol{P}_{l2} + \boldsymbol{G}_M \boldsymbol{P}_{l1}, \tag{3.73}$$

with $\boldsymbol{G}_N$ and $\boldsymbol{G}_M$ suitably defined matrices which extract the relevant axial forces and bending moments by the peak vectors $\boldsymbol{P}_{l1}$ and $\boldsymbol{P}_{l2}$.

Taking into account all the remarks previously reported it is possible to formulate an optimal design problem subjected to dynamic (seismic) loads.

Let assume that the design variables can alternatively belong to a continuous and/or to a discrete domain, so that the minimum volume design problem can be formulated as follows:

$$V^* = \min_{\boldsymbol{t}, \boldsymbol{\rho}, \boldsymbol{\rho}_{l1}, \boldsymbol{\rho}_{l2}, \boldsymbol{\rho}_{l3}, \boldsymbol{\rho}_{l4}} V(\boldsymbol{t}) \tag{3.74a}$$

subjected to:

$$t_d \in T_d, \quad (d = 1, 2, \dots, n_d), \tag{3.74b}$$

$$t_c^{\min} \le t_c \le t_c^{\max} \quad (c = n_d + 1, n_d + 2, \dots, n_b \times s), \tag{3.74c}$$

$$\boldsymbol{H}\boldsymbol{t} \ge \bar{\boldsymbol{h}}, \tag{3.74d}$$

$$\boldsymbol{\varphi}_e = \boldsymbol{N}^T \boldsymbol{P}_0 - \boldsymbol{R} \le \boldsymbol{0}, \tag{3.74e}$$

$$\boldsymbol{\varphi}_s = \boldsymbol{N}^T \boldsymbol{P}_{0s} + \check{\boldsymbol{P}} + \boldsymbol{N}^T \boldsymbol{\rho} - \boldsymbol{R} \le \boldsymbol{0}, \tag{3.74f}$$

$$\boldsymbol{A}^T \boldsymbol{\rho} = \boldsymbol{0}, \tag{3.74g}$$

$$\boldsymbol{\varphi}_{l1} = \boldsymbol{N}^T \left(\boldsymbol{P}_{0l} + \boldsymbol{P}_{l1} + \boldsymbol{\rho}_{l1} \right) - \boldsymbol{R} \le \boldsymbol{0}, \tag{3.74h}$$

$$\boldsymbol{\varphi}_{l2} = \boldsymbol{N}^T \left(\boldsymbol{P}_{0l} + \boldsymbol{P}_{l2} + \boldsymbol{\rho}_{l2} \right) - \boldsymbol{R} \le \boldsymbol{0}, \tag{3.74i}$$

$$\boldsymbol{\varphi}_{l3} = \boldsymbol{N}^T \left(\boldsymbol{P}_{0l} + \boldsymbol{P}_{l3} + \boldsymbol{\rho}_{l3} \right) - \boldsymbol{R} \le \boldsymbol{0}, \tag{3.74j}$$

$$\boldsymbol{\varphi}_{l4} = \boldsymbol{N}^T \left(\boldsymbol{P}_{0l} + \boldsymbol{P}_{l4} + \boldsymbol{\rho}_{l4} \right) - \boldsymbol{R} \le \boldsymbol{0}, \tag{3.74k}$$

$$\boldsymbol{A}^T \boldsymbol{\rho}_{l1} = \boldsymbol{0},\ \boldsymbol{A}^T \boldsymbol{\rho}_{l2} = \boldsymbol{0},\ \boldsymbol{A}^T \boldsymbol{\rho}_{l3} = \boldsymbol{0},\ \boldsymbol{A}^T \boldsymbol{\rho}_{l4} = \boldsymbol{0}. \tag{3.74l}$$

3.2.3 Formulations for base isolated structures

Seismic loads on the structure are sometimes catastrophic events. As known, numerous techniques are available in order to reduce the seismic effect on the structures and base-isolation is one of them (see e.g. [11]).

The main feature of the base isolation systems is that to increase the first natural period of the whole structure-base isolation system in such a way to make the structure less sensitive to seismic actions. This effect can be obtained by means of different approaches, alternatively adopting a passive control, an active control or a semi-active control. Basically, these approaches rely on introducing some devices between the soil foundations and the overhanging structure. These devices must possess suitable mechanical characteristics such that to increase the first natural period of the isolated structure through a decoupling of the structure motion from the soil one. The differences among the above referenced systems lie in the fact whether the mechanical features of the device can change, depending on the load history, or not. Clearly, passive control devices are such that their characteristics do not change depending on that of the seismic action, while the active control ones are able to do that.

To the author's knowledge, the base isolation system is, at present, one of the most efficient and economic technique based on passive devices, able to decouple the ground motion from the super-structure one, such that the structural damage is prevented.

Aim of the present subsection is to formulate two optimal design problems: the first one is formulated as the search for the optimal stiffness features (design variables) which minimize the displacement of a base isolation system for a structure with known geometry and such that the overhanging structure behaves elastically under the action of the solely fixed loads and eventually exhibits an elastic shakedown behavior for the combination of fixed loads and repeated seismic loads.

In the second proposed formulation suitable parameters defining the structural geometry as well as the stiffness and damping features of the related base isolation system play the role of design variables and the optimal search problem will be formulated as the minimum volume of the isolated structure constrained to behave elastically when subjected to the solely fixed loads and to elastically shake down when subjected to the combination of fixed loads and repeated seismic loads.

Before to show the proposed formulations, considering that an isolated structure is a non-classically damped one, let show the method to find the linear elastic response of the relevant structure.

So, let consider a base-clamped frame with lumped masses subjected to repeated seismic loads, which equation of motion (3.63) is here rewritten without the subscript f for the sake of clarity:

$$\boldsymbol{M}\ddot{\boldsymbol{u}}(\tau) + \boldsymbol{V}\dot{\boldsymbol{u}}(\tau) + \boldsymbol{K}\boldsymbol{u}(\tau) = -\boldsymbol{M}\boldsymbol{\tau}\bar{\psi}_k(\tau), \tag{3.75}$$

where the vector $\boldsymbol{\tau}$ is the already defined influence vector.

If one want to equip this structure with an isolation system (assumed to have an equivalent linear behavior) has to treat the isolated structure as a dynamical system with substructure (see e.g. [68]). At this purpose let consider that the isolation system is characterized by the following parameters: mass m_b, damping coefficient v_b and stiffness k_b. The n_{iso} equation of motion of the isolated system can be written in the following way:

$$\begin{bmatrix} m_{tot} & \boldsymbol{\tau}^T\boldsymbol{M} \\ \boldsymbol{\tau}^T\boldsymbol{M} & \boldsymbol{M} \end{bmatrix} \begin{bmatrix} \ddot{u}_b \\ \ddot{\boldsymbol{u}} \end{bmatrix} + \begin{bmatrix} v_b & \boldsymbol{0} \\ \boldsymbol{0} & \boldsymbol{V} \end{bmatrix} \begin{bmatrix} \dot{u}_b \\ \dot{\boldsymbol{u}} \end{bmatrix} + \begin{bmatrix} k_b & \boldsymbol{0} \\ \boldsymbol{0} & \boldsymbol{K} \end{bmatrix} \begin{bmatrix} u_b \\ \boldsymbol{u} \end{bmatrix} = - \begin{bmatrix} m_{tot} \\ \boldsymbol{M}\boldsymbol{\tau} \end{bmatrix} \bar{\psi}_k(\tau), \tag{3.76}$$

that can be also written in a compact form:

$$\boldsymbol{M}_{iso}\ddot{\boldsymbol{u}}_{iso} + \boldsymbol{V}_{iso}\dot{\boldsymbol{u}}_{iso} + \boldsymbol{K}_{iso}\boldsymbol{u}_{iso} = \boldsymbol{F}_{iso}(\tau) \tag{3.77}$$

being $m_{tot} = m_b + \boldsymbol{\tau}^T\boldsymbol{M}\boldsymbol{\tau}$ the total mass of the system and u_b the absolute displacement at the isolation level.

It is worth noting that the base isolation system damping coefficient v_b can be computed once assigned the relevant isolation system damping ratio ζ_b, so that the following quantity can be determined:

$$\omega_b = \sqrt{\frac{k_b}{m_{tot}}}, \tag{3.78}$$

$$v_b = 2m_{tot}\omega_b\zeta_b, \tag{3.79}$$

where ω_b is the natural frequency related to the base isolation system (as known, the related period can be easily deduced $T_b = 2\pi/\omega_b$).

It should be observed that the mass, damping and stiffness matrices in equation (3.77) do not satisfy the Caughey-O'Kelly condition [18] namely, the relevant system is not a classically damped one. As a consequence, the elastic-dynamic analysis has to be effected in the state-space variable as synthetically described in the following.

Let introduce the state-space variable vector $\boldsymbol{y} = |\boldsymbol{u}_{iso}{}^T \quad \dot{\boldsymbol{u}}_{iso}^T|^T$, so equation (3.77) can be rewritten in the following form:

$$\hat{\boldsymbol{A}}\dot{\boldsymbol{y}} + \hat{\boldsymbol{B}}\boldsymbol{y} = \hat{\boldsymbol{F}}(\tau), \tag{3.80}$$

that is explicitly:

$$\begin{bmatrix} \boldsymbol{V}_{iso} & \boldsymbol{M}_{iso} \\ \boldsymbol{M}_{iso} & \boldsymbol{0} \end{bmatrix} \begin{bmatrix} \dot{\boldsymbol{u}}_{iso} \\ \ddot{\boldsymbol{u}}_{iso} \end{bmatrix} + \begin{bmatrix} \boldsymbol{K}_{iso} & \boldsymbol{0} \\ \boldsymbol{0} & -\boldsymbol{M}_{iso} \end{bmatrix} \begin{bmatrix} \boldsymbol{u}_{iso} \\ \dot{\boldsymbol{u}}_{iso} \end{bmatrix} = \begin{bmatrix} \boldsymbol{F}_{iso}(\tau) \\ \boldsymbol{0} \end{bmatrix}. \tag{3.81}$$

Solving the eigenvalue problem:

$$\hat{\boldsymbol{A}}\boldsymbol{\Psi}\boldsymbol{\alpha} = -\hat{\boldsymbol{B}}\boldsymbol{\Psi}, \tag{3.82}$$

in which $\boldsymbol{\alpha}$ is a diagonal matrix containing the eigenvalues and $\boldsymbol{\Psi}$ is the modal matrix normalized with respect to $\hat{\boldsymbol{A}}$, it is possible to decouple the system adopting the coordinate transformation $\boldsymbol{y} = \boldsymbol{\Psi x}$ and than, to solve a system of $2n_{iso}$ first order differential equations with complex coefficients. Generally speaking, in non-classically damped systems the elements of $\boldsymbol{\alpha}$ and $\boldsymbol{\Psi}$ are complex and appear in conjugate pairs. As usual (see, e.g. [68]) for any complex eigenvalue $\alpha_j = \beta_j + i\gamma_j$, it is possible to identify the natural frequency as $\omega_j = \sqrt{\beta_j^2 + \gamma_j^2}$, and the damping ratio as $\zeta_j = -\beta_j/\omega_j$ corresponding to a classically damped system.

The solution of the system (3.77) together with the corresponding initial conditions provides the structural response in terms of horizontal displacements. Once these last are known, the complete frame node displacement vector can be determined utilizing the appropriate reordering matrix, and eventually the related element generalized stress vector $\boldsymbol{P}$ due to the dynamic actions.

In order to formulate a base isolation system minimum displacement design problem, let us consider a frame structure with known geometry subjected to fixed and repeated seismic loads. Aim of the present formulation is to determine the optimal values of the base isolation stiffness which minimizes the base isolation displacement and such that the structure behaves elastically for fixed loads and eventually shakes down for the load combination defined by the simultaneous presence of fixed and high level seismic actions.

The design problem can be written in the following form:

$$u_b^* = \min_{k_b, \boldsymbol{\rho}} u_b(k_b) \tag{3.83a}$$

subjected to:

$$k_b \geq k_b^{\min} \tag{3.83b}$$

$$u_b = \max_{k \in I(n)} \max_{0 \leq \tau \leq t_f} \left(|u_{b0}| + |u_{bk}(\tau)| \right) \tag{3.83c}$$

$$\boldsymbol{\varphi}_e = \boldsymbol{N}^T \boldsymbol{P}_0 - \boldsymbol{R} \leq \boldsymbol{0}, \tag{3.83d}$$

$$\boldsymbol{\varphi}_s = \boldsymbol{N}^T \boldsymbol{P}_{0s} + \check{\boldsymbol{P}} + \boldsymbol{N}^T \boldsymbol{\rho} - \boldsymbol{R} \leq \boldsymbol{0}, \tag{3.83e}$$

$$\boldsymbol{A}^T \boldsymbol{\rho} = \boldsymbol{0}, \tag{3.83f}$$

being u_b the base isolation system total displacement, u_{b0} the base isolation system displacement related to the fixed loads, k_b the stiffness of the base isolation system and $k_b^{\min}$ the assigned minimum value for the defined stiffness and where the seismic response is obtained by means of the modal complex analysis above described.

A second formulation of the optimal design problem is now proposed. It is related to the search of the minimum volume design of the structure provided with a base isolation system with damped and stiffness features variable within assigned ranges. Following the same approach as before, the design problem can be written in the following form:

$$V^* = \min_{\boldsymbol{t},\boldsymbol{\rho}} V(\boldsymbol{t}) \tag{3.84a}$$

subjected to:

$$k_b^{\min} \leq k_b \leq k_b^{\max} \tag{3.84b}$$

$$\zeta_b^{\min} \leq \zeta_b \leq \zeta_b^{\max} \tag{3.84c}$$

$$\varphi_b = P_b - R_b \leq 0 \tag{3.84d}$$

$$t_d \in T_d, \quad (d = 1, 2, \ldots, n_d), \tag{3.84e}$$

$$t_c^{\min} \leq t_c \leq t_c^{\max} \quad (c = n_d + 1, n_d + 2, \ldots, n_b \times s), \tag{3.84f}$$

$$\boldsymbol{H}\boldsymbol{t} \geq \bar{\boldsymbol{h}}, \tag{3.84g}$$

$$\boldsymbol{\varphi}_e = \boldsymbol{N}^T \boldsymbol{P}_0 - \boldsymbol{R} \leq \boldsymbol{0}, \tag{3.84h}$$

$$\boldsymbol{\varphi}_s = \boldsymbol{N}^T \boldsymbol{P}_{0s} + \check{\boldsymbol{P}} + \boldsymbol{N}^T \boldsymbol{\rho} - \boldsymbol{R} \leq \boldsymbol{0}, \tag{3.84i}$$

$$\boldsymbol{A}^T \boldsymbol{\rho} = \boldsymbol{0}, \tag{3.84j}$$

being $k_b^{\min}$ and $k_b^{\max}$, $\zeta_b^{\min}$ and $\zeta_b^{\max}$ assigned lower and upper bounds of stiffness and damping ranges related to the base isolation system. In equation (3.84d) a mechanical constraint on the limit capacity of the isolation system is introduced, where P_b is the maximum absolute value of the shear force due to the combination of fixed and seismic actions and R_b is the base isolation system resistance. It is worth noticing that the value assigned to R_b usually depends on the maximum allowed base isolation system displacement, so that the solution to problem (3.84) provides a complete design coherent with the technological requirements satisfied through the solution to problem (3.83).

Chapter 4

Computational procedures

Since 1970 structural optimization has been the subject of intensive research. In this field, one of the most important aspect is represented by the computational procedures adopted to solve the optimization problem. From the above disclosure, it is clear that the optimal design problems formulated in Chapter 3 are non-linear mathematical programming ones. This kind of problems are usually solved making reference to iterative procedures consisting in the linearization of the original functions by using their derivatives with respect to the design variables. In this way, an approximate problem whose optimality conditions are the same of the initial problem can be constructed. So, utilizing this iterative procedure the actual optimal solution can be reached. In the present thesis, this procedure has been widely used to solve problems involving continuous variables and it is an extension to the present context of what done by Giambanco et al. [46].

On the other hand, one of the objectives of this thesis was to provide optimal design formulations that could be as much as possible consistent with real-world applications. In practice, in sizing optimization problem with stress constraints the design variables belong to a discrete set of variables and so the problem requires combinatorial optimization methods based on probabilistic searching. During the last three decades there has been a growing interest in problem solving systems based on algorithms that rely on analogies to natural processes. The best-known algorithms in this class include evolutionary programming [39], genetic algorithms [51], evolution strategies [83], ant colony optimization [38], particle swarm optimization [59] and harmony search method [42].

None of the above algorithms had been used in the past for sizing optimization of structures with shakedown and instantaneous collapse constraints, and therefore the choice to use in the present thesis the harmony search is based on a recent comparative study [54] of the above algorithms for optimization problems with only elastic stress constraints, in which the harmony search results to be a good compromise between convergence and performance. The harmony search method has been specialized to solve problems as formulated in Chapter 3 involving discrete variables but the procedures presented in the following can be easily extended to problems involving continuous variables.

4.1 Iterative technique

Let recall the optimal design problem formulation (3.39) assuming that all the design variables can vary in a continuous range whose bounds are represented by $\boldsymbol{t}^{\min}$ and $\boldsymbol{t}^{\max}$:

$$V^* = \min_{\boldsymbol{t},\boldsymbol{Y},\boldsymbol{Y}_i} V(\boldsymbol{t}), \tag{4.1a}$$

subjected to:

$$\boldsymbol{t}^{\min} \leq \boldsymbol{t} \leq \boldsymbol{t}^{\max}, \tag{4.1b}$$

$$\boldsymbol{H}\boldsymbol{t} \geq \bar{\boldsymbol{h}}, \tag{4.1c}$$

$$\boldsymbol{\varphi}_e = \boldsymbol{N}^T \boldsymbol{P}_0 - \boldsymbol{R} \leq \boldsymbol{0}, \tag{4.1d}$$

$$\boldsymbol{\varphi}_{si} = \boldsymbol{N}^T \left[\boldsymbol{P}_{s0} + (-1)^i \boldsymbol{P}_s\right] - \boldsymbol{S}\boldsymbol{Y} - \boldsymbol{R} \leq \boldsymbol{0} \quad (i = 1, 2), \tag{4.1e}$$

$$\boldsymbol{Y} \geq \boldsymbol{0}, \tag{4.1f}$$

$$\boldsymbol{\varphi}_{li} = \boldsymbol{N}^T \left[\boldsymbol{P}_{l0} + (-1)^i \boldsymbol{P}_l\right] - \boldsymbol{S}\boldsymbol{Y}_i - \boldsymbol{R} \leq \boldsymbol{0} \quad (i = 1, 2), \tag{4.1g}$$

$$\boldsymbol{Y}_i \geq \boldsymbol{0}, \quad (i = 1, 2). \tag{4.1h}$$

Due to the high non linearity of the relevant search problem an appropriate iterative technique has been utilized as described in the following; it is a specialization of an already proposed one in the framework of the elastic shakedown design [46].

The proposed technique is based on the main assumption that all the quantities depending on the design variables can be expressed as a linear functions of these variables, i.e. as the sum of their values at the previous step plus the product of their partial derivatives with respect to the design variables times the increments of the design variables.

At each step, the computational procedures is constituted by three subsequent phases and at each phase some variables are assumed as known while the other ones are brought up to date, so that at the end of all phases all the variable values are updated. Obviously, the procedure stops when the relevant design variable values at two subsequent steps differ less than a suitably assigned tolerance.

It is worth noting that, as stated by Giambanco et al. [46], the design reached by means of this iterative technique coincides with the design obtainable by solving problem (4.1) because the design and behavioral variable values obtained by means of the proposed technique fulfill all the Kuhn-Tucker equations related to the original design problem (4.1).

Making reference to problem and to the k^{th} typical step, the three relevant phases are described as follows:

1. the purely elastic response of the structure is evaluated utilizing the design variable values $\boldsymbol{t}^{k-1}$ obtained at the end of the previous step ($\boldsymbol{t}^0 = \boldsymbol{t}_0$ is the initial design):

$$\boldsymbol{P}_0{}^{(k-1)} = \boldsymbol{B}^{T(k-1)} \boldsymbol{K}^{-1(k-1)} \boldsymbol{F}_0{}^{(k-1)} + \boldsymbol{P}_0^{*(k-1)} \tag{4.2a}$$

$$\boldsymbol{P}_{s0}{}^{(k-1)} = \boldsymbol{B}^{T(k-1)} \boldsymbol{K}^{-1(k-1)} \boldsymbol{F}_{s0}{}^{(k-1)} + \boldsymbol{P}_{s0}^{*(k-1)} \tag{4.2b}$$

$$\boldsymbol{P}_{sj}{}^{(k-1)} = \boldsymbol{B}^{T(k-1)} \boldsymbol{E} \boldsymbol{\Phi}^{(k-1)} \frac{\boldsymbol{\Phi}^{T(k-1)} \boldsymbol{M} \boldsymbol{\tau} [S_s(T_j)]^{(k-1)}}{\omega_j^{2(k-1)}} \tag{4.2c}$$

$$P_{s\ell}{}^{(k-1)} = \sqrt{\sum_j \sum_k \rho_{jk} P_{s\ell j}{}^{(k-1)} P_{s\ell k}{}^{(k-1)}} \tag{4.2d}$$

$$\boldsymbol{P}_{l0}{}^{(k-1)} = \boldsymbol{B}^{T(k-1)} \boldsymbol{K}^{-1(k-1)} \boldsymbol{F}_{l0}{}^{(k-1)} + \boldsymbol{P}_{l0}^{*(k-1)} \tag{4.2e}$$

$$\boldsymbol{P}_{lj}{}^{(k-1)} = \boldsymbol{B}^{T(k-1)} \boldsymbol{E} \boldsymbol{\Phi}^{(k-1)} \frac{\boldsymbol{\Phi}^{T(k-1)} \boldsymbol{M} \boldsymbol{\tau} [S_l(T_j)]^{(k-1)}}{\omega_j^{2(k-1)}} \tag{4.2f}$$

$$P_{l\ell}{}^{(k-1)} = \sqrt{\sum_j \sum_k \rho_{jk} P_{l\ell j}{}^{(k-1)} P_{l\ell k}{}^{(k-1)}} \tag{4.2g}$$

2. the increments $\Delta \boldsymbol{t}^{(k)}$ of the design variable values and the remaining variables of problem (4.1) are obtained by the solution of the following linearized minimum search problem:

$$\min_{\left(\Delta \boldsymbol{t}^{(k)}, \boldsymbol{Y}^{(k)}, \boldsymbol{Y}_i^{(k)}\right)} \left.\frac{\partial V}{\partial \boldsymbol{t}}\right|_{(k-1)} \Delta \boldsymbol{t}^{(k)} \tag{4.3a}$$

subjected to:

$$\boldsymbol{t}^{\min} \leq \boldsymbol{t}^{(k-1)} + \Delta \boldsymbol{t}^{(k)} \leq \boldsymbol{t}^{\max}, \tag{4.3b}$$

$$\boldsymbol{H}\left(\boldsymbol{t}^{(k-1)} + \Delta \boldsymbol{t}^{(k)}\right) - \bar{\boldsymbol{h}} \geq \boldsymbol{0}, \tag{4.3c}$$

$$\boldsymbol{\varphi_e}^{(k)} = \boldsymbol{\varphi_e}^{(k-1)} + \left.\frac{\partial \boldsymbol{\varphi_e}}{\partial \boldsymbol{t}}\right|_{(k-1)} \Delta \boldsymbol{t}^{(k)} \leq \boldsymbol{0}, \tag{4.3d}$$

$$\boldsymbol{\varphi_{si}}^{(k)} = \boldsymbol{\varphi_{si}}^{(k-1)} + \left.\frac{\partial \boldsymbol{\varphi_{si}}}{\partial \boldsymbol{t}}\right|_{(k-1)} \Delta \boldsymbol{t}^{(k)} \leq \boldsymbol{0} \quad (i = 1, 2), \tag{4.3e}$$

$$\boldsymbol{Y}^k \geq \boldsymbol{0}, \tag{4.3f}$$

$$\boldsymbol{\varphi_{li}}^{(k)} = \boldsymbol{\varphi_{li}}^{(k-1)} + \left.\frac{\partial \boldsymbol{\varphi_{li}}}{\partial \boldsymbol{t}}\right|_{(k-1)} \Delta \boldsymbol{t}^{(k)} \leq \boldsymbol{0} \quad (i = 1, 2), \tag{4.3g}$$

$$\boldsymbol{Y}_i^k \geq \boldsymbol{0} \quad (i = 1, 2), \tag{4.3h}$$

where the partial derivative with respect to $\boldsymbol{t}$ are related with all the quantities depending on it ($\boldsymbol{N}$, $\boldsymbol{P}_0$, $\boldsymbol{P}_{0s}$, $\boldsymbol{P}_s$, $\boldsymbol{P}_{0l}$, $\boldsymbol{P}_l$, $\boldsymbol{R}$) except for the matrix $\boldsymbol{S}$. Actually, in order to obtain the linearized form of the relevant search problem the terms:

$$\left.\frac{\partial \boldsymbol{S}}{\partial \boldsymbol{t}}\right|_{(k-1)} \boldsymbol{Y}^{(k)}, \tag{4.4a}$$

$$\left.\frac{\partial \boldsymbol{S}}{\partial \boldsymbol{t}}\right|_{(k-1)} \boldsymbol{Y}_i^{(k)} \quad (i = 1, 2), \tag{4.4b}$$

in equations (4.3e) and (4.3g) respectively, have been disregarded. The neglecting of these terms does not influence the obtainable optimal design (see e.g. [46]) while the variables $\boldsymbol{Y}^{(k)}$, $\boldsymbol{Y}_i^{(k)}$, $(i = 1, 2)$, appear in $\boldsymbol{\varphi_{si}}^{(k-1)}$, $\boldsymbol{\varphi_{li}}^{(k-1)}$, $(i = 1, 2)$, respectively.

3. The design variable values are updated by

$$\boldsymbol{t}^{(k)} = \boldsymbol{t}^{(k-1)} + \boldsymbol{\beta}^{(k)} \Delta \boldsymbol{t}^{(k)} \tag{4.5}$$

   where the elements of the diagonal matrix $\boldsymbol{\beta}^{(k)}$ are suitably chosen weight coefficients which can also vary at each step.

Clearly, the procedure stops when $\Delta \boldsymbol{t}^{(k)} = \mathbf{0}$ within a suitably prefixed tolerance.

This procedure has been used to solve all the optimal design problems when they involved continuous design variables. Nevertheless, a further computational aspect has to be shown for the optimal design problem of structure with limited ductility.

As it is easy to observe, problem (3.41) is a strongly non-linear one and, as a consequence, it can be solved only making recourse to appropriate simplified and/or approximate methods. It is worth noticing that the main non linearity is related to the presence of the constraints (3.41j, 3.41k); actually, if no bounds are prescribed the remaining problem, even if non-linear, can be solved by making recourse to the above linearization method (when it involves just continuous variables). In order to computationally solve the complete problem (3.41), a simple parametric approach is proposed, later on tested in the application stage.

Let assume for the optimal design problem formulation (3.41) that all the design variables can vary in a continuous range whose bounds are represented by $\boldsymbol{t}^{\min}$ and $\boldsymbol{t}^{\max}$. In this way the minimum volume problem can be solved in an approximate way, operating two subsequent steps:

1. at first the following problem is solved for a suitably chosen number of assigned values of the perturbation multiplier $\bar{\omega}$, i.e. with the above exposed iterative technique:

$$\min_{\boldsymbol{t}, \hat{\boldsymbol{Y}}, \boldsymbol{Y}_i} V(\boldsymbol{t}), \tag{4.6a}$$

   subjected to:

$$\boldsymbol{t}^{\min} \leq \boldsymbol{t} \leq \boldsymbol{t}^{\max}, \tag{4.6b}$$

$$\boldsymbol{H}\boldsymbol{t} \geq \bar{\boldsymbol{h}}, \tag{4.6c}$$

$$\boldsymbol{\varphi}_e = \boldsymbol{N}^T \boldsymbol{P}_0 - \boldsymbol{R} \leq \mathbf{0}, \tag{4.6d}$$

$$\boldsymbol{\varphi}_{si} = \boldsymbol{N}^T \left[\boldsymbol{P}_{s0} + (-1)^i \boldsymbol{P}_s \right] - \boldsymbol{S}\hat{\boldsymbol{Y}} + \bar{\omega}\hat{\boldsymbol{R}} - \boldsymbol{R} \leq \mathbf{0} \quad (i = 1, 2), \tag{4.6e}$$

$$\hat{\boldsymbol{Y}} \geq \mathbf{0}, \tag{4.6f}$$

$$\boldsymbol{\varphi}_{li} = \boldsymbol{N}^T \left[\boldsymbol{P}_{l0} + (-1)^i \boldsymbol{P}_l \right] - \boldsymbol{S}\boldsymbol{Y}_i - \boldsymbol{R} \leq \mathbf{0} \quad (i = 1, 2), \tag{4.6g}$$

$$\boldsymbol{Y}_i \geq \mathbf{0}, \quad (i = 1, 2). \tag{4.6h}$$

2. Subsequently, the minimum structural volume is determined as function of the solely variable ω:

$$V^* = \min_{\omega} V(\omega), \tag{4.7a}$$

$$\frac{1}{2} \hat{\boldsymbol{Y}}^T(\omega) \boldsymbol{S} \hat{\boldsymbol{Y}}(\omega) + \omega \left(|U_{te}|_{\max} - \bar{U}_t \right) \leq 0, \tag{4.7b}$$

It should be noted that if the problem had been formulated with discrete variables the first step of this procedure had to be faced with another solution procedure, such as the one that will be shown in the next section.

4.2 The harmony search algorithm

The harmony search (HS) algorithm was proposed by Geem et al. [42] by adopting the idea that existing meta-heuristic algorithms are found in the observation of natural phenomena. In particular this algorithm is based on natural musical performance processes that occur when a musician searches for a better state of harmony, such as during jazz improvisation. In fact, when jazz musicians play together they select the musical notes in their instruments to give the best overall harmony with the rest of the group. Each musician plays notes, remembering what he had played in a previous session. Sometimes he prefers to improvise a few notes, and if the result is aesthetically pleasing, it will remain in the memory of all the musicians, who will use this harmony for a later session. In other words, jazz improvisation seeks to find musically a perfect state of harmony as determined by an aesthetic standard, just as the optimization process seeks to find a global solution (a perfect state) as determined by an objective function. The pitch of each musical instrument determines the aesthetic quality, just as the objective function value is determined by the set of values assigned to each decision variable.

For optimization, people have traditionally used gradient-based algorithms that give right information in order to find the right direction to the optimal solution. On the contrary, HS does not require differential gradients, thus it can consider discontinuous functions as well as continuous functions and moreover it can handle discrete variables as well as continuous variables.

For the purpose of the present thesis, this algorithm has been used to solve optimal design problems involving discrete variables. In order to show the algorithm procedures, let consider the following standard optimal design problem in which the vector of the design variables $\boldsymbol{t}$ is a row one:

$$V^* = \min_{\boldsymbol{t},\boldsymbol{Y},\boldsymbol{Y}_i} V(\boldsymbol{t}), \tag{4.8a}$$

subjected to:

$$t_i \in T_i \equiv \{t_i(1), t_i(2), \ldots, t_i(q)\} \quad \forall i \in I(n_d) \tag{4.8b}$$

$$\boldsymbol{H}\boldsymbol{t}^T \geq \bar{\boldsymbol{h}}, \tag{4.8c}$$

$$\boldsymbol{\varphi}_e = \boldsymbol{N}^T\boldsymbol{P}_0 - \boldsymbol{R} \leq \boldsymbol{0}, \tag{4.8d}$$

$$\boldsymbol{\varphi}_{si} = \boldsymbol{N}^T\left[\boldsymbol{P}_{s0} + (-1)^i\boldsymbol{P}_s\right] - \boldsymbol{S}\boldsymbol{Y} - \boldsymbol{R} \leq \boldsymbol{0} \quad (i = 1, 2), \tag{4.8e}$$

$$\boldsymbol{Y} \geq \boldsymbol{0}, \tag{4.8f}$$

$$\boldsymbol{\varphi}_{li} = \boldsymbol{N}^T\left[\boldsymbol{P}_{l0} + (-1)^i\boldsymbol{P}_l\right] - \boldsymbol{S}\boldsymbol{Y}_i - \boldsymbol{R} \leq \boldsymbol{0} \quad (i = 1, 2), \tag{4.8g}$$

$$\boldsymbol{Y}_i \geq \boldsymbol{0}, \quad (i = 1, 2). \tag{4.8h}$$

where t_i is the i^{th} discrete variable that can assume one of the q values within the discrete set T_i and n_d is the total number of discrete variables.

The solution of the described optimum design problem can be reached in seven basic steps which are summarized in the following and sketched in Figure 4.1:

1. Harmony search parameters are initialized.

   The HS algorithm parameters that are required to solve the optimization problem (4.8) are specified in this step. In particular, HMS is the number of solution vectors simultaneously handled in the algorithm and

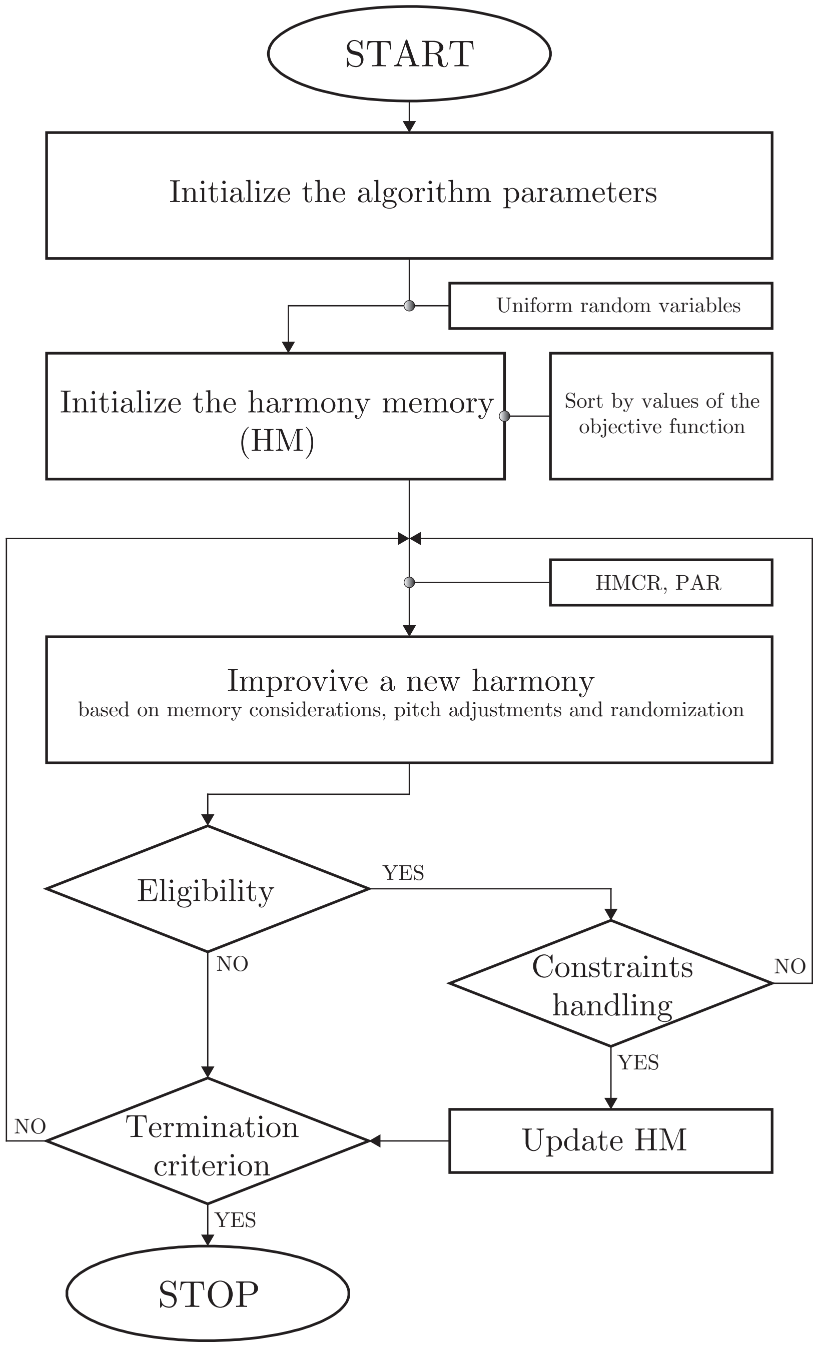

Figure 4.1: Basic flowchart diagram for Harmony Search algorithm.

it represents the size of the harmony memory matrix, HMCR is the rate $(0 \leq \text{HMCR} \leq 1)$ where the algorithm picks one value randomly from harmony memory matrix, thus, $(1 - \text{HMCR})$ is the rate where HS picks one value randomly from total value range, PAR $(0 \leq \text{PAR} \leq 1)$ is the rate where the harmony search tweaks the value which was originally picked from memory, thus, $(1 - \text{PAR})$ is the rate where the algorithm keeps the original value obtained from memory, and finally, MI is the maximum number of iterations.

Originally fixed parameter values were considered by Geem et al. [42]. However, some researchers have proposed changeable parameter values. Degertekin [33], in order to increase the algorithm performances, suggested that PAR may decrease linearly with iterations:

$$\text{PAR}\,(\text{I}) = \text{PAR}^{\max} - \left(\text{PAR}^{\max} - \text{PAR}^{\min}\right) \frac{\text{I}}{\text{MI}} \tag{4.9}$$

being I the iteration number and $\text{PAR}^{\max}$, $\text{PAR}^{\min}$ two suitable parameters. In fact, the search space to be explored should be vast in the first stages of the algorithm and should be then limited within a neighborhood of the optimum design.

2. Harmony memory matrix $\boldsymbol{HM}$ is initialized.

   Each row of the harmony memory matrix contains the values of an "harmony $\boldsymbol{t}$", i.e. the values of the design variables which are randomly selected from the design pool and the value of the objective function $V(\boldsymbol{t})$. Hence the matrix has $n_d + 1$ columns and HMS rows which number is selected in the first step. So, the harmony memory matrix can be written in the following form:

$$\boldsymbol{HM} = \left[\begin{array}{cccc|c} t_1^{(1)} & t_2^{(1)} & \cdots & t_{n_d}^{(1)} & V\left(\boldsymbol{t}^{(1)}\right) \\ t_1^{(2)} & t_2^{(2)} & \cdots & t_{n_d}^{(2)} & V\left(\boldsymbol{t}^{(2)}\right) \\ \vdots & & \ddots & \vdots & \vdots \\ t_1^{(\text{HMS})} & t_2^{(\text{HMS})} & \cdots & t_{n_d}^{(\text{HMS})} & V\left(\boldsymbol{t}^{(\text{HMS})}\right) \end{array}\right] \tag{4.10}$$

   It is worth mentioning that just the feasible designs which satisfy the constraints (4.8c) to (4.8h) are inserted into the harmony memory matrix. Indeed, some authors suggest to insert those designs having a small unfeasibility in the matrix using a penalty on their objective function (see e.g. [62, 82]).

The solution vectors contained by the harmony memory matrix are sorted so that the volume corresponding to the first solution vector $\boldsymbol{t}^{(1)}$ is the minimum and $\boldsymbol{t}^{(\mathrm{HMS})}$ is the worst. In other words, the feasible solutions are sorted in descending order according to their objective function $V(\boldsymbol{t})$. Furthermore, at this stage the iteration number is set $\mathrm{I} = 1$.

3. A new harmony $\boldsymbol{t}^{(\mathrm{new})}$ is improvised.

   In generating a new harmony matrix the new value of the i^{th} design variable can be chosen from any discrete value within the range of the i^{th} column of the harmony memory matrix with the probability HMCR which varies between 0 and 1. In other words, the new value of t_i can be one of the discrete values of the column vector $\left[t_i^{(1)}, t_i^{(2)}, \ldots, t_i^{(\mathrm{HMS})}\right]^T$ with the probability of HMCR. The same is applied to all other design variables. In the random selection, the new value of the i^{th} design variables can also be chosen randomly from the entire pool with the probability of $1-\mathrm{HMCR}$. This sub-operation called, "memory consideration", is effected generating a random number (rn) uniformly distributed over the interval $[0, 1]$ and than:

$$t_i^{(\mathrm{new})} \longleftarrow \begin{cases} t_i \in \quad \left[t_i^{(1)}, t_i^{(2)}, \ldots, t_i^{(\mathrm{HMS})}\right]^T & \text{if } rn \leq \mathrm{HMCR} \\ t_i \in \quad T_i \equiv \{t_i(1), t_i(2), \ldots, t_i(q)\} & \text{if } rn > \mathrm{HMCR} \end{cases} \tag{4.11}$$

   where, as above stated q is the total number of values in the design set T_i.

   If the new value of the design variable is selected from among those of harmony memory matrix (first choice in 4.10), this value is then checked whether it should be pitch-adjusted. This sub-operation can be effected using the pitch-adjustment parameter PAR as the defined in the first step and other random number (rn) uniformly distributed over the interval

$[0, 1]$ so that:

$$\text{pitch adjusting decision} \longleftarrow \begin{cases} \text{Yes} & \text{if } rn \leq \text{PAR} \\ \\ \text{No} & \text{if } rn > \text{PAR} \end{cases} \tag{4.12}$$

Supposing that the new pitch-adjustment decision for $t_i^{(\text{new})}$ came out to be yes from the test and if the value selected for $t_i^{(\text{new})}$ from the harmony memory is the k^{th} element in the general discrete set T_i, then the neighboring value $k+1$ or $k-1$ is taken for new $t_i^{(\text{new})}$. This operation permit to escape local minima and improves the harmony memory for diversity with a greater change of reaching the global optimum.

4. Check on the eligibility of $\boldsymbol{t}^{(\text{new})}$ to be stored in harmony memory matrix.

   After the definition of the new harmony vector $\boldsymbol{t}^{(\text{new})}$, the related value of the objective function $V\left(\boldsymbol{t}^{(\text{new})}\right)$ is calculated. If this value is better than the worst harmony vector in the harmony matrix, in that case it is eligible to be included in the harmony matrix and the following step can be effected. If it is worse than the worst harmony vector in the harmony matrix and a new iteration is required, so that the iteration number is set $\text{I}+1$ and step (3) is repeated. It is worth noting that this check is done before to control that all the constraints (4.8c) to (4.8h) are satisfied, because from a computational point of view this operation requires less time computing than the following one.

5. Constraints handling.

   Once the new harmony vector $\boldsymbol{t}^{(\text{new})}$ is obtained using the above mentioned rules, it is then checked whether it violates problem constraints. If the new harmony vector is unfeasible, it is discarded, the iteration number is set $\text{I}+1$ and step (3) is repeated.

   In particular, as one can see, the problem (4.8) is a multi-constrained one involving a technological constraint (4.8c), a constraint on the elastic stresses (4.8d), constraints on the shakedown behavior (4.8e,4.8f) and constraint preventing the instantaneous collapse (4.8g,4.8h). So, the feasibility is checked by four subsequent sub-operation:

a) first of all, the linear technological constraint (4.8c) is checked. If $\boldsymbol{Ht}^{(\text{new})^T} \geq \bar{\boldsymbol{h}}$, the following sub-operation can be conducted. When, at least one of the value $\boldsymbol{Ht}^{(\text{new})^T} - \bar{\boldsymbol{h}}$ is less than zero a new iteration is required.

b) for the referenced structure subjected to the first load combination the purely elastic response to the applied loads is calculated in terms of generalized stresses $\boldsymbol{P}_0$. If $\boldsymbol{N}^T\boldsymbol{P}_0 \leq \boldsymbol{R}$ the following sub-operation can be conducted. When, at least one of the value $\boldsymbol{N}^T\boldsymbol{P}_0 - \boldsymbol{R}$ is greater than zero a new iteration is required.

c) for the referenced structure subjected to the second load combination in order to control if it is able to shake down, a shakedown analysis has to be conducted. Once the purely elastic responses $\boldsymbol{P}_{s0}$ and $\boldsymbol{P}_s$ are calculated the following linear programming problem has to be solved:

$$\xi^s = \max_{\xi,\boldsymbol{Y}} \xi, \tag{4.13a}$$

subjected to:

$$\varphi_{s1} = \boldsymbol{N}^T\left[\boldsymbol{P}_{s0} + \xi\boldsymbol{P}_s\right] - \boldsymbol{SY} - \boldsymbol{R} \leq \boldsymbol{0}, \tag{4.13b}$$

$$\varphi_{s2} = \boldsymbol{N}^T\left[\boldsymbol{P}_{s0} - \xi\boldsymbol{P}_s\right] - \boldsymbol{SY} - \boldsymbol{R} \leq \boldsymbol{0}, \tag{4.13c}$$

$$\boldsymbol{Y} \geq \boldsymbol{0}. \tag{4.13d}$$

If $\xi^s \geq 1$ the following sub-operation can be conducted. If $\xi^s < 1$ a new iteration is required.

d) for the referenced structure subjected to the third load combination in order to control if it is able to prevent the instantaneous collapse, a limit analysis has to be conducted. Once the purely elastic responses $\boldsymbol{P}_{l0}$ and $\boldsymbol{P}_l$ are calculated the following linear programming problem has to be solved:

$$\xi^l = \max_{\xi,\boldsymbol{Y}_1,\boldsymbol{Y}_2} \xi, \tag{4.14a}$$

subjected to:

$$\varphi_{l1} = \boldsymbol{N}^T\left[\boldsymbol{P}_{l0} + \xi\boldsymbol{P}_l\right] - \boldsymbol{SY}_1 - \boldsymbol{R} \leq \boldsymbol{0}, \tag{4.14b}$$

$$\varphi_{l2} = \boldsymbol{N}^T\left[\boldsymbol{P}_{l0} - \xi\boldsymbol{P}_l\right] - \boldsymbol{SY}_2 - \boldsymbol{R} \leq \boldsymbol{0}, \tag{4.14c}$$

$$\boldsymbol{Y}_1 \geq \mathbf{0}, \quad \boldsymbol{Y}_2 \geq \mathbf{0}. \tag{4.14d}$$

If $\xi^l \geq 1$ the structure satisfy all the above constraints and following step can be effected. If $\xi^l < 1$ a new iteration is required.

6. Harmony memory matrix is updated.

   After that it has been controlled that the the new harmony $\boldsymbol{t}^{(\text{new})}$ satisfies all the constraints the harmony memory matrix is updated. In step (4), the eligibility of $\boldsymbol{t}^{(\text{new})}$ has been checked and rated in terms of the objective function value, so it is included in the harmony memory matrix and the worst harmony (e.g. $\boldsymbol{t}^{(\text{HMS})}$) is excluded from it:

$$\boldsymbol{HM} = \left[\begin{array}{cccc|c} t_1^{(1)} & t_2^{(1)} & \cdots & t_{n_d}^{(1)} & V\left(\boldsymbol{t}^{(1)}\right) \\ t_1^{(2)} & t_2^{(2)} & \cdots & t_{n_d}^{(2)} & V\left(\boldsymbol{t}^{(2)}\right) \\ \vdots & & \ddots & \vdots & \vdots \\ t_1^{(\text{new})} & t_2^{(\text{new})} & \cdots & t_{n_d}^{(\text{new})} & V\left(\boldsymbol{t}^{(\text{new})}\right) \end{array}\right]. \tag{4.15}$$

   The harmony memory matrix is then sorted again in descending order by the objective function value, the iteration number is set I + 1 and step (3) is repeated.

7. Termination criterion.

   Steps (3) to (6) are repeated until the termination criterion which is the pre-selected maximum number of iteration MI is reached. This number is selected large enough so that within this number of the design iteration no further improvement is observed in the objective function.

Chapter 5

Case studies

In the framework of numerical applications, special reference is made to steel frame structures. Several case studies have been proposed and the most significant are exposed in the present chapter. They are described in a sequence following the developments of the thesis: starting with a probabilistic dynamic shakedown analysis, going on the optimal design of frames subjected to cyclic loads, and finally, the optimal design of frames subjected to dynamic loads.

5.1 A probabilistic dynamic shakedown analysis

In this section, the concepts shown in section (2.3) are explored trough a numerical application related to steel frames subjected to wind loads.

The plane steel frame considered in this application is constituted by five floors and two spans. As shown in Figure 5.1 the topology of the frame is fully described by the span lengths (here assumed as $L_1 = 600$ cm, $L_2 = 400$ cm) and by the inter-story height ($H = 400$ cm). The material model, above assumed as elastic perfectly plastic (Figure 5.2), is completely defined trough the yield stress σ_y and the Young modulus E. For each element, these two parameters are considered as uncertainties. In particular a log-normal distribution is assigned both for yield stress (mean 235 MPa and standard deviation 15 MPa) and for elasticity modulus (mean 210 GPa and standard deviation 10 GPa). Obviously, this choice makes aleatory both the stiffness and the resistance of the structure.

All the elements constituting the frame have a box cross section (Fig-

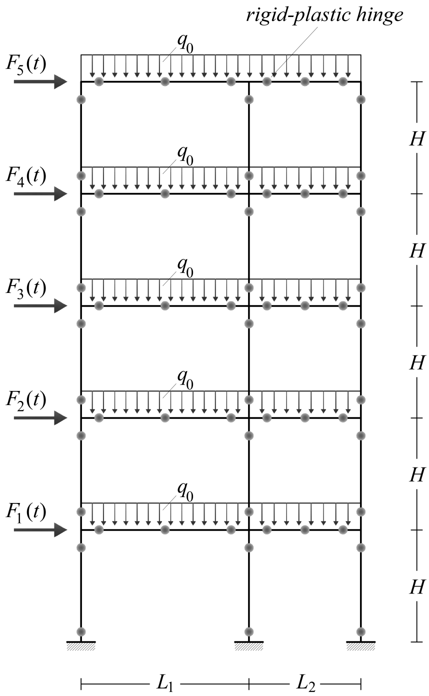

Figure 5.1: Five floors steel frame: geometry and load conditions

ure 5.3a) with length $b = 200$ mm, height $h = 300$ mm and constant thickness $t = 10$ mm. Furthermore, as one can see in Figure 5.1, two rigid perfectly plastic hinges are located at the extremes of each element and an additional one is positioned in the middle of all beams. As known, the convex yielding domain of a plastic hinge depends on the particular cross section chosen and it can be piece-wise linearized. In the present example, as shown in Figure 5.3b, the yielding domain has been assumed in such a way to consider the interaction between the bending moment M and the axial stress N. It's worth noticing that the yielding axial stress can be obtained as $N_y = \sigma_y A$ and the yielding bending moment as $M_y = \sigma_y M_p$, being A and M_p the area and the plastic moment of the cross section.

When the structure is subjected to to an arbitrary excitation history (see e.g. section 2.3), which stationary segment $\boldsymbol{F}(t)$, $0 \leq t \leq T$ induces the maximum plastic demand in time on the structure, the fictitious elastic stress

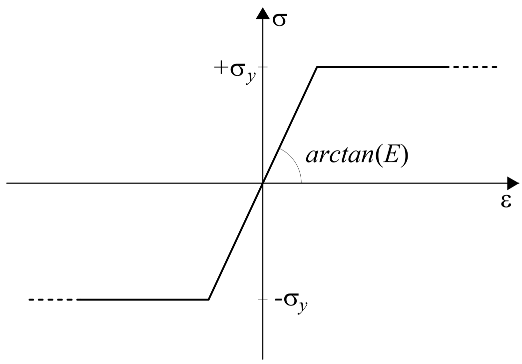

Figure 5.2: Elastic perfectly plastic material model

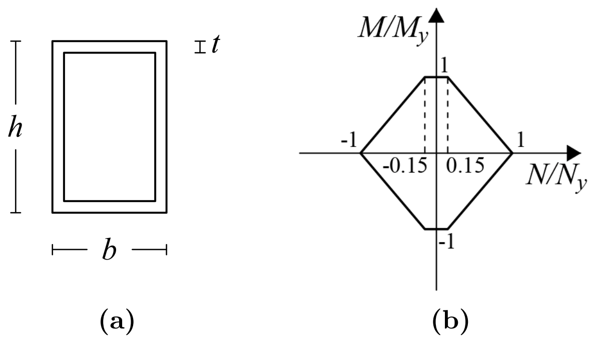

Figure 5.3: (a) Box cross section of the beam elements; (b) Typical rigid perfectly plastic domain of the plastic hinges.

response can be determined integrating the following equation of motion:

$$\boldsymbol{M}\ddot{\boldsymbol{u}}(t) + \boldsymbol{V}\dot{\boldsymbol{u}}(t) + \boldsymbol{K}\boldsymbol{u}(t) = \boldsymbol{F}(t) \tag{5.1}$$

and than the elastic stress response can be deduced:

$$\boldsymbol{P}(t) = \boldsymbol{B}^T\boldsymbol{u}(t) + \boldsymbol{P}^*(t) \tag{5.2}$$

where $\boldsymbol{M}$, $\boldsymbol{V}$, $\boldsymbol{K}$ are the mass, the damping and the stiffness matrices respectively, $\boldsymbol{u}$ is the displacement vector and the over dot means time derivative. Furthermore, $\boldsymbol{P}$ is the the stress vector at the strain points, $\boldsymbol{B}$ is the so-called pseudo-force matrix and $\boldsymbol{P}^*$ is the analogous of $\boldsymbol{P}$ but due to the loads acting upon the elements considered perfectly clamped.

As already explained in this thesis, in common applications of engineering interest can be useful to adopt lumped masses structural model and static condensation procedures, in order to take into account the dynamically significant degree of freedom of the system only. This fact does not affect the discussion carried out so far as the dynamic shakedown theorem is based on the linear dynamic steady-state response. So, in the present section the structural model of masses lumped at each floor has been chosen. The lumped mass of each floor has been calculated through the following relation $M = q_0 * (L_1 + L_2)/g$, where g is the acceleration of gravity and q_0 and $L_1 + L_2$ are the dead loads and the length of each floor respectively, as one can see in Figure 5.6. The horizontal displacements of the floors have been chosen as dynamically significant degree of freedom. Let define $\boldsymbol{u}_t$ the vector of horizontal floor displacement and $\boldsymbol{u}_r$ the vector collecting the rest of displacements so that the following equation can be written:

$$\boldsymbol{u} = \boldsymbol{E} \begin{bmatrix} \boldsymbol{u}_t \\ \boldsymbol{u}_r \end{bmatrix} \tag{5.3}$$

being $\boldsymbol{E}$ a suitable reordering matrix, also able to impose kinematic constraints (e.g. that the nodes of the same floor have the same horizontal displacement).

In this way, the following static condensation procedures of equation of motion, useful to evaluate the response of the uncertain system under stochastic excitation can be adopted:

$$\begin{bmatrix} \boldsymbol{M}_{tt} & \boldsymbol{0} \\ \boldsymbol{0} & \boldsymbol{0} \end{bmatrix} \begin{bmatrix} \ddot{\boldsymbol{u}}_t \\ \ddot{\boldsymbol{u}}_r \end{bmatrix} + \begin{bmatrix} \boldsymbol{C}_{tt} & \boldsymbol{0} \\ \boldsymbol{0} & \boldsymbol{0} \end{bmatrix} \begin{bmatrix} \dot{\boldsymbol{u}}_t \\ \dot{\boldsymbol{u}}_r \end{bmatrix} + \begin{bmatrix} \boldsymbol{K}_{tt} & \boldsymbol{K}_{tr} \\ \boldsymbol{K}_{rt} & \boldsymbol{K}_{rr} \end{bmatrix} \begin{bmatrix} \boldsymbol{u}_t \\ \boldsymbol{u}_r \end{bmatrix} = \begin{bmatrix} \hat{\boldsymbol{F}}(t) \\ \boldsymbol{0} \end{bmatrix} \tag{5.4}$$

where $\boldsymbol{C}_{tt}$ is the damping matrix of the reduced system whose a constant damping ratio ζ is imposed in the modal space, $\boldsymbol{K}_{tt}$, $\boldsymbol{K}_{tr}$, $\boldsymbol{K}_{rt}$, $\boldsymbol{K}_{rr}$ are suitable sub matrices obtained from the reordered external stiffness matrix $\boldsymbol{E}^T\boldsymbol{K}\boldsymbol{E}$ of the complete system, and $\hat{\boldsymbol{F}}(t)$ is the forcing function. Furthermore $\boldsymbol{M}_{tt}$ is the lumped mass matrix. After simple manipulation of equation (5.4) the solving set is made by a reduced system of differential equation and a set of algebraic ones:

$$\boldsymbol{M}_{tt}\ddot{\boldsymbol{u}}_t + \boldsymbol{C}_{tt}\dot{\boldsymbol{u}}_t + \bar{\boldsymbol{K}}\boldsymbol{u}_t = \hat{\boldsymbol{F}}(t) \tag{5.5a}$$

$$\boldsymbol{u}_r = -\boldsymbol{K}_{rr}^{-1}\boldsymbol{K}_{rt}\boldsymbol{u}_t \tag{5.5b}$$

where $\bar{\boldsymbol{K}} = \boldsymbol{K}_{tt} - \boldsymbol{K}_{tr}\boldsymbol{K}_{tt}^{-1}\boldsymbol{K}_{rt}$ is the condensed stiffness matrix. In this way the complete vector of displacements $\boldsymbol{u}$ can be obtained simply reordering the vectors $\boldsymbol{u}_t$ and $\boldsymbol{u}_r$. In the proposed application the damping ratio ζ is given with a log-normal distribution with mean 0.05 and standard deviation 0.65 (see e.g. [53]).

Furthermore, $\hat{\boldsymbol{F}}(t)$ is assumed to be a stationary segment of a stochastic wind process. Among the several methods available in literature (see e.g. [22, 35, 36, 58]), the model for the simulation of wind velocity fields proposed by Deodatis [34]. As known, the forcing function $\hat{\boldsymbol{F}}(t)$ represents a wind load model under the assumption of neglecting the wind-structure interaction, if some of its component (relatively to the structural nodes where the wind load can be concentrated) can be described by the following relation:

$$\hat{f}_j(t) = \eta_j(\bar{v}_j(t) + v_j(t))^2 \quad j = 1, 2, \ldots, n, \tag{5.6}$$

where $\bar{v}_j(t)$ is the mean wind velocity at the point z_j and $v_j(t)$ is the corresponding fluctuating part. Furthermore, η_j is a coefficient equal to $0.5\rho\bar{C}_j A_j$, being ρ the air density, $\bar{C}_j$ an hydrodynamic coefficient determined experimentally and A_j the impact area of the j^{th} node in the direction of the mean wind.

With the aim to describe the fluctuating part in such a way that the obtained forcing function will be a periodic one, let consider a one-dimensional, multivariate stochastic vector process $\boldsymbol{v}(t)$, which has n components $v_1(t)$, $v_2(t)$, …, $v_n(t)$ with mean equal to zero. The cross-spectral density matrix is given by

$$\boldsymbol{S}(\omega) = \begin{bmatrix} S_{11}(\omega) & S_{12}(\omega) & \cdots & S_{1n}(\omega) \\ S_{21}(\omega) & S_{22}(\omega) & \cdots & S_{2n}(\omega) \\ \vdots & \vdots & \ddots & \vdots \\ S_{n1}(\omega) & S_{n2}(\omega) & \cdots & S_{nn}(\omega) \end{bmatrix}, \tag{5.7}$$

that usually is a complex matrix.

According to Deodatis [34], the typical component of vector process $\boldsymbol{v}(t)$, that will be stationary and ergotic, can be simulated by the following series:

$$v_j(t) = 2\sum_{m=1}^{n}\sum_{l=1}^{N} |H_{jm}(\omega_{ml})|\sqrt{\Delta\omega}\cos\left[\omega_{ml}(t) - \theta_{jm}(\omega_{ml}) + \Phi_{ml}\right], \quad j = 1, 2, ..., n, \tag{5.8}$$

as $N \to \infty$. In equation (5.8), $H_{jm}(\omega_{ml})$ is a typical element of a matrix $\boldsymbol{H}(\omega)$, which is obtained decomposing the cross spectral density matrix in the following product

$$\boldsymbol{S}(\omega) = \boldsymbol{H}(\omega)\boldsymbol{H}^{T*}(\omega), \tag{5.9}$$

where (in this section) the apex $()^*$ means complex conjugate. This decomposition can be performed using the Cholesky's method, in which case

$$\boldsymbol{H}(\omega) = \begin{bmatrix} H_{11}(\omega) & 0 & \cdots & 0 \\ H_{21}(\omega) & H_{22}(\omega) & \cdots & 0 \\ \vdots & \vdots & \ddots & \vdots \\ H_{n1}(\omega) & H_{n2}(\omega) & \cdots & H_{nn}(\omega) \end{bmatrix}, \tag{5.10}$$

is a lower triangular matrix. Furthermore, $\Delta\omega = \omega_{up}/N$ is the sample frequency, with ω_{up} cut-off frequency, ω_{ml} is a frequency interval namely:

$$\omega_{ml} = (l-1)\Delta\omega + \frac{m}{n}\Delta\omega,\ l = 1, 2, \ldots, N, \tag{5.11}$$

as stated by Shinozuka et al. [85], $\theta_{jm}(\omega)$ is the complex angle given by:

$$\theta_{jm}(\omega) = \tan^{-1}\frac{\mathrm{Im}\left[H_{jm}(\omega)\right]}{\mathrm{Re}\left[H_{jm}(\omega)\right]}, \tag{5.12}$$

where $\mathrm{Im}\left[H_{jm}(\omega)\right]$ and $\mathrm{Re}\left[H_{jm}(\omega)\right]$ are respectively the imaginary and the real part of the complex function $H_{jm}(\omega)$ when it is written in polar form. Finally, Φ_{ml}, $m = 1, 2, \ldots, n$, $l = 1, 2, \ldots, N$, represents n sequences of independent random phase angles distributed uniformly over the interval $[0, 2\pi]$.

The period of the simulated function (5.8) is given by:

$$T = \frac{2\pi n}{\Delta\omega} = \frac{2\pi n N}{\omega_{up}}, \tag{5.13}$$

as shown in [34]. It's clear that the stochastic process expressed can be simulated quite well by equation (5.8) when the parameters N, ω_{up} and Δt are chosen in such a way to avoid aliasing problems. Finally, this kind of simulation can result cumbersome when it is coupled whit a Monte Carlo method. For that reasons, many computational techniques based on Fast Fourier Transform have been proposed in recent years (see e.g. [34, 37]).

A sample of wind load can be simulated by the equation (5.6). At this purpose let define the quantities used in this example: $\rho = 1.25$ Kg/m^3, $\bar{C}_j = 1.3$ and $A_j = 24$ m^2 for $j = 1, 2..., 5$. Furthermore, the mean wind speed at each floor has been determined with the following power law:

$$\bar{v}_j = v_{10}\,\beta\left(\frac{z_j}{10}\right)^{\alpha} \tag{5.14}$$

where $v_{10} = 40$ m/s is the wind speed at 10 m above the ground, $\beta = 0.65$ is the factor of the power law, z_j is the height of the jth floor and $\alpha = 1/6.5$ is the exponent of the power law.

In order to simulate the fluctuating part of the wind v_j, the entries of the cross-spectral density matrix, given by equation (5.7), have to be defined. For the power spectral density function of the longitudinal wind velocity fluctuation at different heights $S_{jj}(\omega) = S_j(\omega)$, $j = 1, 2, \ldots, 5$, the model proposed by Kaimal et al. [56] has been selected:

$$S_j(\omega) = \frac{1}{2}\,\frac{200}{2\pi}\,v_*^2\,\frac{z_j}{\bar{v}_j}\,\frac{1}{\left[1 + 50\dfrac{\omega z}{2\pi\bar{v}_j}\right]^{5/3}}, \quad j = 1, 2, \ldots, 5 \tag{5.15}$$

where, beyond the already defined quantities, v_* is the shear velocity of the flow, expressed by:

$$v_* = v_{10}\,\beta\,\frac{k_a}{\log\left(\dfrac{10}{z_0}\right)} \tag{5.16}$$

in which $k_a = 0.4$ is the Von Karman's constant and $z_0 = 0.02$ is the ground roughness height.

The cross spectral density functions have been evaluated with the following relation:

$$S_{jk}(\omega) = \sqrt{S_j(\omega)S_k(\omega)}\gamma_{jk}(\omega) \quad j, k = 1, 2, \ldots, 5,\ j \neq k \tag{5.17}$$

where γ_{jk} is the coherence function between $v_j(t)$ and $v_k(t)$. The model suggested by Davenport [31] is chosen for the coherence functions between the velocity fluctuation at two different heights z_1 and z_2:

$$\gamma_{jk}(\Delta z, \omega) = \exp\left[-\frac{\omega}{2\pi}\frac{C_z \Delta z}{\frac{1}{2}\left[\bar{v}_1 + \bar{v}_2\right]}\right] \tag{5.18}$$

where $\bar{v}_1$ and $\bar{v}_2$ are the wind mean speed at heights z_1 and z_2 respectively, $\Delta z = |z_1 - z_2|$ and C_z is a constant that can be set equal to 10 for design purpose [86].

For each generated sample the shakedown safety factor can be evaluated with the following linear programming problem:

$$\xi^* = \max_{\xi,\, \boldsymbol{\rho}} \xi \tag{5.19a}$$

subjected to:

$$\boldsymbol{\varphi} = \boldsymbol{N}^T \left(\boldsymbol{P}_0 + \boldsymbol{\rho}\right) + \xi \check{\boldsymbol{P}} - \boldsymbol{R} \leq \boldsymbol{0}, \tag{5.19b}$$

$$\boldsymbol{A}^T \boldsymbol{\rho} = \boldsymbol{0}, \tag{5.19c}$$

where:

$$\check{\boldsymbol{P}} = \max_{0 \leq t \leq T} \boldsymbol{N}^T \hat{\boldsymbol{P}}(t) \tag{5.20}$$

is the elastic envelope stress vector which select for each yielding mode the maximum of the plastic demand in time [26, 27, 64].

Assuming that $X \subset \mathbb{R}^n$ is the failure region specified as the exceedance of an uncertain load multiplier ξ over its shakedown value ξ^* and that $\boldsymbol{\theta} \in \mathbb{R}^n$ is a vector containing all the uncertain parameters regarding both the structural behavior and the load conditions, the failure probability can be calculated in a generic form as

$$P(X) = \int \mathbb{I}_X(\boldsymbol{\theta})\, q(\boldsymbol{\theta})\, d\boldsymbol{\theta} \tag{5.21}$$

where $\mathbb{I}_X : \mathbb{R}^n \mapsto \{0, 1\}$ is an indicator function that is $\mathbb{I}_X(\boldsymbol{\theta}) = 1$ when $\boldsymbol{\theta} \in F$ and $\mathbb{I}_X(\boldsymbol{\theta}) = 0$ otherwise, and $q : \mathbb{R}^n \mapsto [0, \infty)$ be a prescribed probability density function (PDF) representing the values that the set of uncertain parameters $\boldsymbol{\theta} = [\theta_1, \theta_2, \cdots, \theta_n]$ can assume. At least in principle, the probability of failure $P(X)$ can be reached trying to integrate directly the integral above exposed. Indeed, due to the large number of uncertainties involved, the probability of failure $P(X)$ can be calculated trough the Monte Carlo simulation method that has been widely used in the past for its robustness and for its ability to solve problems with complex failure regions such as that shown in the present section.

However, this method is lack to find the small probability of failure because the number of samples that must be generated to achieve a predetermined accuracy, and therefore also the number of analyses to be performed, is proportional to the ratio $1/P(X)$. In the present example, this problem is enhanced by the fact that, in order to evaluate the shakedown multiplier, each sample requires not only a time history analysis but also a problem of linear programming.

In this context, the use of the method proposed by Au and Beck [4], called Subset Simulation, is to be considered more appropriate. This method is based on the idea that a small probability of failure can be expressed as a product of large values of conditional failure by introducing appropriate intermediate failure events.

Given the failure domain X, let $X_1 \supset X_2 \supset \cdots \supset X_m = X$ be a decreasing nested sequence of failure regions so that $X_k = \cap_{i=1}^{k} X_i$, $k = 1, 2, \ldots, m$. The probability of failure $P(X)$ can be represented as the probability of falling in the final subset X_m. From the definition of conditional probability, let write:

$$\begin{aligned} P(X) = P(X_m) = P(\cap_{i=1}^{m-1} X_i) = P(X_m \mid \cap_{i=1}^{m-1} X_i) X_i) P(\cap_{i=1}^{m-1} X_i) = \\ = P(X_m \mid X_{m-1}) P(\cap_{i=1}^{m-1} X_i) = \cdots = P(X_1) \prod_{i=1}^{m-1} P(X_{i+1} \mid X_i). \end{aligned} \tag{5.22}$$

Equation (5.22) shows that, instead of directly calculating the probability of failure, this one can be calculated as the product of many conditional probabilities.

Since the failure region has been defined as $X = \{\boldsymbol{\theta} : \xi(\boldsymbol{\theta}) > \xi^*(\boldsymbol{\theta})\}$, then intermediate failure region can be defined as $X_i = \{\boldsymbol{\theta} : \xi(\boldsymbol{\theta}) > \xi_i^*(\boldsymbol{\theta})\}$. In this

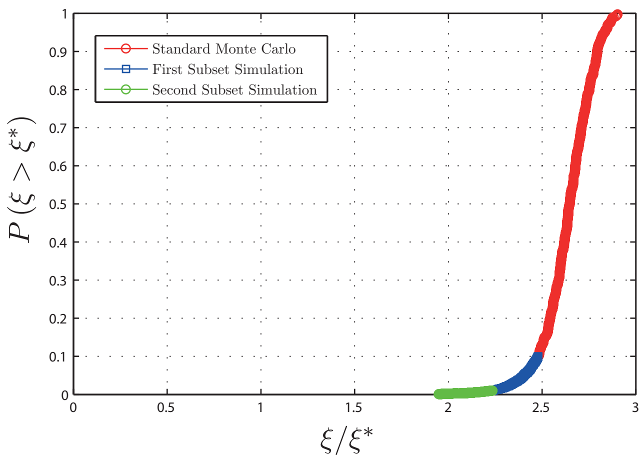

Figure 5.4: Probability of failure in shakedown conditions

way, the probability of failure can be rewritten as:

$$P(X) = P(\xi > \xi^*) = P(\xi > \xi_1^*) \prod_{i=1}^{m-1} P(\xi > \xi_{i+1}^* \mid \xi > \xi_i^*) \tag{5.23}$$

where $0 < \xi_1^* < \xi_2^* \cdots < \xi_m^* = \xi^*$ is a decreasing sequence of threshold levels. These levels are generated adaptively using information from simulated samples so that the conditional probabilities are approximately equal to a common specified value p_0 (experience shows that $p_0 = 0.1$ is a prudent choice [5, 67]).

To calculate the probability of failure expressed by equation (5.23), one needs to calculate $P(\xi > \xi_1^*)$ and $P(\xi > \xi_{i+1}^* \mid \xi > \xi_i^*)$. The first one is an unconditional probability that can be estimated by well-known Monte Carlo simulation. The second represent conditional probabilities that can be simulated through a class of powerful algorithms called Markov Chain Monte Carlo based on Metropolis-Hastings algorithm [3, 4].

Afterwords, the procedure used by the Subset Simulation can be summarized as follows:

1. generation of N sample vectors by direct Monte Carlo simulation for the unconditional case such that they are independent and identically

distributed from the proposal PDF q and evaluation of the structural response for each of them;

2. choice of the value ξ_1^* such that $[(1-p_0)N]$ responses lie outside the subset X_1 and p_0N conditional samples belong to $X_1 = (\xi > \xi_1^*)$;

3. starting from each of the sample at "conditional level 1", generation by the Metropolis-Hastings algorithms of $(1-p_0)N$ additional conditional samples so that the level 1 is repopulated and has again N conditional samples.

4. repetition of the operations shown in steps 2 and 3 for higher conditional levels until the samples at conditional level m have been generated.

So, Subset Simulation provides a useful tool for wind performance assessment through efficient estimation of failure probabilities grounding on dynamic shakedown analysis.

The result in terms of probability of failure $P(X)$ for the above exposed uncertain steel frame subjected to the shown stochastic wind load model are obtained for $N = 1000$ samples generated and for a threshold level $p_0 = 0.1$. In particular, they are reported in terms of probability of failure in dynamic shakedown condition in Figure 5.4.

5.2 Case studies of frames under quasi-static cyclic loads

The optimal designs of steel frames have been obtained referring to the formulations proposed in section (3.1).

First example

At first, the minimum volume design problem (3.23) has been solved, utilizing the iterative technique based on an appropriate linearization of the relevant optimization problem (as explained in Chapter 4), for the six floor frame plotted in Figure 5.5. The frame is constituted by square box cross section elements (Figure 5.6a) with edge length $\ell = 250$ mm. The constant thickness t of each

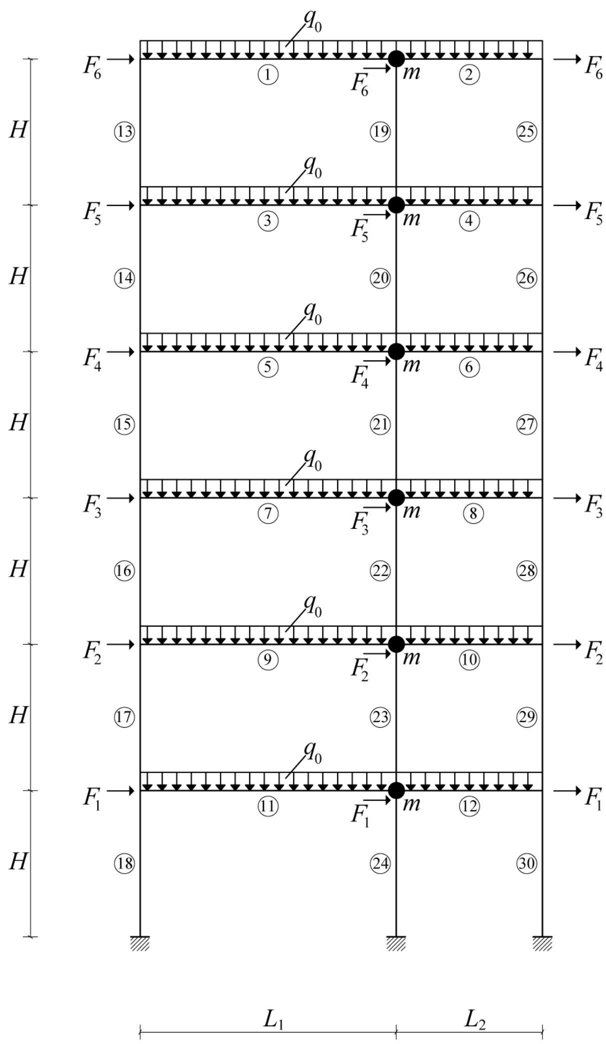

Figure 5.5: Six floor steel frame: geometry and load conditions.

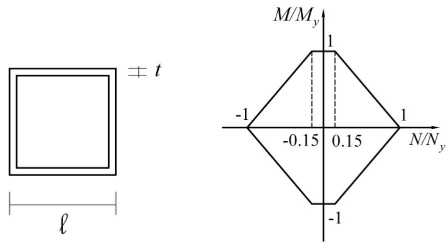

Figure 5.6: Six floor standard design: (a) Typical square box cross section; (b) Rigid plastic domain of the typical plastic hinge.

cross section element has been assumed as a continuous design variable. Furthermore, the frame is constituted by two spans of length $L_1 = 7\,\mathrm{m}$, $L_1 = 4\,\mathrm{m}$, and the inter-story height is $H = 4$ m. The material is steel S235H so that the Young modulus $E = 250$ GPa and yield stress $\sigma_y = 235$ MPa have been assumed.

Two rigid perfectly plastic hinges are located at the extremes of all elements, considered to be purely elastic. Moreover, an additional plastic hinge is located in the middle point of the longer beams because they are loaded by a uniform dead load. The interaction between the bending moment M and the axial force N has been taken into account. In Figure 5.6b, the dimensionless rigid plastic domain of the typical plastic hinge is plotted in the plane $(N/N_y, M/M_y)$, being N_y and M_y the yield generalized stress corresponding to N and M, respectively. It is worth noticing that the relevant domain is a very common satisfactory simplified model deduced from some standards [40, 80] and suggested for practical applications (see, e.g. [66, 84]); the related limit behavior is here utilized for pillar's cross sections as well as for beam's cross sections. Furthermore, in the present context, within the aims of the proposed study, the influence of the shear forces on the safety conditions will not be taken into account.

Finally, in order to ensure that the cross sections of the elements be able to fully exhibit the relevant plastic deformations (plastic hinge behavior) preventing dangerous phenomena of local instability, the cross section element thicknesses will be constrained within the range 8 mm $\leq t \leq$ 40 mm, as suggested in the referenced standards.

As stated in section (3.1.2), the structure is subjected to three loads combination of fixed and seismic loads. In particular, the structure is subjected to a fixed uniformly distributed vertical load on the beams $q_0 = 40\,\mathrm{kN/m}$ and to seismic actions defined trough two different response spectra as defined by the Italian code [80]. The selected response spectra for serviceability conditions (up-crossing probability in the lifetime of 81%) and instantaneous collapse (up-crossing probability in the lifetime of 5%) are those corresponding to Palermo, with a soil type B, life time 100 years and class IV (Figure 5.7). Seismic masses are assumed to be equal at each floor $m = q_0\,(L_1 + L_2)\,/g = 44.85\,\mathrm{kN \cdot sec^2/m}$ (with g acceleration of gravity), and located in the intermediate node at each floor (Figures 5.5). Furthermore, the fixed loads present in the second and in the third combination are reduced setting $\xi_{s0} = \xi_{l0} = 0.8$.

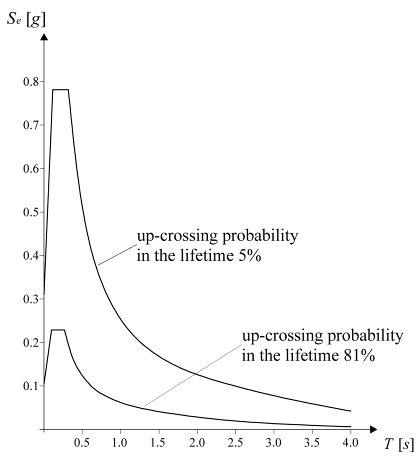

Figure 5.7: Selected response spectra for serviceability conditions (up-crossing probability in the lifetime 5%) and instantaneous collapse (up-crossing probability in the lifetime 81%).

As suggested by the cited code, a forth load combination is considered in this example in order to take into account the wind effect upon the structure. In particular the optimal structure must prevent the instantaneous collapse when subjected to a combination of fixed load $\boldsymbol{F}_{w0} = 0.8\boldsymbol{F}_{w0}$ and to perfect cyclic wind action $\boldsymbol{F}_w = 1.25\bar{\boldsymbol{F}}_w$ that are concentrated horizontal loads applied

Volume: 1.360										
El.	1	2	3	4	5	6	7	8	9	10
t	8.00	8.00	8.00	8.00	9.62	8.00	9.61	12.76	9.61	17.00
El.	11	12	13	14	15	16	17	18	19	20
t	9.61	21.31	8.00	8.00	8.00	8.00	8.00	8.17	8.00	8.96
El.	21	22	23	24	25	26	27	28	29	30
t	11.66	14.77	18.11	20.85	8.00	8.00	8.00	8.03	9.14	14.59

Table 5.1: Optimal volume (m^3) and thicknesses (mm) of the six floor frame standard design.

on all the nodes and described by the following vector:

$$\bar{\boldsymbol{F}}_w = |24.0 \quad 27.4 \quad 30.6 \quad 32.6 \quad 36.2|^T \tag{5.24}$$

where the typical component $\bar{F}_{wj}$ is the resultant force at the j^{th} floor. Vector $\bar{\boldsymbol{F}}_w$ is computed referring to the Italian code for a building in Palermo, assuming a class type B, a category type III and an impact surface for the typical floor equal to 20 m^2. It is worth noticing that the typical load F_j, $(1, 2, \ldots, 6)$ represented in Figure 5.5 is deduced as $F_j = \bar{F}_{wj}/3$.

In this way, the following constraints has been appended to the problem (3.23):

$$\boldsymbol{\varphi}_{wi} = \boldsymbol{N}^T \left[\boldsymbol{P}_{w0} + (-1)^i \boldsymbol{P}_w + \boldsymbol{\rho}_{wi}\right] - \boldsymbol{R} \leq \boldsymbol{0} \quad (i = 1, 2), \tag{5.25}$$

$$\boldsymbol{A}^T \boldsymbol{\rho}_{wi} = \boldsymbol{0} \quad (i = 1, 2). \tag{5.26}$$

where $\boldsymbol{P}_{w0}$ is the elastic stress response to $\boldsymbol{F}_{w0}$, $\boldsymbol{P}_w$ is the elastic stress response to the wind load $\boldsymbol{F}_w$, and $\boldsymbol{\rho}_{wi}$, $(i = 1, 2)$, are two independent self-stress vectors.

The results in terms of optimal volume and optimal thicknesses are reported in Table 5.1. The obtained design features have been investigated through the determination of the relevant Bree diagrams related to the combinations of suitably reduced fixed loads and seismic actions, as well as of amplified fixed loads and wind actions.

In Figure 5.8a and 5.8b, the cited diagrams are plotted so that ξ_0 represents the fixed load multiplier and ξ_c the cyclic load one. It is easy to observe that,

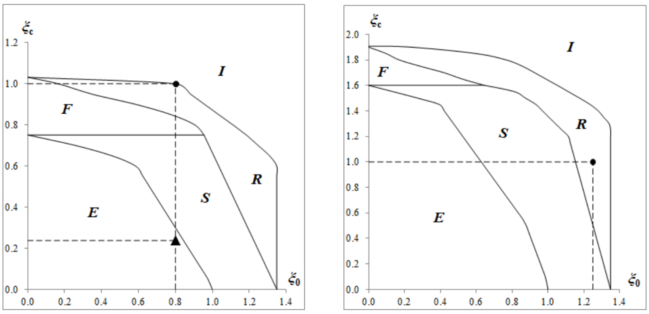

(a) **(b)**

Figure 5.8: Six floor standard design: (a) Bree diagram related to the combination of reduced fixed loads and seismic actions (▲ serviceability condition, • instantaneous collapse condition); (b) Bree diagram related to the combination of amplified fixed loads and wind actions (• instantaneous collapse condition).

as expected, all the imposed behavioral constraints are satisfied. In particular, the structure shows to especially suffer the load combination involving the seismic loads: actually, it exhibits a purely elastic behavior in serviceability seismic conditions, it guarantees a certain safety margin with respect to the instantaneous collapse for fixed and wind actions, and it finds itself in a condition of impending collapse for fixed and high seismic loads. Furthermore, it must be noticed that:

- a dangerous condition of ratchetting is reached even for load multipliers lower than the prescribed ones for the combination of loads involving seismic actions;
- in any examined case the safety margin related to fixed loads, considered as acting alone, does not appear sufficiently consistent.

Actually, for the obtained design the elastic limit fixed load multiplier is equal to 1.00 and the instantaneous collapse one is equal just to 1.35. Such undesirable behavior can be avoided by introducing in the elastic constraint (3.23e) a load multiplier so that it is rewritten in the following form:

$$\varphi_e = \boldsymbol{N}^T 1.25 \boldsymbol{P}_0 - \boldsymbol{R} \leq \boldsymbol{0}. \tag{5.27}$$

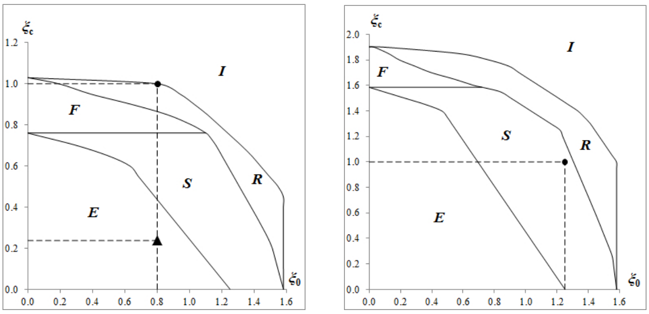

(a) (b)

Figure 5.9: Six floor improved design: (a) Bree diagram related to the combination of reduced fixed loads and seismic actions (▲ serviceability condition, • instantaneous collapse condition); (b) Bree diagram related to the combination of amplified fixed loads and wind actions (• instantaneous collapse condition).

The Bree diagrams related to the new design obtained for are plotted in Figure 5.9a and 5.9b. The improvement of the behavior is related with a very moderate volume increment ($\Delta V\% = 1.85\%$). It is also worth noticing that in this case the safety features of the optimal structure with regard to the limit condition related to wind action definitely improve; actually, the optimal frame eventually shakes down preventing a dangerous incremental collapse behavior.

Furthermore, in order to analyze the structural response investigating on its safety behavior features with regard to the element slenderness, the last obtained structure has been studied performing an elastic plastic analysis under a suitably selected load history taking into account the P-Δ effects. It has been verified that the structure shows incremental collapse for load multipliers lower and lower; in particular it reaches a condition of impending collapse for the combination of fixed and high seismic load when $\xi_0 = 0.8$ and $\xi_c = 0.82$.

These results justify the considerations that led to improve the optimal design formulation in order to take into account for element slenderness as shown in section (3.1.3). Furthermore, it is necessary to compare in the next example the different results obtainable if continuous or discrete variables are

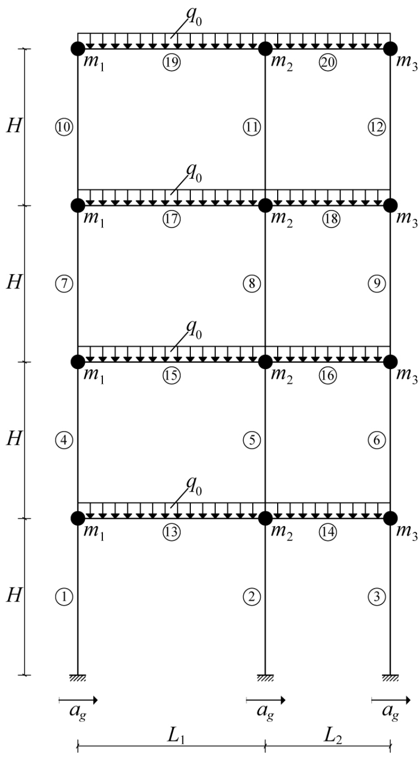

Figure 5.10: Four floors steel frame: geometry and load conditions.

considered.

Second example

Let consider a new plane steel frame (Figure 5.10) in which the wind loads are neglected. At first, the optimal design problem (3.23) has been solved searching for the standard minimum volume.

The frame is constituted by rectangular box cross section elements (Figure 5.11) with b = 200 mm, h = 300 mm, and constant thickness t variable between $t_c^{\min} = 4$ mm and $t_c^{\max} = 24$ mm. The imposed bounds for the thickness have been deduced by the more common standard elements on sale. The cross section of all the elements is disposed so that the axis related to the greater moment of inertia is orthogonal to the plane of the relevant frame.

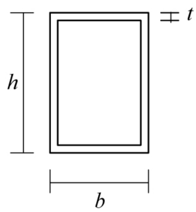

Figure 5.11: Typical rectangular box cross section.

Furthermore, $L_1 = 600$ cm, $L_2 = 400$ cm, $H = 500$ cm, Young modulus $E = 250$ GPa and yield stress $\sigma_y = 235$ MPa have been assumed.

As in the previous example, two rigid perfectly plastic hinges are located at the extremes of all the elements, considered to be elastic, and an additional hinge is located in the middle point of the longer beams and the interaction between bending moment M and axial force N has been taken into account trough the typical rigid plastic domain for square and/or rectangular box cross section.

As stated in section (3.1), the structure is subjected to three loads combination of fixed and seismic loads. In particular, the structure is subjected to a fixed uniformly distributed vertical load on the beams $q_0 = 40$ kN/m and to seismic actions defined trough two different response spectra as defined by the Italian code [80]. The selected response spectra for serviceability conditions (up-crossing probability in the lifetime of 81%) and instantaneous collapse (up-crossing probability in the lifetime of 5%) are those corresponding to Palermo, with a soil type B, life time 100 years and class IV.

Let assume that the seismic masses are lumped in the relevant structure nodes and that they are equal for each floor, $m_1 = 9.79\,\text{kN}\cdot\text{sec}^2/\text{m}$, $m_2 = 16.31\,\text{kN}\cdot\text{sec}^2/\text{m}$, $m_3 = 6.52\,\text{kN}\cdot\text{sec}^2/\text{m}$ (Figure 5.10). The value assumed for the seismic masses depends on the remark that during the earthquake not all the gravitational loads are considered as acting on the structure, so that $m_i = (0.8\,q_0\ell_i)/g$, where g is the acceleration of gravity, and ℓ_i, $i = 1, 2, 3$ is the relevant influence beam length. Furthermore, the fixed loads present in the second and in the third combination are reduced, setting $\xi_{s0} = \xi_{l0} = 0.8$.

Being the problem a strongly nonlinear one, in order to reach the numerical solution an appropriate computational technique has been utilized (see e.g.

Volume: 0.573										
El.	1	2	3	4	5	6	7	8	9	10
t	5.2	11.1	8.7	4.0	10.3	4.0	4.0	5.3	4.0	4.0
El.	11	12	13	14	15	16	17	18	19	20
t	4.0	4.0	6.1	12.1	6.2	7.5	5.2	4.0	5.2	4.0

Table 5.2: Continuous variable standard design volume (m^3) and thicknesses (mm).

Chapter 4). The obtained results are reported in Table 5.2 in terms of optimal volume and optimal thicknesses.

Let now study the same steel frame, always searching for the standard design, but assuming the design variables as appertaining at the discrete sets $T_d \equiv \{4, 6, 8, \ldots, 24\,\text{mm}\}$, $d = 1, 2, \ldots, 20$. For the numerical computation, the Harmony Search Algorithm (HS) shown in section (4.2) has been used. This special approach consist in the using of appropriate random search processes instead of gradient search one, so that derivative information are unnecessary. The HS Algorithm is substantially based on the analogy between the performance process of natural music and the searching for the solution to optimization problems. The obtained results for the discrete variable standard design are reported in Table 5.3 always in terms of optimal volume and optimal thicknesses.

As it is possible to observe the structural volume related to the discrete variable design is quite greater than the continuous variable design ($\Delta V\% = 14.14\%$). Furthermore, a very large amount of elapsed real time (4889 s) is related to the obtaining of the discrete variable design, while the elapsed real time related to the continuous variable design is just 1873 s. As a consequence, a suitable sub-optimal distribution of discrete thicknesses has been considered starting from the continuous variable optimal design solution and increasing the thickness of each element till the one directly above in the discrete range, as reported in Table 5.4.

As it is possible to observe, the volume related to the sub-optimal discrete variable standard design is substantially coincident with the volume obtained for the discrete variable standard design ($\Delta V\% = 2.67\%$) and, yet, the latter is slightly greater than the former. This last result is negligible from an engi-

Volume: 0.654										
El.	1	2	3	4	5	6	7	8	9	10
t	12.0	8.0	10.0	4.0	12.0	4.0	6.0	4.0	4.0	4.0
El.	11	12	13	14	15	16	17	18	19	20
t	4.0	4.0	8.0	12.0	8.0	10.0	6.0	4.0	6.0	6.0

Table 5.3: Discrete variable standard design volume (m^3) and thicknesses (mm).

Volume: 0.637										
El.	1	2	3	4	5	6	7	8	9	10
t	6.0	12.0	10.0	4.0	12.0	4.0	4.0	6.0	4.0	4.0
El.	11	12	13	14	15	16	17	18	19	20
t	4.0	4.0	8.0	14.0	8.0	8.0	6.0	4.0	6.0	4.0

Table 5.4: Sub-optimal discrete variable standard design volume (m^3) and thicknesses (mm).

neering point of view and it depends on the different numerical tools utilized. Anyway, in the present case, it can be stated that the sub-optimal discrete variable standard design is certainly acceptable representing a very good approximation of the real optimal one with computational cost absolutely reduced. In order to compare and better interpret the features of the obtained designs the relevant Bree diagrams have been determined and plotted in the plane ξ_0, ξ_c (Figure 5.13, 5.14, 5.15), where ξ_0 and ξ_c are the multipliers of the fixed and cyclic load, respectively.

An examination of these graphs allows us to observe that: all the obtained designs fulfill the prescribed constraints; just the continuous variable design finds itself in a condition of impending instantaneous collapse for the load combination related to high intensity seismic actions; both the discrete variable (optimal and sub-optimal) standard designs show the same safety factors with respect the assigned limit state, even if they are characterized by different thickness distributions.

As already stated, for the chosen plane frame it is necessary to suitably take into account the element slenderness. Therefore, the same frame plotted

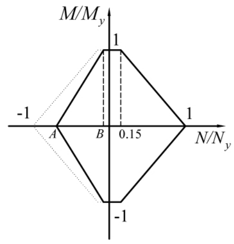

Figure 5.12: Rigid plastic domain of the plastic hinge related to the pillars accounting for buckling. $A = -P_{cr}/\eta N_y$ and $B = -0.15 P_{cr}/\eta N_y$

Volume: 0.694										
El.	1	2	3	4	5	6	7	8	9	10
t	10.1	22.6	10.4	7.2	15.5	7.0	4.6	9.6	4.0	4.0
El.	11	12	13	14	15	16	17	18	19	20
t	4.6	4.0	6.1	4.0	6.1	4.0	6.0	4.0	5.3	4.0

Table 5.5: Safe buckling continuous variable design volume (m^3) and thicknesses (mm).

in Figure 5.10 has been designed by solving problem (3.31) and considering alternatively element buckling (with $\eta = 1.5$), P-Δ effects and both.

In particular in order to take into account for the pillar slenderness the rigid plastic domain represented in Figure 5.12 is utilized.

The results obtained assuming a continuous domain for the design variables are reported in Tables 5.5, 5.6 and 5.7, while the analogous results obtained assuming the discrete sets $T_d \equiv \{4, 6, 8, \ldots, 24\,\text{mm}\}$, $d = 1, 2, \ldots, 20$ for the design variables and utilizing the referred harmony search (HS) are reported in Tables 5.8, 5.9 and 5.10.

In Figures 5.16, 5.17, and 5.18 the Bree diagrams related to all the obtained optimal structures are represented. Finally, in Figure 5.19, 5.20, and 5.21, the Bree diagrams related to the sub-optimal discrete variable standard design are plotted taking alternatively into account the buckling effects, the P-Δ effects and both. These last diagrams clearly show the effectiveness of the introduced relevant constraints.

Volume: 0.591										
El.	1	2	3	4	5	6	7	8	9	10
t	5.0	11.2	9.3	4.0	10.6	4.1	4.0	5.3	4.0	4.0
El.	11	12	13	14	15	16	17	18	19	20
t	4.0	4.0	6.1	13.5	6.6	8.5	5.5	4.0	5.4	4.0

Table 5.6: Safe P-Δ continuous variable design volume (m^3) and thicknesses (mm).

Volume: 0.716										
El.	1	2	3	4	5	6	7	8	9	10
t	10.1	22.7	11.7	7.2	15.5	7.3	4.6	9.6	4.1	4.0
El.	11	12	13	14	15	16	17	18	19	20
t	4.6	4.0	6.1	7.4	6.1	4.0	6.1	4.0	5.3	4.0

Table 5.7: Safe buckling/P-Δ continuous variable design volume (m^3) and thicknesses (mm).

Volume: 0.825										
El.	1	2	3	4	5	6	7	8	9	10
t	16.0	24.0	14.0	10.0	16.0	8.0	10.0	12.0	4.0	6.0
El.	11	12	13	14	15	16	17	18	19	20
t	6.0	4.0	6.0	4.0	6.0	6.0	6.0	6.0	6.0	4.0

Table 5.8: Safe buckling discrete variable design volume (m^3) and thicknesses (mm).

Volume: 0.647										
El.	1	2	3	4	5	6	7	8	9	10
t	12.0	8.0	8.0	4.0	10.0	8.0	4.0	6.0	4.0	4.0
El.	11	12	13	14	15	16	17	18	19	20
t	4.0	4.0	12.0	6.0	8.0	10.0	6.0	4.0	6.0	4.0

Table 5.9: Safe P-Δ discrete variable design volume (m^3) and thicknesses (mm).

Volume: 0.816										
El.	1	2	3	4	5	6	7	8	9	10
t	12.0	24.0	16.0	8.0	16.0	8.0	6.0	12.0	6.0	4.0
El.	11	12	13	14	15	16	17	18	19	20
t	8.0	4.0	8.0	4.0	6.0	4.0	6.0	4.0	6.0	8.0

Table 5.10: Safe buckling/P-Δ discrete variable design volume (m^3) and thicknesses (mm).

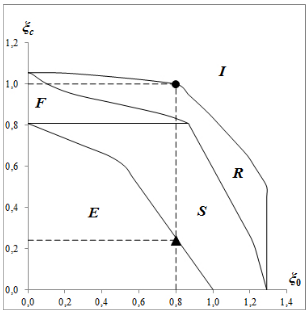

Figure 5.13: Four floors continuous variable standard design: Bree diagram (▲ serviceability condition, • instantaneous collapse condition).

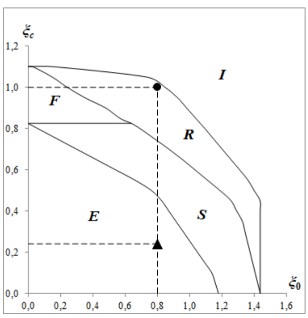

Figure 5.14: Four floors discrete variable standard design: Bree diagram (▲ serviceability condition, • instantaneous collapse condition).

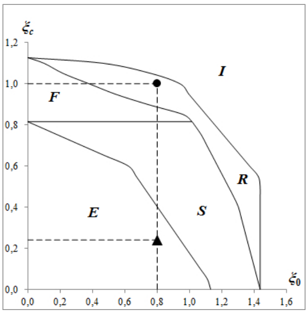

Figure 5.15: Four floors sub-optimal discrete variable standard design: Bree diagram (▲ serviceability condition, • instantaneous collapse condition).

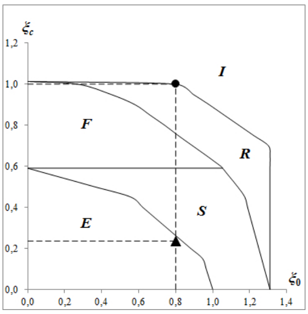

Figure 5.16: Four floor safe buckling continuous variable design: Bree diagram (▲ serviceability condition, • instantaneous collapse condition).

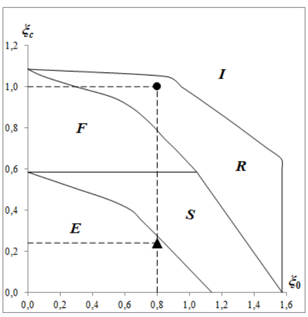

Figure 5.17: Four floor safe buckling discrete variable design: Bree diagram (▲ serviceability condition, • instantaneous collapse condition).

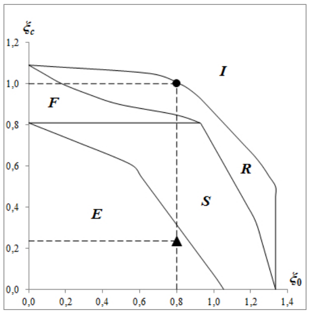

Figure 5.18: Four floor safe P-Δ continuous variable design: Bree diagram (▲ serviceability condition, • instantaneous collapse condition).

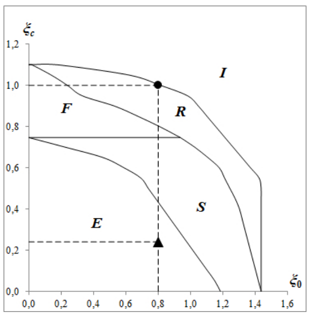

Figure 5.19: Four floor safe P-Δ discrete variable design: Bree diagram (▲ serviceability condition, • instantaneous collapse condition).

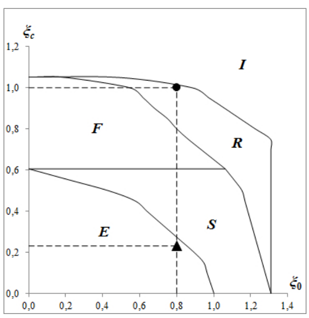

Figure 5.20: Four floor safe buckling/P-Δ continuous variable design: Bree diagram (▲ serviceability condition, • instantaneous collapse condition).

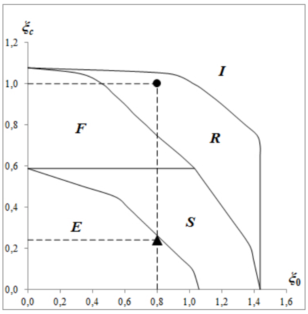

Figure 5.21: Four floor safe buckling/P-Δ discrete variable design: Bree diagram (▲ serviceability condition, ● instantaneous collapse condition).

Third example

Different optimal designs of the plane steel frame plotted in Figure 5.22 have been obtained referring to the formulation (3.41) previously proposed. At first, the optimal design problem (3.41) has been solved searching for the unlimited ductility minimum volume structure, i.e. eliminating the terms related to the perturbation, and assuming continuous design variables.

The studied frame is constituted by three floors and all the elements have square box cross section with edge length $\ell = 200$ mm and constant thickness t variable between $t_c^{\min} = 4$ mm and $t_c^{\max} = 24$ mm (Figure 5.23). The imposed design variable bounds for the thicknesses have been deduced by referring to the more common standard elements on sale. Furthermore, $L_1 = 600$ cm, $L_2 = 400$ cm, $H = 450$ cm, Young modulus $E = 250$ GPa and yield stress $\sigma_y = 235$ MPa have been assumed.

As in the previous examples, two rigid perfectly plastic hinges are located at the extremes of all the elements, considered to be elastic, and an additional hinge is located in the middle point of the longer beams. Moreover, the interaction between bending moment M and axial force N has been taken into account in the rigid plastic domain of the plastic hinges. The structure beams are all subjected to the same fixed uniformly distributed vertical load $q_0 = 30$ kN/m. Referring to the dynamic loads, let assume that the seismic masses are located at all the structure nodes; due to the described gravitational load q_0 they are equal at each floor and it results: $m_1 = 7.34$ kN $\cdot$ sec^2/m, $m_2 = 12.23$ kN $\cdot$ sec^2/m, $m_3 = 4.90$ kN $\cdot$ sec^2/m (Figure 5.22). The values

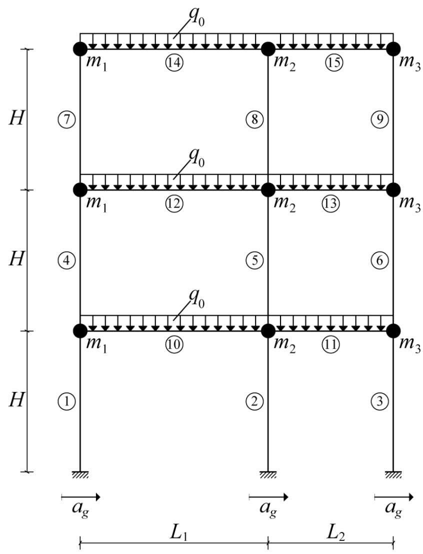

Figure 5.22: Three floor steel frame: geometry and load condition.

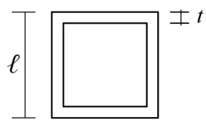

Figure 5.23: Typical square box cross section.

assigned to the seismic masses, as usual, are computed considering that during the earthquake the gravitational loads does not act all simultaneously on the structure, so that it is possible to evaluate $m_i = (0.8\, q_0 \ell_i)/g$, where g is the acceleration of gravity, and ℓ_i, $i = 1, 2, 3$ relevant influence beam length.

Also in this example, the structure is subjected to three loads combination of fixed (q_0) and seismic loads. The selected response spectra, as defined by the Italian code [80], for serviceability conditions (up-crossing probability in the lifetime of 63%) and instantaneous collapse (up-crossing probability in the lifetime of 10%) are those corresponding to Palermo, with a soil type B, life time 100 years and class IV. The fixed loads present in the second and in the third combination are reduced, setting $\xi_{s0} = \xi_{l0} = 0.8$. Furthermore, a technological constraint is imposed so that the pillars of the same floor have

Volume: 0.486					
El.	1	2	3	4	5
t	17.6	17.6	17.6	8.0	8.0
El.	6	7	8	9	10
t	8.0	6.6	6.6	6.6	8.3
El.	11	12	13	14	15
t	4.0	8.3	4.0	8.8	6.3

Table 5.11: Continuous variable unlimited ductility optimal design: volume (m^3) and thicknesses (mm).

Volume: 0.542 ω : 71.6					
El.	1	2	3	4	5
t	17.2	17.2	17.2	9.2	9.2
El.	6	7	8	9	10
t	9.2	9.2	9.2	9.2	8.3
El.	11	12	13	14	15
t	5.4	8.3	6.2	9.2	8.9

Table 5.12: Continuous variable limited ductility optimal design: volume (m^3) and thicknesses (mm).

the same thickness and the element slenderness is taken into account as in previous example.

As previously stated, the search problem is a strongly nonlinear one. As a consequence, the numerical solution can be reached by making recourse to the appropriate computational techniques shown in Chapter 4. The obtained results are reported in Table 5.11 in terms of optimal volume and optimal thicknesses.

Afterwards, the optimal design problem (3.41) has been solved for the same structure, imposing a bound on its structure ductility. To reach a numerical solution, the parametric approach described in Chapter 4 has been utilized and problems (4.6) and (4.7) has been solved. In particular, the residual dis-

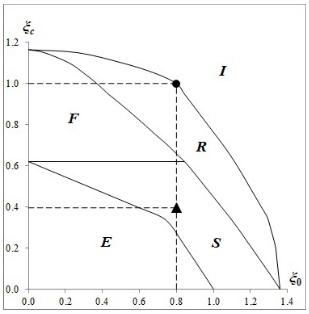

Figure 5.24: Continuous variable unlimited ductility optimal design: Bree diagram (▲ serviceability condition, ● instantaneous collapse condition).

placements related to the top floor has been bounded to be not greater than 12 cm.

The obtained results are reported in Table 5.12 in terms of optimal volume and optimal thicknesses. In the same table, the obtained value of the perturbation multiplier related to the minimum volume is reported.

As expected the limited ductility design is heavier than the former one. The safety characteristics of the two obtained optimal designs can be interpreted by means of the related Bree diagrams plotted in Figures 5.24, 5.25, where ξ_0 and ξ_c are the multipliers of the fixed and cyclic (seismic) load, respectively. It is worth noticing that the constraint imposed on the chosen displacement improves the resistance capacity of the optimal structure. Actually, the obtained strength and stiffness increment for the pillars guarantees a related increment of the global safety factor for the optimal structure.

Following the same approach as before, the plane frame in Figure 5.22 has been studied always searching for the unlimited ductility optimal design, but assuming all the design variables as appertaining at the same discrete set $T_d \equiv \{4, 6, 8, \ldots, 24\,\text{mm}\}$, $d = 1, 2, \ldots, 15$. For the numerical computation the above discrete variable optimization problem has been solved by utilizing the appropriate Harmony Search (HS) exposed in Chapter 4.

The obtained results are reported in Table 5.13 in terms of optimal volume and optimal thicknesses.

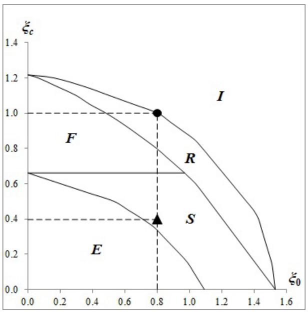

Figure 5.25: Continuous variable limited ductility optimal design: Bree diagram (▲ serviceability condition, • instantaneous collapse condition).

Volume: 0.505					
El.	1	2	3	4	5
t	18.0	18.0	18.0	10.0	10.0
El.	6	7	8	9	10
t	10.0	6.0	6.0	6.0	10.0
El.	11	12	13	14	15
t	4.0	8.0	4.0	8.0	6.0

Table 5.13: Discrete variable unlimited ductility optimal design: volume (m^3) and thicknesses (mm).

Volume: 0.552 ω : 70.8					
El.	1	2	3	4	5
t	18.0	18.0	18.0	10.0	10.0
El.	6	7	8	9	10
t	10.0	8.0	8.0	8.0	10.0
El.	11	12	13	14	15
t	4.0	8.0	8.0	10.0	8.0

Table 5.14: Discrete variable limited ductility optimal design: volume (m^3) and thicknesses (mm).

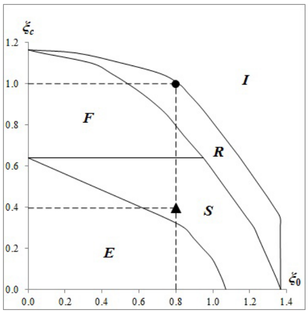

Figure 5.26: Discrete variable unlimited ductility optimal design: Bree diagram (▲ serviceability condition, ● instantaneous collapse condition).

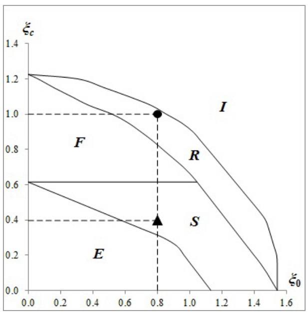

Figure 5.27: Discrete variable limited ductility optimal design: Bree diagram (▲ serviceability condition, ● instantaneous collapse condition).

Finally, the limited ductility optimal design has been determined for the same discrete variable structure, yet imposing a bound (12 cm) on the residual displacement of the top floor. The obtained results are reported in Table 5.14 in terms of optimal volume and optimal thicknesses. Furthermore, in the same table the founded value of the perturbation multiplier is reported.

Even in this case, the limited ductility design is heavier than the former one but, as it is possible to verify by analyzing the related Bree diagrams plotted in Figure 5.26, 5.27, the modest volume increment is related to a very useful increment of the global safety factor for the optimal structure.

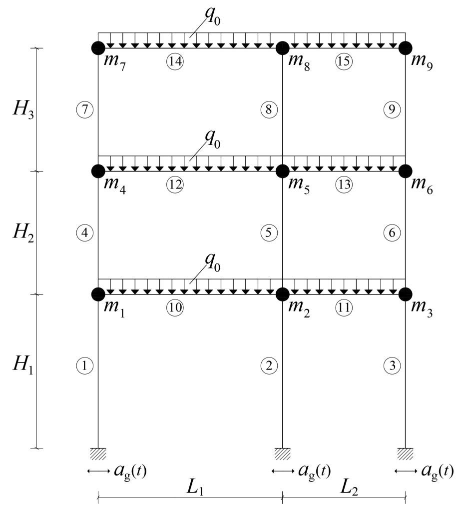

Figure 5.28: Three floor steel frame: geometry and load condition.

5.3 Case studies of frames under dynamic loads

With reference to the formulations proposed in section (3.2), three different applications have been addressed. At first the minimum volume design problem (3.74) has been solved for the frame plotted in Figure 5.28 constituted by rectangular box cross section elements (Figuere 5.29) with b = 200 mm, h = 300 mm, and constant thickness t variable in the continuous range between $t_c^{\min} = 4$ mm and $t_c^{\max} = 40$ mm. The following technological constraint on the pillars has been introduced: the thickness of the typical pillar must be not greater than the thickness of the pillar below. The cross sections of all the elements are disposed so that the axis related to the greater moment of inertia is orthogonal to the plane of the relevant frame. Furthermore, $L_1 = 600$ cm, $L_2 = 400$ cm, $H_1 = 500$ cm, $H_2 = H_3 = 500$ cm, Young modulus $E = 250$ GPa and yield stress $\sigma_y = 235$ MPa have been assumed.

The frame is modeled as an elastic perfectly plastic discrete structure; actually, it is constituted by perfectly elastic beam elements delimited by two rigid perfectly plastic hinges located at their extremes. Furthermore, an additional rigid perfectly plastic hinge is located in the middle point of the longer beams. The plastic admissibility of the structure is evaluated in correspondence of each

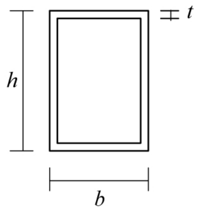

Figure 5.29: Typical rectangular box cross section.

hinge making reference to the domain already described in in section 5.2.

The structure is subjected to a fixed uniformly distributed vertical load $q_0 = 40\,\text{kN/m}$, and to seismic actions modeled as in section (3.2.2). As usual, the value assumed for the seismic masses depends on the remark that during the earthquake not all the gravitational loads are considered as acting on the structure, so $m_i = (0.8\, q_0 \ell_i)/g$, where g is the acceleration of gravity, $i = 1, 2, \ldots, 9$ is the number of masses and ℓ_i is the influence length of the i^{th} mass. Furthermore, according with the previously described load combinations, $\xi_{s0} = \xi_{l0} = 0.8$ has been utilized.

With the aim of defining the seismic input the parameters of the Kanai-Tajimi [87] filter have been selected, as usual for stiff soil characteristics, as $\omega_g = 5\pi$ rad sec^{-1} and $\zeta_g = 0.6$, whereas the white noise intensity has been assumed as $S_0^s = 0.0028\,\text{m}^2\,\text{sec}^{-3}$ for serviceability conditions and $S_0^l = 0.0064\,\text{m}^2\,\text{sec}^{-3}$ for instantaneous collapse ones. It is worth noticing that the same seismic ground motion will be used for all the effected applications.

Being the problem a strongly nonlinear one, in order to reach the numerical solution an appropriate Harmony Search (see e.g. section 4.2) has been utilized. As known, the Harmony Search is a solution strategy suitable for large optimization problem involving continuous and/or discrete design variables and, furthermore, it does not require the use of derivatives. The obtained results are reported in Table 5.15 in terms of optimal volume and optimal thicknesses. The safety characteristics of the obtained optimal designs can be interpreted by means of the related Bree diagram plotted in Figure 5.30 where ξ_0 and ξ_c are the multipliers of the fixed and seismic load, respectively. It is wort noting that the limit curve of the Bree diagram is obtained referring to an approximate limit analysis for the reasons exposed in section (3.2).

Volume: 0.864					
El.	1	2	3	4	5
t	13.4	25.6	21.2	6.4	23.9
El.	6	7	8	9	10
t	14.6	4.2	7.8	10.3	9.9
El.	11	12	13	14	15
t	27.9	11.9	13.7	6.0	5.6

Table 5.15: Optimal volume (m^3) and thicknesses (mm) of the frame plotted in Figure 5.28.

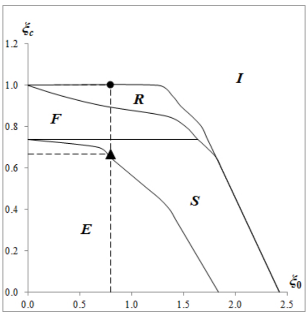

Figure 5.30: Bree diagram related to the combination of fixed loads and seismic actions (▲ serviceability condition, ● instantaneous collapse condition).

As previous referred, the second application regards the solution to problem (3.83) which searches for the optimal mechanical characteristics of a base isolation system supporting a given known structure. At this purpose, let us make reference to the frame plotted in Figure 5.31.

The overhanging structure is assumed to be equal to that used in the previous case for both geometry and mechanical characteristics; it differs only by the addition of two beams at the soil level and for a different thickness distribution, as reported in Table 5.16. The thicknesses of the beam elements have been chosen as the ones which ensures an elastic response to the fixed loads, adopting a safety factor with value not lower than 1.4. The relevant volume results $0.349\,\mathrm{m}^3$. The minimum value for the stiffness of the base isolation system has been assigned $k_b^{\min} = 0.05\mathrm{kN/mm}$ and a fixed damping ratios (10%)

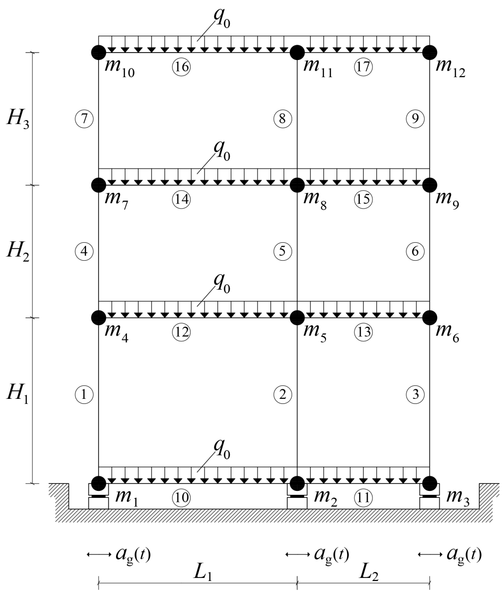

Figure 5.31: Base isolated steel frame: geometry and load condition.

for the base isolation system has been imposed.

As imposed with the constraints of problem (3.83) the optimal solution is related with a base isolated structure which must exhibit an elastic behavior for fixed loads and an elastic shakedown behavior for the combination of reduced fixed loads and high seismic actions. The numerical solution has been reached by a suitable parametric procedure coded in MatLab which explores for a discrete interval of base isolation stiffness values the response in terms of base isolation displacement and shakedown load amplifier.

As it is possible to observe from Figure 5.32 the problem provides a solution respecting the relevant constraints for values of stiffness of the isolation system less than $k_b = 0.255$kN/mm (shakedown multiplier with value equal to 1). Furthermore, for that limit value of stiffness the minimum base isolation displacement $u_b = 51.5$mm has been found (Figure 5.33). In order to show the optimal design structural sensitivity the Bree diagram has been plotted in Figure 5.34.

It is easy to remark that the utilization of the base isolation system allows to

Volume: 0.349						
El.	1	2	3	4	5	6
t	4.1	4.2	4.1	4.1	4.1	4.1
El.	7	8	9	10	11	12
t	4.1	4.0	4.1	5.4	4.2	5.5
El.	13	14	15	16	17	-
t	4.1	5.3	4.2	5.6	4.1	-

Table 5.16: Volume (m^3) and thicknesses (mm) assumed for the base-isolated frame plotted in Figure 5.30.

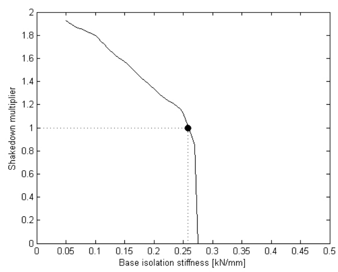

Figure 5.32: Base isolation stiffness VS Base isolation displacement diagram: • optimal value.

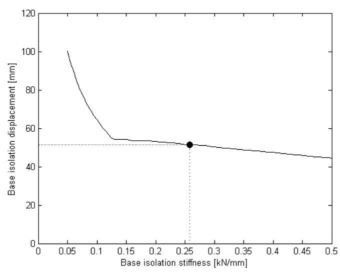

Figure 5.33: Base isolation stiffness VS Shakedown multiplier diagram: • serviceability condition.

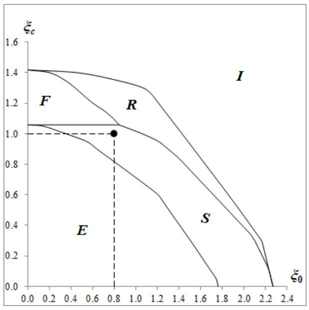

Figure 5.34: Bree diagram related to the combination of fixed loads and seismic actions (• limit condition).

obtain an optimal structure with a volume definitely lower than the previously computed one (volume reduction of about 60%) but which guarantees a full usability of the structure during its lifetime preventing any collapse mode even under high level seismic loads. Such a good feature it is not invalidate by the cost of the base isolation system which normally it is not greater than $15 \div 20\%$ of the structure cost.

The last exposed example describes a design approach which can be certainly applied to the design of new structures but it possesses its fundamental interest in existing structures to be improved against seismic actions.

Actually, the complete general approach in order to compute the optimal design of a new structure provided with a base isolation system is described by problem (3.84) in which geometrical structure features and mechanical base isolation system ones are considered as variables of the relevant optimization problem.

As a consequence, a third application has been effected related to the search for the minimum volume design of the same frame structure provided with a base isolation system with damped and stiffness features variable within assigned ranges (mixed formulation).

The data of the problem are the same as the ones assumed for the first application, and more: $k_b^{\min} = 0.05\text{kN/mm}$, $k_b^{\max} = 0.5\text{kN/mm}$, $\zeta_b^{\min} = 0.10$, $\zeta_b^{\max} = 0.15$.

The numerical procedure utilized to reach the solution to problem (3.84) is the already described harmony search, here adapted with further design

Volume: 0.317						
El.	1	2	3	4	5	6
t	4.1	4.0	4.0	4.1	4.0	4.0
El.	7	8	9	10	11	12
t	4.1	4.0	4.0	4.1	4.1	4.2
El.	13	14	15	16	17	-
t	4.1	4.3	4.1	4.0	4.1	-

Table 5.17: Optimal volume (m^3) and thicknesses (mm) of the base-isolated frame plotted in Figure 5.30.

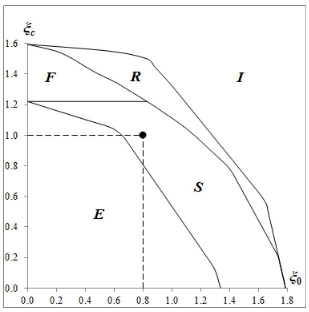

Figure 5.35: Bree diagram related to the combination of fixed loads and seismic actions (● limit condition).

variables and constraints.

The results are obtained in terms of stiffness $k_b = 0.184$kN/mm and damping ratio $\zeta_b = 0.143$ of the base isolation system, and in terms of optimal thicknesses and volume as reported in Table 5.17. The maximum base isolation system displacement $u_b = 54.1$mm has been found. The Bree diagram of the obtained design is plotted in Figure 5.35.

As it is possible to observe this last improved design exhibits a very sure shakedown behavior, it suffers a base isolation system displacement definitely acceptable from a technological point of view and guarantees a further cost saving of about 10%.

Chapter 6

Conclusions

In the present thesis the analysis and design problem of elastic perfectly plastic structures subjected to dynamic loads has been studied.

Starting from the vast scientific literature on this topic and with the aim to refer to cases of great practical interest, e.g. civil and industrial buildings affected by catastrophic events such as earthquakes and strong wind loads, new optimal design problem formulations together with suitable solution procedures have been provided. Further, a particular dynamic shakedown analysis for uncertain elastic plastic structures subjected to stochastic loads has been proposed.

In general, the response of an elastic plastic structure subject to quasi-static or dynamic load histories, can be analyzed through incremental analysis procedures. Actually, the loads acting upon the structures are random by nature, and from a deterministic point of view, it is impossible to control the structural response for each of the infinite possible load histories. So, it is usual to describe the loads through a suitable domain representing the maximum and minimum expected values.

An elastic-plastic structure subject to such load model can exhibit different structural behaviors depending on the load intensity, such for example it could respond in a purely elastic manner, it could suffer plastic deformations or it could collapse immediately to the loads application.

When the structure suffers plastic deformations in a first and than it responds in an elastic manner, it is said that the structure shakes down to an elastic state. As known, the elastic shakedown is a safe criterion to treat elastic-plastic structure because it allows the developing of some plastic strain avoiding dangerous phenomena as low cycle fatigue, ratcheting and instantaneous collapse.

When the structure is subjected to a domain of perfectly cyclic loads varying in time in a quasi-static manner, one can refer to the well-known classical shakedown analysis. When the loads to consider are variable in time so rapidly that inertia and damping forces cannot be neglected, one has to refer to the dynamic shakedown analysis in which a suitable domain of excitations can be considered.

Whenever one wants to consider the conditions under which an elastic plastic structure shakes down under a stochastic dynamic load, the use of an excitation domain is improper. In fact, ensure that the structure shakes down for any excitation belonging to the given domain means ensuring the shakedown for an event with probability one and so the stochasticity of the problem disappears. In the present thesis, starting from the concept of arbitrary excitation history namely a load history made by finite excitations paused by intervals of no-motion of arbitrary length, a probabilistic assessment of dynamic shakedown analysis has been given. In particular, by matching every excitation with the stationary segment of a scalar normal stochastic process it was possible to define a probabilistic shakedown safety factor. This load model seems to be adequate to represent wind load upon the structure and a numerical application related to plane steel frames has been effected in order to show the effectiveness of the proposed method. This analysis can lead to the formulation of a reliability-based optimization problem. The research in this topic are still in progress and they will constitute the subject of future developments.

It is easy to understand that the above mentioned analyses can be effected for structures whose geometry, load conditions and mechanical characteristics are completely known. If the geometry of the structure or other parameters are treated as free variables, one has to solve an optimization problem.

Solving a structural design problem means the reaching, among all the feasible designs, of the one which minimizes or maximizes a chosen quantity. In the present thesis reference has been made to the so-called "sizing optimization problems with stress constraints" in which the minim volume of a frame structure has been searched treating as variables the thicknesses of the cross sections of all the beam elements. The structure has been considered subjected to multiple load combinations and thus different stress constrains have been imposed to the optimal design.

In particular, a first group of formulations have been proposed idealizing the seismic loads on the structure as a perfect cyclic quasi-static load and taking into account inertia and damping effects in an approximate way trough the use of the response spectrum method. Three different load combinations have been considered in correspondence of which three different structural behaviors have been imposed so that the structure must behave in a purely elastic manner when subjected to fixed (dead) loads, it must respond eventually in an elastic manner when subjected to a combination of fixed and low intensity seismic loads (i.e. it must shakes down) and finally, it must prevent the instantaneous collapse when subjected to fixed and high intensity seismic loads.

This formulation, being based on first order theories such as shakedown and limit analysis, has been improved in order to take into account dangerous effects as buckling and P-Δ effects. Furthermore, due to the special loading model assumed, the exact amount of plastic strains accumulated in the transient phase is not known. So, making reference to the so-called "bounding techniques" a special formulation has been proposed for structures with limited ductility.

A second group of optimal design problem formulations has been presented making reference to the so-called "repeated seismic excitation model" in which seismic waves are represented trough a spectral decomposition as a convex domain of excitations. With this special load model it is possible to formulate an optimization problem in which the seismic actions are treated in all their dynamic nature. As usual three different load combinations have been considered in correspondence of which three different structural behaviors have been imposed. In particular, the structure must exhibit a purely elastic behavior when subjected to fixed loads, it must eventually dynamically shakes down when subjected to fixed loads and repeated seismic loads of low intensity and, it must prevent the instantaneous collapse when subjected to fixed loads and repeated seismic loads of high intensity. It is worth noting that the last condition has been imposed in an approximate way because the exact one is unfeasible from a practical point of view. Furthermore, some special formulations for base-isolated structure have been exposed.

As known, to solve an optimization problem spacial computational procedures must be adopted. When the problem is formulated with variable varying in a continuous range many iterative procedures consisting in the linearization of the original functions by using their derivatives with respect to the design variables are available. In the present thesis, due to the high non linearity of the relevant search problems, a suitable iterative technique based on the main assumption that all the quantities depending on the design variables can be expressed as a linear functions of these variables, i.e. as the sum of their values at the previous step plus the product of their partial derivatives with respect to the design variables times the increments of the design variables, has been utilized. It is worth noting that the design reached by means of this iterative technique coincides with the design obtainable by solving the original problem because the design and behavioral variable values obtained by means of the proposed technique fulfill all the Kuhn-Tucker equations related to the original design problem.

When the design variables belong to discrete sets, in order to solve the problem, combinatorial optimization method are more appropriate. In the last decades, many algorithms relying analogies to natural processes have been presented. Among them, the so-called “harmony search method” has been here specialized to solve discrete variable design problems with shakedown and limit constraints.

In the framework of numerical applications, special reference is made to frame structures. For each optimal design the related Bree diagrams are plotted and the different features of the special behavior of the obtained structures are discussed. The results allow to confirm the theoretical expectations in terms of behavioral features of the obtained optimal designs and, furthermore, they provide useful information on many case of technical interest.

Acknowledgments

At the end of this three years of doctoral course, I feel obliged to thank all those who contributed to my scientific growth and with whom I had the privilege of working.

I feel to express my deep sense of gratitude to my tutor Prof. Luigi Palizzolo for the opportunity that he gave me to attend and complete this course of doctoral studies. He was my real mentor offering me his knowledge and abilities and furthermore, he represented a certain scientific and human guide. Thanks.

Equally, I would like to thank Prof. Salvatore Benfratello and to Prof. Francesco Giambanco who, believing in me, encouraged me to undertake my doctoral studies.

Thanks to Prof. Mario Di Paola for all the fruitful discussions and suggestions on the topics of this thesis. Thanks to Prof. Giuseppe Failla for his quick answers to all my questions.

Sincere thanks are also for Prof. Antonina Pirrotta, Prof. Ahsan Kareem and Dr. Seymour Spence, to whom I have to be grateful for the months that I spent at the University of Notre Dame improving my studies and my research. I will never forget all the help that Seymour gave to me, made me feel at home.

I would like to thank also all the people working at the Department of Civil, Environmental,Aerospace, Materials Engineering of University of Palermo who for various reasons have contributed to this thesis. In particular, thanks to the advisory board of this doctorate and to the librarians Dott. Rita Cinà and Ruggero Garaffa for the patient bibliographic searches.

I want to express my good luck for a prosperous and full of happiness future to my friends and colleagues Francesco, Gioacchino and Emma, who shared with me knowledge and scientific interests.

I wish to thanks my parents Giuseppe and Piera, for all their great sacrifices that allowed me to became an architect first and to complete the doctoral studies later.

Finally, I dedicate this thesis to Veronica that with love, patience and confidence supported me all these years, with the hope that she continues to do that for the rest of our lives.

Bibliography

[1] J. Atkočiūnas and A. Venskus. Optimal shakedown design of frames under stability conditions according to standards. *Computers & Structures*, 89 (3-4):435–443, 2011. doi: 10.1016/j.compstruc.2010.11.014.

[2] J. Atkočiūnas, D. Merkevičiūtė, and A. Venskus. Optimal shakedown design of bar systems: Strength, stiffness and stability constraints. *Computers & Structures*, 86(17-18):1757–1768, 2008. doi: 10.1016/j.compstruc.2008.01.008.

[3] S.K. Au and J.L. Beck. A new adaptive importance sampling scheme for reliability calculations. *Structural Safety*, 21(2):135 – 158, 1999. ISSN 0167-4730. doi: 10.1016/S0167-4730(99)00014-4.

[4] S.K. Au and J.L. Beck. Estimation of small failure probabilities in high dimensions by subset simulation. *Probabilistic Engineering Mechanics*, 16(4):263 – 277, 2001. ISSN 0266-8920. doi: 10.1016/S0266-8920(01)00019-4.

[5] S.K. Au, Z.J. Cao, and Y. Wang. Implementing advanced monte carlo simulation under spreadsheet environment. *Structural Safety*, 32(5):281 – 292, 2010. ISSN 0167-4730. doi: 10.1016/j.strusafe.2010.03.004.

[6] S. Benfratello, L. Cirone, and F. Giambanco. Bounds on transient phase plastic deformations in optimal design of steel frames subjected to cyclic loads. *Computational Mechanics*, 44(1):1–13, 2009. doi: 10.1007/s00466-008-0350-7.

[7] S. Benfratello, F. Giambanco, L. Palizzolo, and P. Tabbuso. Multicriteria

design of frames with constraints on buckling. In *Atti del XX congresso AIMETA, Associazione Italiana Meccanica Teorica e Applicata*, 2011.

[8] S. Benfratello, F. Giambanco, L. Palizzolo, and P. Tabbuso. On the structural optimization in presence of base isolating devices. In *Proceedings of the 3rd International Conference on Engineering Optimization*, 2012.

[9] S. Benfratello, F. Giambanco, L. Palizzolo, and P. Tabbuso. Optimal design of steel frames accounting for buckling. *Meccanica*, 48(9):2281–2298, 2013. doi: 10.1007/s11012-013-9745-4.

[10] S. Benfratello, L. Palizzolo, and P. Tabbuso. Dynamic shakedown design of structures under repeated seismic loads. In *Research and Applications in Structural Engineering, Mechanics and Computation - Proceedings of the 5th International Conference on Structural Engineering, Mechanics and Computation, SEMC 2013*, pages 241–246, 2013. doi: 10.1201/b15963-47.

[11] S. Benfratello, L. Palizzolo, and P. Tabbuso. Optimal design of elastic plastic frames accounting for seismic protection devices. *Structural and Multidisciplinary Optimization*, 49(1):93–106, 2014. doi: 10.1007/s00158-013-0959-9.

[12] S. Benfratello, L. Palizzolo, and P. Tabbuso. Seismic shakedown design of frames based on a probabilistic approach. In *WIT Transactions on the Built Environment*, volume 137, pages 359–370, 2014. doi: 10.2495/HPSM140341.

[13] S. Benfratello, L. Palizzolo, and P. Tabbuso. Comparison between unrestricted dynamic shakedown design and a new probabilistic approach for structures under seismic loadings. In *Proceedings of the 4th International Conference on Engineering Optimization*, 2014.

[14] H. Bleich. Uber die bemessung statisch unbestimmter stahltragwerke unter berüecksichtigung des elastich-plastischen verhaltens des baustoffes. *Bauingenieur*, 13:261–267, 1932.

[15] G. Borino and C. Polizzotto. Dynamic shakedown of structures under repeated seismic loads. *Journal of Engineering Mechanics*, 121(12):1306–1314, 1995. doi: 10.1061/(ASCE)0733-9399(1995)121:12(1306).

[16] G. Borino and C. Polizzotto. Dynamic shakedown of structures with variable appended masses and subjected to repeated excitations. *International Journal of Plasticity*, 12(2):215–228, 1996. doi: 10.1016/S0749-6419(96)00004-6.

[17] G. Borino, S. Caddemi, and C. Polizzotto. Mathematical programming methods for the evaluation of dynamic plastic deformations. In D.Lloyd Smith, editor, *Mathematical Programming Methods in Structural Plasticity*, volume 299 of *International Centre for Mechanical Sciences*, pages 349–372. Springer Vienna, 1990. ISBN 978-3-211-82191-6. doi: 10.1007/978-3-7091-2618-9_17.

[18] T.K. Caughey and M.E.J. O'kelly. Classical normal modes in damped linear dynamic systems. *Journal of Applied Mechanics*, 32(3):583–588, 1965.

[19] G. Ceradini. Sull'adattamento dei corpi elastoplastici soggetti ad azioni dinamiche. *Giornale del Genio Civile*, 4-5:239–250, 1969.

[20] G. Ceradini. Dynamic shakedown in elastic-plastic bodies. *Journal of the Engineering Mechanics Division*, 106(3):481–499, 1980.

[21] G. Ceradini and C. Gavarini. Applicazione della programmazione lineare ai problemi di adattamento plastico statico o dinamico. *Giornale del Genio Civile*, 8:471–476, 1969.

[22] X. Chen and A. Kareem. Proper orthogonal decomposition-based modeling, analysis, and simulation of dynamic wind load effects on structures. *Journal of Engineering Mechanics*, 131(4):325–339, 2005. doi: 10.1061/(ASCE)0733-9399(2005)131:4(325).

[23] A.K. Chopra. *Dynamics of structures*, volume 3. Prentice Hall New Jersey, 1995. ISBN 978-0132858038.

[24] P.W. Christensen and A. Klarbring. *An Introduction to Structural Optimization.* Solid Mechanics and Its Applications. Springer, 2008. ISBN 9781402086656. doi: 10.1007/978-1-4020-8666-3.

[25] R.W. Clough and J. Penzien. *Dynamics of Structures.* McGraw-Hill Education - Europe, London, United Kingdom, international 2 revised edition, 1993. ISBN 9780071132411.

[26] C. Comi and A. Corigliano. Dynamic shakedown in elastoplastic structures with general internal variable constitutive laws. *International Journal of Plasticity*, 7(7):679–692, 1991. doi: 10.1016/0749-6419(91)90051-Y.

[27] A. Corigliano, G. Maier, and S. Pycko. Dynamic shakedown analysis and bounds for elastoplastic structures with nonassociative, internal variable constitutive laws. *International Journal of Solids and Structures*, 32(21): 3145–3166, 1995. doi: 10.1016/0020-7683(94)00265-X.

[28] L. Corradi. On compatible finite element models for elastic plastic analysis. *Meccanica*, 13(3):133–150, 1978. ISSN 0025-6455. doi: 10.1007/BF02128357.

[29] L. Corradi. A displacement formulation for the finite element elastic-plastic problem. *Meccanica*, 18(2):77–91, 1983. ISSN 0025-6455. doi: 10.1007/BF02128348.

[30] L. Corradi and G. Maier. Dynamic non-shakedown theorem for elastic perfectly-plastic continua. *Journal of the Mechanics and Physics of Solids*, 22(5):401 – 413, 1974. ISSN 0022-5096. doi: 10.1016/0022-5096(74)90005-2.

[31] G. A. Davenport. The dependence of wind load upon meteorological parameters. In University of Toronto Press, editor, *Proceedings of the International Research Seminar on Wind Effects on Building and Structures*, pages 19–82, 1967.

[32] A. De Martino and M. Di Paola. Dynamic shakedown analysis under stochastic loads. In *Proceedings of the Euromech 413 Colloquium on "Stochastic Dynamics of Nonlinear Mechanical Systems"*, 2001.

[33] S.O. Degertekin. Improved harmony search algorithms for sizing optimization of truss structures. *Computers & Structures*, 92-93:229–241, 2012. doi: 10.1016/j.compstruc.2011.10.022.

[34] G. Deodatis. Simulation of ergodic multivariate stochastic processes. *Journal of Engineering Mechanics*, 122(8):778–787, 1996. ISSN 0733-9399. doi: 10.1061/(ASCE)0733-9399(1996)122:8(778).

[35] M. Di Paola. Digital simulation of wind field velocity. *Journal of Wind Engineering and Industrial Aerodynamics*, 74-76:91–109, 1998. doi: 10.1016/S0167-6105(98)00008-7.

[36] M. Di Paola and I. Gullo. Digital generation of multivariate wind field processes. *Probabilistic Engineering Mechanics*, 16(1):1–10, 2001. doi: 10.1016/S0266-8920(99)00032-6.

[37] Q. Ding, L. Zhu, and H. Xiang. Simulation of stationary gaussian stochastic wind velocity field. *Wind and Structures, An International Journal*, 9 (3):231–243, 2006. ISSN 1226-6116. doi: 10.12989/was.2006.9.3.231.

[38] M. Dorigo. *Optimization, Learning and Natural Algorithms (in Italian)*. PhD thesis, Dipartimento di Elettronica, Politecnico di Milano, Milan, Italy, 1992.

[39] L.J. Fogel, A.J. Owens, and M.J. Walsh. *Artificial intelligence through simulated evolution*. Wiley, Chichester, WS, UK, 1966.

[40] European Committee for Standardization. Eurocode 3: Design of steel structures, part 1-1: General rules. Technical report, 1993.

[41] C. Gavarini. Sul rientro in fase elastica delle vibrazioni forzate elastoplastiche. *Giornale del Genio Civile*, 4-5:251–261, 1969.

[42] Z.W. Geem, J.H. Kim, and G.V. Loganathan. A new heuristic optimization algorithm: Harmony search. *Simulation*, 76(2):60–68, 2001.

[43] F. Giambanco, M. Lo Bianco, and L. Palizzolo. Approximate technique for dynamic elastic-plastic analysis. *Journal of Applied Mechanics, Transactions ASME*, 61(4):907–913, 1994.

[44] F. Giambanco, L. Palizzolo, and C. Polizzotto. Optimal shakedown design of beam structures. *Structural Optimization*, 8(2-3):156–167, 1994. doi: 10.1007/BF01743313.

[45] F. Giambanco, L. Palizzolo, and L. Cirone. Elastic plastic analysis iterative solution. *Computational Mechanics*, 21(2):149–160, 1998. ISSN 0178-7675. doi: 10.1007/s004660050291.

[46] F. Giambanco, L. Palizzolo, and L. Cirone. Computational methods for optimal shakedown design of fe structures. *Structural Optimization*, 15 (3-4):284–295, 1998. doi: 10.1007/BF01203544.

[47] F. Giambanco, L. Palizzolo, and A. Caffarelli. Computational procedures for plastic shakedown design of structures. *Structural and Multidisciplinary Optimization*, 28(5):317–329, 2004. doi: 10.1007/s00158-004-0402-3.

[48] F. Giambanco, L. Palizzolo, and A. Caffarelli. Computational procedures for plastic shakedown design of structures. *Structural and Multidisciplinary Optimization*, 28(5):317–329, 2004. doi: 10.1007/s00158-004-0402-3.

[49] F. Giambanco, S. Benfratello, L. Palizzolo, and P. Tabbuso. Structural design of frames able to prevent element buckling. In *Civil-Comp Proceedings*, volume 99, 2012. doi: 10.4203/ccp.99.18.

[50] F Giambanco, L Palizzolo, and L Cirone. An iterative approach to dynamic elastic-plastic analysis. *Journal of Applied Mechanics-Transaction of the ASME*, 65(4):811–819, DEC 1998. ISSN 0021-8936. doi: {10.1115/1.2791916}.

[51] D.E. Goldberg. *Genetic Algorithms in Search, Optimization and Machine Learning*. Addison-Wesley Longman Publishing Co., Inc., Boston, MA, USA, 1st edition, 1989. ISBN 0201157675.

[52] R.T. Haftka and Z. Gürdal. *Elements of Structural Optimization*. Solid Mechanics and Its Applications. Springer, 1992. ISBN 9780792315056. doi: 10.1007/978-94-011-2550-5.

[53] A. Haldar and S. Mahadevan. *Reliability assessment using stochastic finite element analysis*. John Wiley & Sons, New York, 2000. ISBN 0-471-36961-6.

[54] O. Hasançebi, S. Çarbaş, E. Doğan, F. Erdal, and M. P. Saka. Performance evaluation of metaheuristic search techniques in the optimum design of real size pin jointed structures. *Computers & Structures*, 87(5-6):284–302, 2009. ISSN 0045-7949. doi: 10.1016/j.compstruc.2009.01.002.

[55] H.S. Ho. Shakedown in elastic-plastic systems under dynamic loadings. *Journal of Applied Mechanics*, 39(2):416–421, 1972. doi: 10.1115/1.3422694.

[56] J.C. Kaimal, J.C. Wyngaard, Y. Izumi, and O.R. Coté. Spectral characteristics of surface-layer turbulence. *Quarterly Journal of the Royal Meteorological Society*, 98(417):563–589, 1972. ISSN 1477-870X. doi: 10.1002/qj.49709841707.

[57] S. Kaliszky and J. Lógó. Optimal design of elasto-plastic structures subjected to normal and extreme loads. *Computers and Structures*, 84(28): 1770–1779, 2006. doi: 10.1016/j.compstruc.2006.04.009.

[58] A. Kareem. Numerical simulation of wind effects: A probabilistic perspective. *Journal of Wind Engineering and Industrial Aerodynamics*, 96 (10-11):1472–1497, 2008. doi: 10.1016/j.jweia.2008.02.048.

[59] J. Kennedy and R. Eberhart. Particle swarm optimization. In *Neural Networks, 1995. Proceedings., IEEE International Conference on*, volume 4, pages 1942–1948 vol.4, Nov 1995. doi: 10.1109/ICNN.1995.488968.

[60] W. T. Koiter. A new general theorem on shake-down of elastic-plastic structures. In *Proc. Koninkl. Ned. Akad. Wet*, volume B 59, pages 24–34, 1956.

[61] J.A. König. *Shakedown of elastic-plastic structures*. Fundamental studies in engineering. Elsevier, New York, 1987. ISBN 9780444989796.

[62] M. Mahdavi, M. Fesanghary, and E. Damangir. An improved harmony search algorithm for solving optimization problems. *Applied Mathematics and Computation*, 188(2):1567 – 1579, 2007. ISSN 0096-3003. doi: 10.1016/j.amc.2006.11.033.

[63] G. Maier. A quadratic programming approachfor certain classes of nonlinear structural problems. *Meccanica*, 3(2):121–130, 1968. ISSN 0025-6455. doi: 10.1007/BF02129011.

[64] G. Maier and G. Novati. Dynamic shakedown and bounding theory for a class of nonlinear hardening discrete structural models. *International Journal of Plasticity*, 6(5):551–572, 1990. doi: 10.1016/0749-6419(90) 90044-F.

[65] E. Melan. Zur plastizität des räumlichen kontinuums. *Ingenieur-Archiv*, 9(2):116–126, 1938. ISSN 0020-1154. doi: 10.1007/BF02084409.

[66] D. Merkevičiūtė and J. Atkočiūnas. Optimal shakedown design of metal structures under stiffness and stability constraints. *Journal of Constructional Steel Research*, 62(12):1270–1275, 2006. ISSN 0143-974X. doi: 10.1016/j.jcsr.2006.04.020.

[67] F. Miao and M. Ghosn. Modified subset simulation method for reliability analysis of structural systems. *Structural Safety*, 33(4-5):251 – 260, 2011. ISSN 0167-4730. doi: 10.1016/j.strusafe.2011.02.004.

[68] G. Muscolino. *Dinamica delle strutture*. Pitagora Editrice, Bologna, Italy, 2012. ISBN 88-371-1858-9.

[69] B.G. Neal. *The plastic methods of structural analysis*. Wiley, 1956.

[70] B.G. Neal and P.S. Symonds. A method for calculating the failure load for a framed structure subjected to fluctuating, loads. *Journal of the ICE*, 35(3):186–197, 1951. doi: 10.1680/IJOTI.1951.12769.

[71] L. Palizzolo, S. Benfratello, and P. Tabbuso. On the optimal design of base isolation devices. In *Atti del XXI congresso AIMETA, Associazione Italiana Meccanica Teorica e Applicata*, 2013.

[72] L. Palizzolo, A. Caffarelli, and P. Tabbuso. Minimum volume design of structures with constraints on ductility and stability. *Engineering Structures*, 68:47–56, 2014. doi: 10.1016/j.engstruct.2014.02.025.

[73] L. Palizzolo, Benfratello S., and Tabbuso P. Discrete variable design of frames subjected to seismic actions accounting for element slenderness. *Computers & Structures*, 147:147–158, 2015. ISSN 0045-7949. doi: 10.1016/j.compstruc.2014.09.016.

[74] C. Polizzotto. A unified treatment of shakedown theory and related bounding techniques. *Solid Mech. Arch.*, 7:19–75, 1982. ISSN 0952-4762.

[75] C. Polizzotto. On shakedown of structures under dynamics agencies. In C. Polizzotto and A. Sawczuk, editors, *Inelastic analysis under variable loads*, pages 5–29. Cogras, Palermo, Italy, 1984.

[76] C. Polizzotto. Dynamic shakedown by modal analysis. *Meccanica*, 19(2): 133–144, 1984. ISSN 0025-6455. doi: 10.1007/BF01560461.

[77] C. Polizzotto. Elastoplastic analysis method for dynamic agencies. *Journal of Engineering Mechanics*, 112(3):293–310, 1986. doi: 10.1061/(ASCE)0733-9399(1986)112:3(293).

[78] C. Polizzotto, G. Borino, S. Caddemi, and P. Fuschi. Theorems of restricted dynamic shakedown. *International Journal of Mechanical Sciences*, 35(9):787 – 801, 1993. ISSN 0020-7403. doi: 10.1016/0020-7403(93)90025-P.

[79] C. Polizzotto, G. Borino, and P. Fuschi. Shakedown of structures subjected to dynamic external actions and related bounding techniques. In Dieter Weichert and Giulio Maier, editors, *Inelastic Behaviour of Structures under Variable Repeated Loads*, volume 432 of *International Centre for Mechanical Sciences*, pages 133–185. Springer Vienna, 2002. ISBN 978-3-211-83687-3.

[80] Consiglio Superiore Dei Lavori Pubblici. Nuove norme tecniche per le costruzioni dm 14/01/2008. Technical report, Repubblica Italiana, 2008.

[81] G.I.N. Rozvany. *Structural Design via Optimality Criteria*. Mechanics of Elastic and Inelastic Solids. Springer, 1989. ISBN 978-94-010-7016-4. doi: 10.1007/978-94-009-1161-1.

[82] M.P. Saka. Optimum design of steel sway frames to bs5950 using harmony search algorithm. *Journal of Constructional Steel Research*, 65(1):36 – 43, 2009. ISSN 0143-974X. doi: 10.1016/j.jcsr.2008.02.005.

[83] H. P. Schwefel. *Numerical Optimization of Computer Models*. John Wiley & Sons, Inc., New York, NY, USA, 1981. ISBN 0471099880.

[84] N. Scibilia. *Progetto di strutture in acciaio*. Dario Flaccovio Editore, Palermo, Italy, 2010. ISBN 9788857900223.

[85] M. Shinozuka, M. Kamata, and C. Yun. Simulation of earthquake ground motion as multi-variate stochastic process. Technical report, Dept. of Civ. Engrg. and Operations Res., Princeton University, 1989.

[86] E. Simiu and R.H. Scanlan. *Wind effects on structures: an introduction to wind engineering*. A Wiley-Interscience publication. Wiley, 1986. ISBN 9780471866138.

[87] H. Tajimi. A statistical method to determining the maximum response of a building structure during an earthquake. In *Proc. 2nd WCEE*, pages 781–797, 1960.